Alternative Reinforcing Strategies for Non-Contact Hooked Bar Lap Splices

Mason Kendall Brown

Thesis submitted to the faculty of the

Virginia Polytechnic Institute and State University

In partial fulfilment of the requirements for the degree of

Master of Science

in

Civil Engineering

Eric J. Jacques, Chair

Carin L. Roberts-Wollmann, Co-Chair

David W. Mokarem

December 13, 2024

Blacksburg Virginia

Keywords: Lap-Splice, hooked bar, steel fibers, number of splices, transverse reinforcement

Alternative Reinforcing Strategies for Non-Contact Hooked Bar Lap Splices

Mason Kendall Brown

ABSTRACT

Closure joints are used in precast bridge construction to join two pieces of precast concrete. The pieces of concrete are joined by a lap splice which consists of longitudinal steel sticking out of each precast element and overlapped over the minimum required development length. State departments of transportation find it desirable to make the width of closure joints short. To achieve this, bridge engineers have been using hooked bars in the closure joints in lieu of straight bars, with the assumption that this would allow for shorter splice lengths. Though engineers in practice are doing this, design guidance does not exist. One research project by Coleman (2024) tested 58 beam-splice specimens to investigate the impacts of a variety of parameters on bond and anchorage and develop design guidance for hooked bar lap splices. This project did not investigate three parameters: the number of lap splices, the placement of transverse reinforcement, and the addition of steel fibers in the closure joint. For this thesis, 15 beam-splice specimens were tested in 4 point-bending to investigate the impact of these parameters on bond and validate the descriptive equation developed by Coleman (2024) to determine the bar stress of a hooked bar lap splice.

The findings of this study suggest that the number of splices and the placement of transverse reinforcement has minimal impact on the bar stress developed, and the equation by Coleman (2024) adequately predicts the bar stress when these parameters were varied. The addition of steel fibers to the closure joint had a substantial impact on increasing the splice strength. In the beams where steel fibers were added in a 1% fiber volume fraction, the descriptive equation by Coleman (2024) underpredicted the bar stress for both unconfined and confined beams with the addition of fibers. Thus, this thesis proposes a factor to multiply the descriptive equation by determining the bar stress when steel fibers are added.

With these findings, using steel fibers in closure joints for precast concrete can be used to reduce splice length in non-contact hooked bar lap splices.

Alternative Reinforcing Strategies for Non-Contact Hooked Bar Lap Splices

Mason Kendall Brown

GENERAL AUDIENCE ABSTRACT

Precast concrete is concrete that is cast off-site in a controlled environment and transported to the site to then be put together at the site of a project. In bridge construction, this is very beneficial to projects since it means that there is more quality control of the specimens and can allow for faster construction times since the components can have time to cure to strength off-site.

To put together pieces of precast concrete to create continuous beams and other components, a closure joint is used. These closure joints consist of two precast pieces of concrete which have longitudinal steel sticking out of each precast element. The pieces of concrete are then joined by overlapping the longitudinal steel in a lap splice. Where a lap splice is used to develop the minimum development, length is required to provide the adequate bar strength such that load will be transferred from one beam to another to create a continuous beam.

State departments of transportation find it desirable to make the width of closure joints short. Since closure joint width is typically controlled by the minimum development length required to connect the pieces of concrete, the main way to reduce the width is to reduce the minimum development length. To achieve this, bridge engineers have been using hooked bars in the closure joints in lieu of straight bars, with the assumption that this would allow for shorter splice lengths. Though engineers in practice are doing this, design guidance does not exist. One research project by Coleman (2024) tested 58 beam-splice specimens to investigate the impacts of a variety of parameters on bond and anchorage and develop design guidance for hooked bar lap splices. This project did not investigate three parameters: the number of lap splices, the placement of transverse reinforcement, and the addition of steel fibers in the closure joint. For this thesis, 15 beam-splice specimens were tested in 4 point-bending to investigate the impact of these parameters on bond and validate the descriptive equation developed by Coleman (2024) to determine the bar stress of a hooked bar lap splice.

The findings of this study suggest that the number of splices and the placement of transverse reinforcement has minimal impact on the bar stress developed, and the equation by Coleman (2024) adequately predicts the bar stress when these parameters were varied. The addition of steel fibers to the closure joint had a substantial impact on increasing the splice strength. In the beams where steel fibers were added in a 1% fiber volume fraction, the descriptive equation by Coleman (2024) underpredicted the bar stress for both unconfined and confined beams with the addition of fibers. Thus, this thesis proposes a factor to multiply the descriptive equation by determining the bar stress when steel fibers are added. With these findings, using steel fibers in closure joints for precast concrete can be used to reduce splice length in non-contact hooked bar lap splices.

Acknowledgements

I would like to thank Dr. Jacques and Dr. Roberts-Wollmann for advising me over the last year and a half. I have learned a lot about how to complete research and about concrete. I would additionally like to thank Dr. Mokarem for serving on my committee.

I would like to thank the Virginia Department of transportation for sponsoring this research.

The experimental work of this thesis was completed in the Thomas M. Murray Structures lab and took many hours to complete. I am very grateful for the help of Dr. Zachary Coleman, who guided me through construction, testing, and analysis techniques, and additionally helped with testing and construction. I would also like to acknowledge the help of friends for their help on the lab floor: Ann Albright, Henry Mcklin, Iliana Walters, Michael Cheney, and Omar Almasarani. I have additionally received help from 2 undergraduates Virginia Babcock, and Ray Bodnar. I would also like to thank Dr. Mokarem, Brett Farmer, and Garret Blankenship for their kindness and help with many aspects of the experimental portion of this work.

I would also like to thank the mentors I have had throughout my life which contributed to my completing my master's degree. I would like to thank my previous advisors and teachers Dana Sanelli, Peter Ammadio, and Paige Blackburn for fostering a passion for civil engineering. I would, furthermore, like to thank my coaches and athletic staff from my undergraduate institution, Coach Colleen Murphy and Sheri Lampin for helping me learn how to face adversity and come back stronger from it.

Lastly, I would like to thank my family and friends. To my Mom and Dad who always taught me to leave can't out of my vocabulary, thank you for pushing me to be the best version of myself I can be. To my sister and brother, Emma and Hudson, thank you for supporting me and always being a comfortable place to come home to. To all of my friends, thank you for all of the good memories and helping support me through all of the phases of my life.

The views expressed in this thesis are those of the author and do not reflect the official policy or position of the United States Air Force, Department of Defense, or the U.S. Government.

TABLE OF CONTENTS

List of Figures

List of Tables

Chapter 1 INTRODUCTION

1.1 MOTIVATION

Precast concrete bridge construction has gained popularity over the last 70 years due to the affordability, speed of construction, and durability of the bridges. The primary benefit of precast bridge construction is that most of the concrete pieces are manufactured off site. This allows manufacturers to have greater quality control over the concrete since environmental factors can be controlled, resulting in fewer weather-related delays and higher quality concrete, which has longer lifespans and lower maintenance requirements. Additionally, precast bridge construction reduces the construction time significantly, with precast concrete bridges having installation times of days compared to months for cast-in-place concrete.

In bridge construction, where bridge components span long distances, closure joints are used to connect pieces of precast concrete to create one continuous structural component. To create a closure joint, two pieces of precast concrete are constructed off-site where the longitudinal steel sticks of each piece stick out of the concrete. Then, the two pieces are joined together by overlapping the longitudinal steel over a minimum development length. Where the development length is the minimum length that the steel must overlap to provide load transfer to create a continuous structural component.

With beam segments typically being rather large in bridge construction, non-contact lap splices are used extensively in these closure joints because of the greater ease with fit up. A non-contact lap splice is a type of lap splice where the two reinforcing bars are placed parallel to each other with a gap separating the two bars rather than them being directly in contact. The rebar is separated by a specified distance and overlap by a specified length to ensure adequate force transfer. This separation allows for construction tolerance for when it is difficult or impossible to place the bars directly against each other. Thus, using non-contact lap splices allows for connecting of adjacent precast concrete elements quickly and more economically than traditional lap splices. Currently the design of non-contact lap splices is governed by ACI 318-19 (2019) or AASHTO (2021).

While closure joints are essential to using precast concrete in bridge design, they are very tedious to construct and can offset some of the benefits of using precast concrete. These joints are tedious to construct since the closure joints must align to adequately transfer load, specialty supports are frequently required, and the reinforcement required often requires tight spacing which can cause congestion in the joint. Furthermore, since closure joints are cast-in place and expected to be used prior to the 28-day strength, there are additional durability concerns for these joints. For these reasons, transportation authorities want engineers to make the width of the closure joints shorter.

One of the ways to reduce the width of the closure joint is to reduce the length of the lap splice. Current code requirements for splice length state that the splice length is equal to the required development length multiplied by a factor from ACI 318-19 (2019) or AASHTO (2021).

One potential solution that bridge engineers have been using in practice is using hooked bars to shorten the development length. They make this substitution under the assumption that hooked bar development and splice length are equivalent. This substitution is not presently permitted by ACI 318-19 (2019) or AASHTO (2021). This is due to minimal test data on hooked bar lap splices.

To address these issues, the Virginia Department of Transportation (VDOT) sponsored a project at Virginia Tech to develop an understanding of non-contact hooked bar lap splices. As part of this project, Zachary Coleman investigated the influence of a variety of parameters on noncontact hooked bar lap splices with 58 beam-splice specimens (Coleman, 2024). From these tests, (Coleman, 2024)contributed to a larger understanding of non-contact hooked bar lap splices and developed a descriptive equation to predict bar stress. From this equation, a design equation was developed, and design guidance for the parameters tested was provided.

One key finding of this study was that hooked bars fail in a manner different from straight bar lap splices. Specifically, Coleman (2024) found that these beams fail by a mechanism of hook side bulging and hook prying: terms which are defined and investigated in section 2.1.1 of the literature review. In typical closure joints which use straight bars, the number of splices and placement of transverse reinforcement do not influence the bar stress developed. With the new failure modes discovered in this preliminary study, the side effect of these failures might cause these parameters to have a greater impact on bond and anchorage. Since the preliminary study did not study these factors, this study will investigate the impact of the number of lap splice pairs and the placement of transverse reinforcement. For the purposes of this research, transverse reinforcement will refer to stirrups perpendicular to the lead of the hooks used to reduce transverse tension. See Figure 1-1 for what the lead and tail of the hook is defined as and for a visual representation of a typical closure pour.

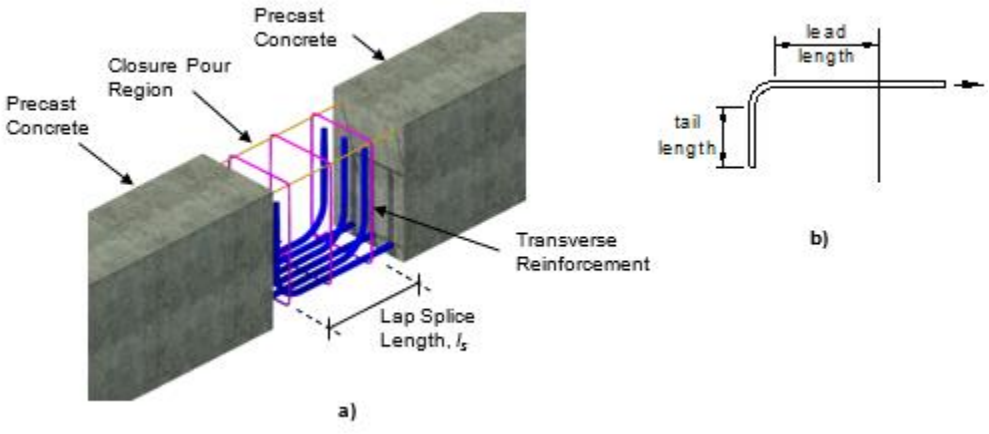

Figure 1-1: Noncontact Hooked Bar Lap Splice (Coleman, 2024)

In this study, it is expected that as the spacing for the transverse reinforcement decreases and that the quantity of reinforcement increases, the bond and anchorage parameters improve. Additionally, one can anticipate that as the number of spliced bar pairs increases, the side effects

should reduce, and the effect on the splice strength should be minimal such that it can be ignored.

In addition to the desire to understand these two parameters there was one more parameter that was of interest to study, and that is the use of fiber reinforced concrete (FRC) in the closure joint. This is largely due to the growing popularity of fiber reinforced concrete due to its enhanced material properties of improved crack control, durability, and the potential for improved strength. With these enhanced material properties, and the industry desire to reduce splice length, fibers offer a potential solution to further reduce splice length when using noncontact hooked bar lap splices.

For these reasons, VDOT has sponsored this research to investigate these three parameters to gain further understanding of non-contact hooked bar lap-splices and to validate the equations developed by Coleman (2024).

1.2 RESEARCH OBJECTIVES

The objective of this work is to broaden the understanding of non-contact hooked bar lap splices when varying the parameters: number of splices, placement of transverse reinforcement, and the addition of a 1% dosage of steel fibers by volume to the closure joint. This work aims to validate equations developed by Coleman (2024) and provide design recommendations for the use of a 1% dosage of steel fibers by volume in the closure joint. The following variables and their influence on splice strength were studied: placement of transverse reinforcement perpendicular to the lead end of the hooks, bar size, splice length, steel fiber reinforcement in the concrete, concrete cover, and number of splices.

1.3 RESEARCH METHODOLOGY

To achieve the objectives of this work, the following approach was taken.

1. **Review of previous research on the influence of the noncontact hooked bars, number of lap splices, transverse reinforcement, and steel fibers.**
2. **An experimental program to study anchorage behavior of non-contact hooked bar lap splices was conducted.** Sixteen 13-ft long beam splice specimens were constructed and subjected to four-point loading to investigate the influence of: the number of lap splices, transverse reinforcement, and the addition of steel fibers on bond and anchorage strength. The details of these beams can be found in a test matrix given in Appendix A.
3. **Compare experimental results to those of beams chosen from Coleman (2024).** From these comparisons, an understanding of the impacts of the parameters on bond is developed.
4. **Compare experimental results to predicted results of the equation developed by Coleman (2024).** Furthermore, it will be determined if design guidance can be recommended based on the findings of this study.
5. **Preparation of a thesis and presentation of the design methods, experimental results, and conclusions.**

1.4 THESIS ORGANIZATION

The structure of this thesis is as follows:

- Chapter 1 is an introduction which details the motivations of this research, research objectives, research methodology, and introduces hypotheses.
- Chapter 2 is a literature review which includes a review of the dissertation by Coleman (2024) and previous research on number of splices, transverse reinforcement, and steel fibers.
- Chapter 3 includes the test matrix for the beams tested and details the methods and procedures for constructing and testing the beams.
- Chapter 4 is a discussion of the results of the study which includes an analysis of bar stress, moment deflection plots, and suitability of the equation developed by Coleman (2024)
- Chapter 5 details the conclusions of this study.

Chapter 2 LITERATURE REVIEW

2.1 INTRODUCTION

This thesis requires an understanding of the impact of the number of spliced bars in a connection, alternative transverse reinforcement, and the effect of fibers on bond. It also requires an understanding of the dissertation *Hooked Bar Anchorages and their Use in Noncontact Lap Splices* (Coleman, 2024). This thesis will use some of the data from Coleman's research to compare results.

2.1.1 COLEMAN (2024)

For bridge construction in which splices between precast beams are used, traditional lap splices result in very large closure joints whose constructability negatively offsets the benefits of using precast concrete beams. To solve this issue, bridge engineers have been using hooked bar lap splices in place of straight bars, using the assumption that hooked bars would allow for shorter lengths of lap splices. The design codes which guide the design of lap splices are not sufficient to justify this substitution. Furthermore, there is limited experimental tests on the behavior of hooked bar lap splice. For this reason, Coleman tested 58 non-contact hooked bar lap splice beam-splice specimens to develop design guidance for the use of noncontact hooked bar lap splices to connect precast elements and address the knowledge gap(Coleman, 2024).

The specimens consisted of two precast beam elements where the longitudinal steel in the form of hooks protruded the designed lap length from the precast element. These precast elements were joined in a closure pour. See the experimental methods section of this thesis for more in depth descriptions of the specimens as this study followed the methods used in this dissertation(Coleman, 2024).

The specimens were subjected to a monotonic four-point loading and were designed to fail in a mode related to anchorage to study splice behavior. For the 58 beams, a variety of parameters were studied to reflect geometric configurations and material properties expected in bridge construction. The variables studied were: presence of multiple layers of reinforcement, spacing of spliced bars, bar size, bundling of spliced bars, presence and detailing of confining reinforcement, hook shape (standard 90° and 180° hooks or U-bars), depth of beams, interlocking lacer bars, depth of fresh concrete below the spliced bars, concrete compressive strength, splice length, steel fiber reinforcement in the concrete, and concrete cover(Coleman, 2024).

Nonlinear finite element models were developed to investigate beam depth, number of lapped bars, and the tail length. These models predicted failures by 3% of the experimental strengths..

In addition to studying the behavior of non-contact hooked bar lap splices, a descriptive equation and design recommendations were made for using non-contact hooked bar lap splices in precast bridge construction (Coleman, 2024).

The key findings of this study are as follows:

1.) Over 50% of United States departments of transportation have used hooked bar lap splices. (Coleman, 2024)

2.) Two failure modes were found that differ from the typical bond and anchorage failure modes for non-contact hooked bar lap splices without transverse reinforcement. The primary failure mode was found to be hook side bulging, and hook prying was a secondary failure mode. Both failure modes are related to the resistance mechanism. For this reason, the splices can be represented by a three-dimensional space truss. (Coleman, 2024)

3.) Noncontact hooked bar lap splices with transverse reinforcement had improved anchorage strength and toughness due to the transverse reinforcement carrying tension forces. The Transverse Reinforcement within the edge pair of hooks was most highly stressed because it resists the compression forces which pushes the edge hooks outwards. These splices fail in either concrete crushing within the radius of the hooks or side face blowout. (Coleman, 2024).

4.) Splice strength increases with an increase in concrete cover, concrete compressive strength, or increase in concrete cover. Splice strength decreased with an increase in splice spacing or the bar size of the hooks.(Coleman, 2024).

5.) Splices with the addition of a 1% fiber volume fraction had substantial increases in splice strength. (Coleman, 2024).

8.) Existing codes do not have an equation that accurately describes the influence parameters used in bridge design which affect splice strength of hooked bar lap splices (Coleman, 2024).

10.) A descriptive equation for the splice strength of non-contact hooked bar lap splices. From the descriptive equation, a design equation was developed for the minimum lap length for hooked bars. (Coleman, 2024).

DESCRIPTIVE AND DESIGN EQUATION

One of the goals of this study is to validate an equation developed by Coleman (2024) that predicts the bar stress of hooked bar lap splices. This equation is given by Eq. 1.

$$f_s^p = \frac{5.55 l_s^{0.67} f_{cm}^{0.33} \left(\frac{(0.1 c_{so} + 0.7 c_b)}{d_b} + K_{tr} \right)^{0.22}}{s_l^{0.033} d_b^{1.00}} \quad \text{Eq.1}$$

where:

f_s^p = is the predicted strength of a hooked bar lap splice

K_{tr} = $6.5 N A_{trl}$

N = the number of legs of transverse reinforcement within one outer bend diameter from the top of the lapped bars, towards the hook tails

A_{tr1} = the area of one leg of transverse reinforcement.
c_{so} = side cover

c_b = bottom cover

d_b = the diameter of the longitudinal reinforcing steel

s_l = distance between lap splices

l_s = the splice length

For this project, transverse reinforcement perpendicular to the lead ends of the hooks are the only reinforcement considered. An example calculation to determine the number of transverse reinforcement legs to consider in the is shown in figure 3-7. The vertical legs of the ties are not effective, and there are four ties with one leg transverse to the lapped hooks, therefore N = 4 and $K_{tr} = 26A_{tr1}$.

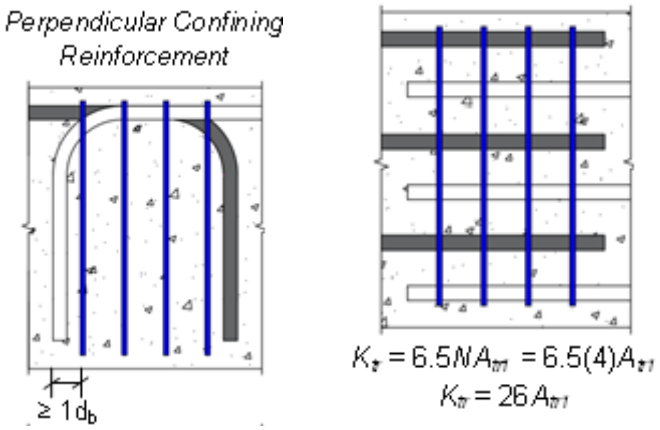

Figure 2-1: Example calculation to determine the number of transverse reinforcement legs N to include in the K_{tr} equation (Coleman, 2024)

For additional arrangements and the methods used for developing the descriptive equation, see Hooked Bar Anchorages and their Use in Noncontact Lap Splices by Coleman (2024).

To simplify Eq1. and provide a design equation, the cover term was replaced with the minimum cover which yielded the new descriptive equation

$$f_s^p = \frac{5.4 l_s^{0.67} f_{cm}^{0.33} \left(\frac{c_{min}}{d_b} + K_{tr}\right)^{0.22}}{s_l^{0.033} d_b^{1.00}} \quad \text{Eq. 2}$$

Then, the descriptive equation was multiplied by the strength reduction factor (0.75) and splice strength was replaced by the yield strength to determine the minimum required splice length of hooked bars.

$$f_y = \frac{(0.75)5.4 l_s^{0.67} f_{cm}^{0.33} \left(\frac{c_{min}}{d_b} + K_{tr}\right)^{0.22}}{s_l^{0.033} d_b^{1.00}} \quad \text{Eq. 3}$$

Finally, the resulting equation was rearranged to solve for the minimum required splice length.

$$l_s = \left(\frac{f_y^{1.5} s_l^{0.05}}{8\sqrt{f_{cm}} \left(\frac{c_{min}}{d_b} + K_{tr} \right)^{0.33}} \right) d_b^{1.5} \quad \text{Eq. 4}$$

The restrictions and limitations of these equations are based on the construction parameters used in the experimental testing from which the equation was developed. Based on this, the design equation can be used when used for beams that have a lap splice with spacings not exceeding 6 in and one-half of the splice length. The design equation is suitable for splices no larger than No. 11 bars. The upper limit on spacing was capped at 6 in. since minimal tests were conducted on specimens with a spacing greater than 6 in. The maximum compressive strength tested was 6 ksi, and thus compressive strengths should not exceed 6 ksi concrete (Coleman,2024).

The design equation is suitable for No. 9 bars or smaller with Grade 80 or lower reinforcing steel, or No. 10 and No. 11 bars with grade 60 or lower reinforcing steel. Since higher levels of confinement were not studied, the ($K_{tr} + c_{min}/d_b$) term may not exceed 8.0. (Coleman, 2024).

The design equation can be applied to top-cast and bundled cast bars without having to increase the required splice length. Furthermore, it is important to note that the bar diameter for bundled bars should not be the diameter of individual bars comprising a bundle, but that the bar diameter should reflect an equivalent bar having the same cross-sectional area of the bundle (Coleman, 2024).

The design equation should not be used in for multiple layers of hooked reinforcement (Coleman, 2024).

The design provisions developed were based solely on monotonically loaded elements. Therefore, to understand the effects of fatigue and reverse cycling, more tests should be conducted (Coleman, 2024).

The descriptive equation developed in this dissertation will be used in the results and discussion section of this thesis.

NEED FOR RESEARCH

With the new failure mode found in this research, it is important to understand if the number of spliced bars and the placement of transverse reinforcement will have an impact on the splice strength developed. Furthermore, given the popularity of using steel fibers and the promise of steel fibers on improving splice strength in this study, this should be further studied to determine the effects of fibers on non-contact lap splices and to determine if the equation could be modified to account for the impact of fibers. For this reason, a test matrix of 16 beams investigating these variables were developed by Coleman, and this test matrix will be the basis of this thesis. The work of this thesis was done in collaboration with the work of Coleman's dissertation. Thus, data, equations, and findings of this dissertation are referenced throughout this thesis.

2.2 NUMBER OF SPLICES

2.2.1 CANBAY AND FROSH (2006)

To simplify the equations for development and splices of reinforcement in ACI 318 - 05, Canbay and Frosh analyzed 203 unconfined and 278 confined beams. The splices were subjected to constant moment. (Canbay Erdem & Frosch Robert, 2006).

One of the variables in this study was the number of spliced bars. The number of bars spliced were three, four, and fiber bars. The reason this was studied is because the new expression would consider the number of spliced bars, where this was deemed a parameter to consider for side splitting failure. (Canbay Erdem & Frosch Robert, 2006).

These tests found that as the weighted average of the cover dimension decreased by increasing the number of bars. The decrease in the cover dimension results in an increase in the minimum required splice length. As the number of bars increase, the increase in required splice length drops. Which means that the increase from four to five bars was greater than the increase from five to six bars. (Canbay Erdem & Frosch Robert, 2006).

For a comparison of experiment vs practice, the authors acknowledged that while the number of bars does affect splice length, increasing the number of bars does not change the splice length significantly, and for the development equation developed four spliced bars were considered. (Canbay Erdem & Frosch Robert, 2006)

NEED FOR RESEARCH

There seems to be little research on the impacts of the number of splices on development length. This seems to be consistent with the findings of the study by Canbay and Frosh. That though there is a small effect from the number of bars for the side-splitting failure modes, that this impact is very small and decreases as the number of bars increases.

In the study motivating this research by Coleman (2024) the failure mode hook side bulging was found. Coleman (2024)found that if the capacity of the tension tie transverse to the bars is less than the demand of the hooks, the cover of the concrete will fracture and the hook ends will fracture outwards.

This indicates that the side effect is more significant in hooked bars than with straight bars. Thus, where traditional development equations ignore the effect of the number of spliced bars on development length due to its small impact, this project hypothesizes that the side effect could be significant enough to include the number of bars in the development equation for non-contact hooked bar lap splices.

Additionally, (Coleman, 2024) found that in non-contact hooked bar lap splices, the outer hooks carry less tension force than the inner bars. This effect is shown in Figure 2-1. This study anticipates that as the number of splices increases, this effect will decrease.

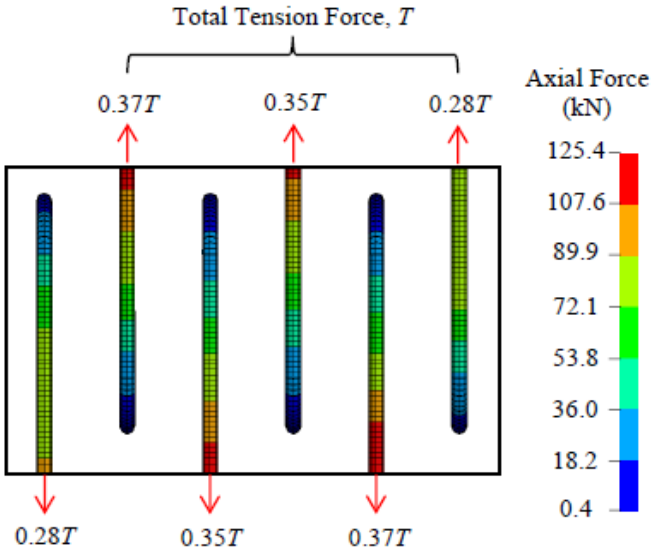

Figure 2-2: Distribution of Axial Forces at Peak Capacity of Showing that Edge Hooks Carry Less Force than Interior Hooks (Coleman, 2024)

2.3 TRANSVERSE REINFORCEMENT

2.3.1 MARQUES AND JIRSA (1975)

Marques and Jirsa (1975) noticed that provisions for hooked bar anchorage design in the ACI 318-71 were not well documented. For this reason, this study aimed to evaluate the capacity of anchored beam reinforcement subjected to the effect of confinement. For this study, 22 specimens were tested simulating a typical exterior beam-column joint, where embedded hooks were used (Marques & Jirsa, 1975).

The effects of axial load, vertical column reinforcement, side concrete cover, and lateral reinforcement through the joint on the performance of standard hooked bars were studied (Marques & Jirsa, 1975).

Variables considered were size of anchorage bars, hook geometry, lead embedment length, confinement, and column axial load. The test studies No. 7 or No. 11 bars using standard 90- or 180-degree hooks conforming to ACI 318-71 specifications. All reinforcement was grade 60 with yield strengths ranging from 64 to 68 ksi. By varying the size of the column, the lead embedment length was varied. The anchored lengths were short to ensure that bond failure would occur before steel yielded. Three types of confinement were considered: longitudinal column bars, column ties through the joint, and concrete cover (Marques & Jirsa, 1975).

The tests were conducted using a loading frame to apply axial loads to the column. The tests were terminated when one of the anchored bars pulled out of the column. Data gathered included lead bar stress, slip, and stress along bar (Marques & Jirsa, 1975).

The key findings of this study are as follows:

1.) As transverse reinforcement confining the hooks is increased. The bond strength increases. Standard hooks embedded in concrete achieved stresses in excess of yield. (Marques & Jirsa, 1975).

2.) Much higher stresses are achievable than were permitted by codes available at the time. To allow for higher stresses, the minimum straight embedment lengths before the hook are required, especially for larger bar sizes. (Marques & Jirsa, 1975)

The results of the study indicate that the location of column bars had little influence, but with ties throughout the joint the stress at failure reached yield in all cases. The results indicated that closely spaced ties are especially beneficial in the case of large, anchored bars (Marques & Jirsa, 1975).

2.3.2 MCLEAN AND SMITH (1997)

Mclean and Smith (1997) found that the existing code provisions for non-contact splices were limited. The code provisions at the time permitted noncontact lap splices provided two requirements were met: the bars could not be spaced farther apart than the smaller of one fifth the splice length or 6 in. and the yielding of the reinforcement was prohibited or discouraged. These requirements were typically violated with column-shaft connections. For this reason, Mclean and Smith investigated the behavior of noncontact reinforcing splices typical of those that would be used for connections between large diameter shafts and smaller diameter columns in bridges (McLean David & Smith Carol, 1997).

Fifteen full scale panel specimens representing a cross-section of a column shaft connection, and one 2 ¼ scale column shaft specimens were tested under monotonic and cyclic loading to understand noncontact lap splice behaviors in bridge column shaft connections (McLean David & Smith Carol, 1997).

The variables investigated in this study were lap splice length, lapped bar spacing, and spacing of transverse reinforcement. The offset spacings of 6, 9, 12, and 15 in. were used. The transverse bars were No. 3 bars with hooks at each end and a measured yield strength of 70 ksi. Specimen performance was evaluated in terms of load capacity, failure mechanism, and strength degradation (McLean David & Smith Carol, 1997).

The results of the study indicated that with smaller offset distances for the non-contact splices, the contribution from the transverse reinforcement is small. Conversely, with larger offset distances the transverse bars are more heavily loaded and more critical to the successful performance of the splice (McLean David & Smith Carol, 1997).

The key findings of this study are as follows.

1) Regardless of splice length, specimens without transverse reinforcement failed due to brittle tensile cracking of the concrete. For this reason, the authors

concluded that transverse reinforcement was necessary (McLean David & Smith Carol, 1997).

2) The truss analogy can be used to model the observed behavior of non-contact lap splices (McLean David & Smith Carol, 1997)

3) Larger offset spacing of the transverse reinforcement resulted in increased number and extent of cracks. (McLean David & Smith Carol, 1997)

NEED FOR RESEARCH

Both studies indicate that transverse reinforcement plays a significant role in both hooked bars and non-contact bars. The study by Coleman (2024) included some research on transverse reinforcement in the closure joint of beams using non-contact hooked bar lap splices. This study indicated that there are improvements in the bond strength when using transverse reinforcement in the closure joint and found that using stirrups perpendicular to the hooks was most beneficial. Between these studies, there is a gap on if the placement of reinforcement for a non-contact hooked bar lap splice has an impact on bond. For this reason, this study will investigate the placement of stirrups perpendicular to the longitudinal bars.

2.4 EFFECT OF FIBERS ON BOND

2.4.1 BACKGROUND ON FIBERS

It is known that concrete is very brittle and will crack due to tensile stress. To address this problem, Engineers use reinforcement typically in the form of steel reinforcing bars in the concrete where tension is expected. The use of reinforcing bars carries the tensile stress of the concrete to the steel, which is strong in tension. Similarly, steel fibers in concrete also act to carry tensile stress after concrete cracking. The key difference between steel fibers and reinforcing bars or a steel mesh, is that steel fibers are mixed into the concrete, and are a part of the concrete matrix forming a composite material. Thus, instead of providing strength at specific locations, steel fibers form a reinforcing network throughout the entire composite material.

Since it’s introduction 40 years ago, the use of steel fibers has gained popularity for several reasons: it increases overall ductility, controls cracks more efficiently than traditional reinforcement, and absorbs tensile stresses in any direction.

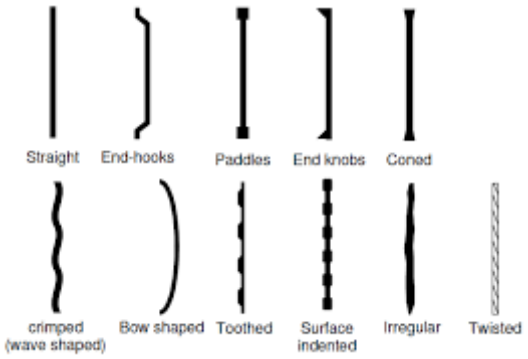

Figure 2-3 : Fiber types (Altera et al., 2021)

As seen in Figure 2-2, steel fibers can come in many different shapes and sizes. The different shapes have different impacts on bond, and therefore the amount of stress the fibers can hold. For this project, steel fibers with end-hooks were used, which are the most used fibers today. Parameters affecting bond behavior are fiber reinforcing index $\left({}^{L}/_{d_f}\right)$, and fiber volume fraction $\left({}^{V_f}/_{V}\right)$. The fiber reinforcing index is defined as the length of the fiber (L) over the diameter of the fiber (d_f), and the fiber volume fraction is defined as the volume of fibers(V_f) over the total volume of the concrete (V).

How steel fibers work is as follows: when a crack occurs, the hooked ends anchored on each side of the crack act as a medium for stress transfer. When the maximum bond strength of the fiber is reached, the fiber pulls out of the concrete adjacent to the crack. After pull out of one fiber, the next fiber will begin carrying the tensile forces, which inhibits the growth of cracks. This is demonstrated in Figure 2-3.

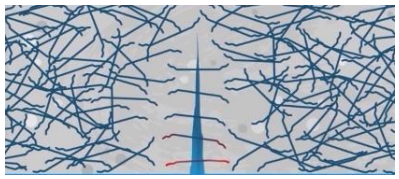

Figure 2-4: Fiber Bridging Crack Visual (Bekaert, 2018)

2.4.2 HARAJILI AND SALLOUKH (1997)

At the time of this paper, there were relatively few experimental studies on the bond characteristics of reinforcing bars embedded in fiber reinforced concrete. Additionally, none of the studies focused on development splice strength using actual beams. To assess the effect of fibers on development and splice strength of reinforcing bars in tension Harajili and Salloukh tested 15 full-scale beam specimens with spliced reinforcement at midspan. These beams were loaded in positive bending with constant moment along the splice region. Variables tested were: bar diameter (No. 5, No. 6, No. 8), fiber type (steel hooked fibers and polypropylene fibers) , fiber volume fraction (2%,1.2%,.45%,.6%), and fiber reinforcing index(60,100,150) (Harajli & Salloukh, 1997).

The beam specimens were designed such that splitting failure would occur at the midspan of the beams. Furthermore, transverse reinforcement was not used in the spliced region (Harajli & Salloukh, 1997).

The key findings of the study are as follows:

1.) Adding steel fibers with up to a 2% volume fraction increased splice strength by up to 55% (Harajli & Salloukh, 1997).

2.) Compared to ordinary transverse reinforcement, steel fibers were more effective in increasing splice strength (Harajli & Salloukh, 1997).

3.) Steel fibers increased the number of cracks, but decreased the growth of cracks. For this reason there was improvement from ordinary transverse reinforcement in the ductility of bodn failure. The descent in load deflection was more gradual in steel fiber beams when compared to plain concrete (Harajli & Salloukh, 1997).

4.) As volume fraction of fibers increases, the bond strength ration increases (Harajli & Salloukh, 1997).

Findings 3 and 4 are captured in Figure 2.3, in which case the final script of the name indicates the percentage of fibers or C for normal concrete. Ignore beam B15-8-P-150-.6 as this beam uses polypropylene fibers.

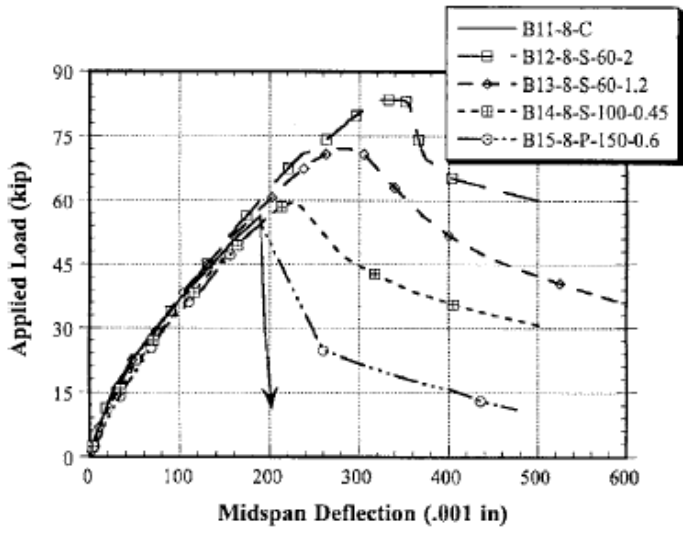

Figure 2-5: Load Deflection Plot at Different Fiber Volume Fractions (Harajli & Salloukh, 1997)

2.4.3 HAMAD(2001)

To understand the effect of steel fiber reinforcement on the bond strength and ductility mode of failure of tension lap splices anchored in HSC test specimens, Hamad et al. (2001) tested 12 full-scale HSC beams designed with bars spliced in a constant moment region at midspan. Variables tested were bar sizes of No. 6, No. 8, and No. 10 bars, and the volume fraction of steel fibers

added in the spliced region, with values .5, 1, or 2%. No transverse reinforcement was used in the spliced region to evaluate the influence of fibers. Beam width was 9.45 in. in all beams tested, and the splice length was 12 in. for all beams tested. Non-air entrained concrete mixtures were designed to provide a nominal 28-day compressive strength of 10,000 psi. Beams were tested in constant positive moment in the middle of the beam specimens (Hamad Bilal et al., 2001).

The key findings of the study were as follows:

1.) Beams with no fibers in the splice region failed in brittle face-and-side splitting modes of failure. As the fiber volume fraction increased, the failure mode was more ductile and gradual with the failure mode being splitting of concrete cover (Hamad Bilal et al., 2001).

2.) As the fiber volume fraction of steel fibers increased, the crack width for a given steel stress decreased. The quantity of cracks increased with increased volume fraction of fibers (Hamad Bilal et al., 2001).

3.) The presence of fibers did not affect the flexural cracking load (Hamad Bilal et al., 2001).

4.) There was a consistent increase in the average bond strength as the fiber content was increased. (Hamad Bilal et al., 2001)

5.) The increase in average splitting bond resistance due to the addition of steel fiberss was substantially higher than increases reported in technical literature using pullout specimens with short embedment lengths (Hamad Bilal et al., 2001).

2.4.4 HAMAD (2011)

To understand the influence of steel fibers distributed in concrete on bond performance and the ductility failure mode of hooked bars anchored in normal strength concrete (NSC), Hamad et al. (2011) tested 12 full-scale beam column type specimens. Variables tested included beam bar size [No. 5, No. 8, or No. 11]. Grade 60 reinforcing bars were used for all tests. Transverse reinforcement was placed in all elements except within the beam-column anchorage zone. This was done to examination of the confining effect of steel fibers. The steel fibers used had hooked ends and an aspect ratio L/d_f of 30/0.55 = 55. The test used the strong floor reaction wall testing facility to assess the effect of steel fibers. This method of loading was used to simulate the fixed-end reaction conditions of a beam column joint (Hamad, 2011).

The key findings of this research are as follows:

1.) The failure mode was side splitting of the concrete cover perpendicular to the hooks and side splitting of the cover where flexural cracks were initiated in the tension corner zone of the beam-column joint.(Hamad, 2011)

2.) For all bar sizes tested, the addition of steel fibers in the concrete mixture led to an increase in peak load of the specimen, an increase in the corresponding steel

stress, and an increase in the ductility of the load-deflection curves. 1.0% fibers reached the highest maximum or peak load, and the best improvements in ductility were achieved with 1.0 and 1.5% volume of fraction fibers. (Hamad, 2011)

2.4.5 METELLI ET. ALL (2017)

To understand the effects of using steel fibers in lapped bars within concrete joints, Metelli et all conducted two series of tests. One series of four beams with three longitudinal bars with diameter d_b of 0.787 in. In this series the fiber volume fraction was equal to 1%. The fiber reinforced concrete (FRC) beams were tested with one or all 3 bars lapped, varying the percentage of bars lapped, corresponding to 33% or 100% of bars lapped. In another series, six beams with four reinforcing bars with a diameter of .63 in. were tested. In these beams the fiber volume fraction was 0.9%. The FRC specimens were made with one bar, two bars, or four bars lapped, corresponding to a percentage of bars laped of 25%, 50%, or 100%. Transverse reinforcement consisted of two stirrups with a diameter of .394 in. and .315 in. provided for each pair of .787 in. and .623 in. lapped bars respectively. The stirrups were spaced evenly along the lap length with the distance to the first link to the end of the lap splice shorter than 1.969 in. These stirrups were designed to comply with Model Code 2010 provisions. Hooked-end steel fibers ($L_f = 35$ mm, $d_f = 0.75$ mm) with a tensile strength of 174 ksi used with a volume fraction of 0.5% were used. The ten beams were tested with a span of 157.48 in. under four-point bending with a constant moment region of 78.74 in. (Metelli et al., 2017).

The key findings were as follows:

1.) The addition of fibers significantly improved lap strength when all bars were spliced. (Metelli et al., 2017).

2.) No weakening effect was observed in the part of the fiber reinforced concrete where the bars were lapped. (Metelli et al., 2017)

3.) Fiber reinforced concrete has higher post cracking resistance than normal concrete, thus the brittleness of the joints with FRC was reduced. (Metelli et al., 2017)

4.) The lap length may be reduced for FRC joints. (Metelli et al., 2017)

NEED FOR RESEARCH

In all the studies provided in this literature review, it was found that using steel fibers increase bond strength, and that ductility was improved with the use of steel fibers. Harjili and Salloukh, found that steel fibers play a more effective role in increasing splice strength than ordinary transverse reinforcement. They found that adding steel fibers up to 2% by volume increased the development/ splice strength by up to 55%. The larger study by Coleman (2024) that the current study is a part of, aims to understand non-contact hooked bar lap splices. The studies from this literature review indicate that steel fibers could help further reduce the lap length for non-contact lap splices from what has already been found with the larger study.

The study by Harjili and Salloukh found that everything else being constant, the bond strength ratio increases as the volume fraction of fibers increases. Thus, this might be something that requires future research but is outside of the scope of this study.

2.5 SUMMARY

In summary, the preliminary study by Coleman (2024) saw a need for more investigations into the number of splices, placement of transverse reinforcement, and the effects of fibers on bond. The literature on number of splices was relatively limited, but due to the failure modes of hook side bulging and hook prying along with the difference in edge bar stress found in Coleman (2024) this variable is investigated in this study. From the literature and the study by Coleman (2024), an increase in bond strength was found in all cases using transverse reinforcement in the closure joint. Using stirrups perpendicular to the hooks was most beneficial. Thus, this study further investigates if the placement of perpendicular stirrups has an effect on bond. Lastly, in all of the studies using FRC, fibers increased bond strength. As this study aims to understand non-contact hooked bar lap splices, it is desirable to understand the effects on fibers and if the governing equations developed by Coleman (2024) may be modified to include a fiber term.

Chapter 3 EXPERIMENTAL PROGRAM

3.1 INTRODUCTION

This chapter introduces the test matrix, then describes the experimental procedure, the testing procedure, and details how material properties were obtained. Furthermore, it details how bar stress for the experimental tests were determined using sectional analysis.

3.2 TEST MATRIX

This study investigated three main parameters on the strength and behavior of noncontact hooked bar lap splices: (1) the placement of transverse reinforcement perpendicular to the spliced hooks, (2) the effect of the number of splices bars, and (3) the addition of steel fibers in the closure joint of the concrete. These were organized into three test series, as shown in Table 3-1. Table 3-1 will introduce each series and provide a short description of what each test series tested.

Table 3-2 shows the test matrix and specimen configuration for all beams in the test series. A total of fifteen beams were tested as a part of this study, while nine beams were included in the analysis but tested by Coleman. Beams in the test matrix under "Beams from Coleman (2024) are beams from the dissertation by (Coleman,2024) and will be noted with an (*) for the remainder of this thesis. The naming convention for the beams in this test matrix follows the naming convention in 3.2.1.

For all beams in this test matrix, the beam span was thirteen feet and beams were tested in 4-point bending.

As this is a part of a larger study sponsored by the Virginia Department of Transportation (VDOT), the naming convention for each series follows that of the project by (Coleman, 2024). The series numbers 1-3 and 5-11 have parameters that were investigated only by (Coleman, 2024). As (Coleman, 2024) also investigated transverse reinforcement, the series number is used in both projects.

This section will give a table defining each series number prior to the test matrix. Following the test Matrix, the beam naming convention will be defined, then how each series will be analyzed is discussed.

Table 3-1: Table Defining Series

Series No	Parameter Studied	Description
4	Transverse Reinforcement (Perpendicular)	Ties in the closure joint perpendicular to the leads of the hooks, varying placement, bar size, and quantity of reinforcement.
12	Number of Spliced Bars	Lap splices of three or four pairs of non-contact hooked bars, varying transverse reinforcement.
13	Steel Fibers in Closure	1% fiber dosage by volume, varying transverse reinforcement, cover, and splice spacing.

Table 3-2: Test Matrix

	Material Properties			*Splice Parameters*		*Cross Section and Cover Depth*				
Beam ID	f_{cm} (ksi)	f_y (ksi)	f_{yt} (ksi)	l_s (in)	s_l (in)	b (in)	h (in)	c_{so} (in)	c_b (in)	c_{si} (in)
Series to Investigate the Influence of Placement of Transverse Reinforcement										
4-#6-[S.Ends]	3.58	66.1	72.9	7.96	4.32	24.19	15.84	1.62	1.64	1.43
4-#6-[S.Ends&Mid]	3.11	66.1	72.9	7.88	4.67	24.25	15.81	1.45	1.45	1.88
4-#9-[S#4.4in. s_l]	3.58	61.6	60.6	12.38	3.96	24.28	23.25	1.85	1.64	1.33
4-#9-[S.Ends]	4.53	61.6	72.9	12.13	4.06	24.13	23.25	1.62	1.45	1.33
4-#11-[S#4.Ends&Mid]	3.51	66.4	60.6	17.06	4.18	16.69	27.94	1.67	1.74	1.09
4-#11-[S#4.4in.s_l]	4.37	66.4	60.6	17.25	4.45	16.69	28.06	1.55	1.71	.936
Series to Investigate the Influence of the Number of Splices										
12-#6-[4 splices]	3.11	66.1	-	10.59	4.44	32.0	15.75	1.57	1.56	-
12-#6-[S.4 splices]	4.37	66.1	-	7.84	3.82	31.88	15.75	1.84	1.96	-
12-#11-[S#4.3 splices]	5.04	66.4	60.6	17.04	4.01	24.25	28.25	1.51	2.00	5.114
Series to Investigate the Influence of Steel Fibers										
13-#6-[F.4 in. s_l]	4.98	66.1	-	6.15	3.93	24.13	15.88	1.77	1.68	1.63
13-#6-[S.F.4 in. s_l]	3.29	66.1	72.9	5.92	4.38	24.06	16.06	1.63	1.83	1.36
13-#9-[F.4 in. s_l]	3.29	61.6	-	9.67	3.93	24.25	23.25	1.89	1.56	1.33
13-#9-[S.F.4 in. s_l]	3.20	61.6	72.9	10.04	4.29	24.13	23.25	1.50	1.71	1.23
13-#9-[F.3in.c_b& c_{so}]	4.56	61.6	-	8.63	4.19	27.13	26.25	3.18	3.24	1.20
13-#9-[S.F.3in.c_b& c_{so}]	3.8	61.6	72.9	8.92	3.72	27.13	27.00	3.51	3.57	1.39
Beams from Coleman (2024)										
2-#6-[4 in. s_l]	3.5	66.1	-	11.29	4.00	24.00	15.67	1.74	1.42	-
2-#9-[4 in. s_l]	4.01	70.0	-	16.92	4.08	24.06	23.29	1.59	1.46	-
2-#11-[4 in. s_l]	3.65	66.8	-	21.44	4.11	16.63	27.69	1.55	1.43	-
4-#6-[S.4 in. s_l]	3.50	66.1	69.5	7.83	4.04	24.0	15.70	1.64	1.61	-
4-#9-[S.4 in. s_l]	4.01	70.0	69.5	11.92	4.05	24.0	23.23	1.45	1.44	-
9-#9-[3 in. c_b& c_{so}]	3.65	66.3	-	13.00	4.14	27.13	26.07	3.03	3.32	-
9-#9-[S. 3 in..c_b& c_{so}]	3.67	66.3	72.9	13.58	4.25	27.13	26.25	2.98	3.07	-
S13-#9-[F.6 in. sl]	3.55	66.3	-	11.88	6.17	34.25	23.40	1.46	1.62	-
S13-#11-[F.8 in. sl]	5.01	66.8	-	15.30	8.30	28.63	27.75	1.52	1.60	-

Definitions: f_{cm} = concrete compressive strength; f_y= yield strength of hooked bars; f_{yt}= yield strength of transverse reinforcement, l_s= splice length; b = beam width; h = beam height; c_{s0}=side cover; c_b= vertical cover; s_l= spacing of spliced bars.

A three-part naming convention is used to identify the beams. To demonstrate the naming convention, see beam S4-#6-[S.Ends]. The first part (S4) refers to the test series for the beam corresponding to the series descriptions in Table 3-1. The second part, (#6) refers to the bar size of the longitudinal steel (the lapped hooks), and the third part in brackets refers to the characteristic feature of the beam. The following bullet points describe the characteristic feature

in the bracket term [] of the naming convention:

- "4 in. s_l" refers to the offset spacing of the lap splice. For all beams, unless otherwise denoted using this notation, the offset spacing is 4 in. Thus, if this term does not exist, assume the offset spacing is 4 in.
- "F." indicates that a 1% dosage of steel fibers was used in the cast-in-place concrete. Thus, if this term does not exist, there are no fibers in the cast in place(CIP) concrete.
- "S." refers to the use of confining reinforcement transverse to the hook leads.
    - "S." refers to the use of No. 3 stirrups
    - "S.#4" refers to the use of No. 4 stirrups
    - "S.Ends" refers to the use of stirrups placed at $2d_b$ from either splice end
    - "S.Ends&Mid" refers to the use of stirrups placed at $2d_b$ from either splice end and one stirrup placed in the middle
    - If there is no Ends & Mid term in addition to the "S." term, stirrups are placed at $3d_b$ along the splice length.
    - If the "S." term does not exist, the closure joint is unconfined
- "3 in. c_b & c_{so}" refers to beams that have 3 in. of side and bottom cover as opposed to 1.5 in. used for all other beams
- "Splices" refers to beams that have a different number of splices than is typical for that bar size in the rest of the test matrix. Typical splice numbers are as follows: three splices for No. 6 and No. 9 beams, and two splices for No. 11 beams. Thus "4 splices" refers to beams that have four splices compared to the typical three for that bar size, and "3 splices" refer to beams that have three splices compared to the typical two for that bar size.

For the example S4-#6-[S.Ends]: the beam belongs to Series 4, has No. 6 bars for the longitudinal steel, and has No. 3 reinforcement tranverse to the hook leads placed at $2d_b$ from either spliced end.

Figure 3-1 demonstrates a typical specimen with transverse reinforcement perpendicular to the leads of the hooks.

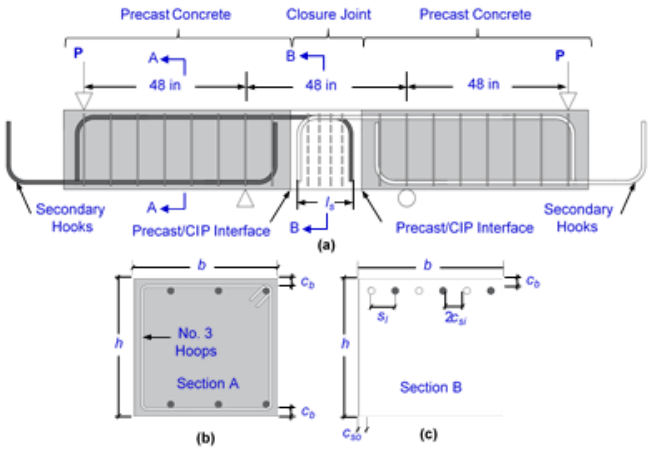

Figure 3-1: Typical Beam-Splice Specimen (a) Elevation View (b) Section through Shear Span, (Coleman, 2024)

3.2.2 SERIES STUDYING TRANSVERSE REINFORCEMENT

This series, with a series designation of 4, will investigate alternative placement of transverse reinforcement.

This series compares beams with different longitudinal bar sizes and varies positions of the transverse reinforcement. Figure 3-2 details the cross section for beams labeled [S.Ends] and [S.Ends&Mid].

For the analysis of the effects of varying reinforcement, beams with the same bar size but different reinforcement configurations will be compared. For the purpose of this thesis, only beams with transverse reinforcement perpendicular to the leads of the hooks are compared. The beams chosen, were beams with the same longitudinal bar size without confinement, or with transverse reinforcement perpendicular to the leads of the hooks spaced at $3d_b$. These comparisons are made as follows.

No. 6 beams: 2-#6-[4 in. s_l]*, 4-#6-[S.Ends], 4-#6-[S.Ends&Mid], 4-#6-[S.4 in. s_l]*

No. 9 beams: 2-#9-[4 in. s_l]*, 4-#9-[S.Ends], 4-#9-[S.4 in. s_l]*, 4-#9-[S#4.4in. s_l]

No. 11 beams: 2-#11-[4 in. s_l], 4-#11-[S#4.Ends&Mid], 4-#11-[S#4.4in.$\boldsymbol{s_l}$]

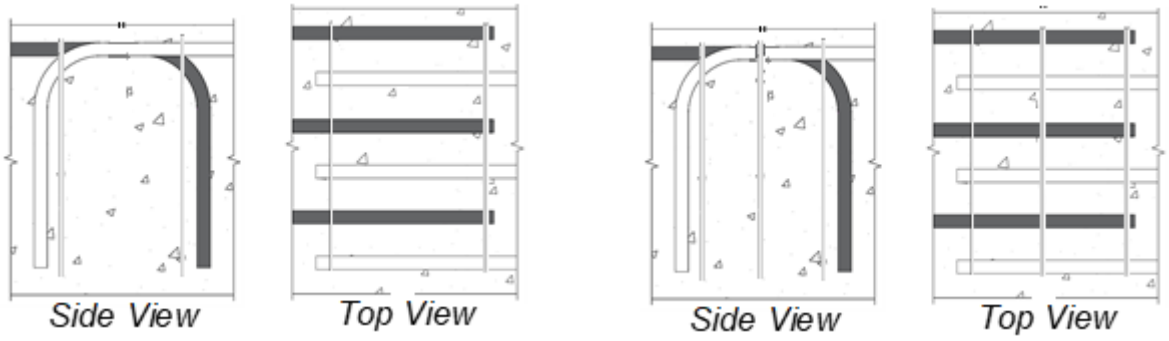

(a) [S.Ends] (b.) [S.Ends&Mid]

Figure 3-2: Cross-section for Transverse Reinforcing Arrangements

3.2.3 SERIES STUDYING THE NUMBER OF SPLICES

This series, with a series designation of 12, investigates the number of splices. For all beams from Coleman (2024), No. 6 beams had three splices and No. 11 beams had two splices.

For the analysis, this series compares beams with one additional splice pair to the beams from Coleman (2024). For No. 6 beams, beams with three splices with and without stirrups from Coleman (2024) are compared to beams with four splices with and without stirrups. For No. 11 beams, beams with two splices and perpendicular reinforcement are compared to beams with three splices and perpendicular reinforcement. These comparisons are made as follows:

No. 6 beams: 2-#6-[4 in. $\boldsymbol{s_l}$]*, 12-#6-[4 splices], 4-#6-[S.4 in. $\boldsymbol{s_l}$]*, 12-#6-[S.4 splices]

No. 11 beams: 4-#11-[S#4.4in.$\boldsymbol{s_l}$]**,** 12-#11-[S#4.3 splices]

3.2.4 SERIES STUDYING STEEL FIBERS IN CLOSURE

This series, with a series designation of 13, investigates steel fibers in the cast-in-place closure pour of the concrete. For the purpose of this study, fiber volume fraction is not studied, and the analysis and recommendations only apply to using a 1% dosage of fibers by volume.

This series investigates steel fibers with and without confinement, and steel fibers with 3 in. of cover with and without confinement

For the analysis, beams with similar configurations without fibers from Coleman (2024) were compared to beams with fibers from this test matrix. Additionally, the offset spacing of the splices were not part of the test matrix for this thesis. Coleman (2024) did two tests with 1% fiber dosage by volume varying offset spacing. For this, one beam with No. 9 longitudinal bars and 6 in. offset spacing was tested and one beam with No. 11 bars and 8 in. offset spacing was tested. Since these two beams were already analyzed by Coleman, the results from these beams are only used for the development of design recommendations using fibers. For understanding fibers in non-contact hooked bar lap splice closures, this beam and the corresponding beam without fibers from Coleman (2024) will be analyzed.

The comparisons for this series are as follows:

No. 6 beams: 2-#6-[4 in. $\boldsymbol{s_l}$]*, 13-#6-[F.4in. $\boldsymbol{s_l}$]**,** 4-#6-[S.4 in. $\boldsymbol{s_l}$]*, 13-#6-[S.F.4in. $\boldsymbol{s_l}$]

No. 9 beams: 2-#9-[4 in. s_l]*, 13-#9-[F.4in. $\boldsymbol{s_l}$], 4-#9-[S.4 in. s_l]*, 13-#9-[S.F.4in. $\boldsymbol{s_l}$]

No. 9 + 3 in. cover beams: 9-#9-[3 in. $\boldsymbol{c_b}$&$\boldsymbol{c_{so}}$]*, 13-#9-[F.3in.$\boldsymbol{c_b}$&$\boldsymbol{c_{so}}$], 9-#9-[S. 3 in..$\boldsymbol{c_b}$&$\boldsymbol{c_{so}}$],

13-#9-[S.F.3in.$\boldsymbol{c_b}$&$\boldsymbol{c_{so}}$]

No. 9 + 6 in offset of Splices: S4-#9-[F.6 in. sl]*, S2-#9-[F.6 in. sl]*

3.4 SPECIMEN FABRICATION

To emulate accelerated bridge construction, each specimen was composed of two precast segments with protruding 90° hooks set at the desired splice spacing in the precast concrete segments. The precast pieces were joined in a closure joint with cast-in-place concrete according to specifications which are detailed below to complete the beams.

3.4.1 CONSTRUCTION OF THE PRECAST SEGMENTS

The precast segments were designed with enough reinforcement so they would not fail in shear or flexure. They were also designed with hooks sticking out on both ends so that the beams could be cut after testing at the intersections of the closure pour. A new closure joint can then be cast for each set of precast segments, allowing for another test.

An example of the typical design of a beam is represented in figure 3-3.

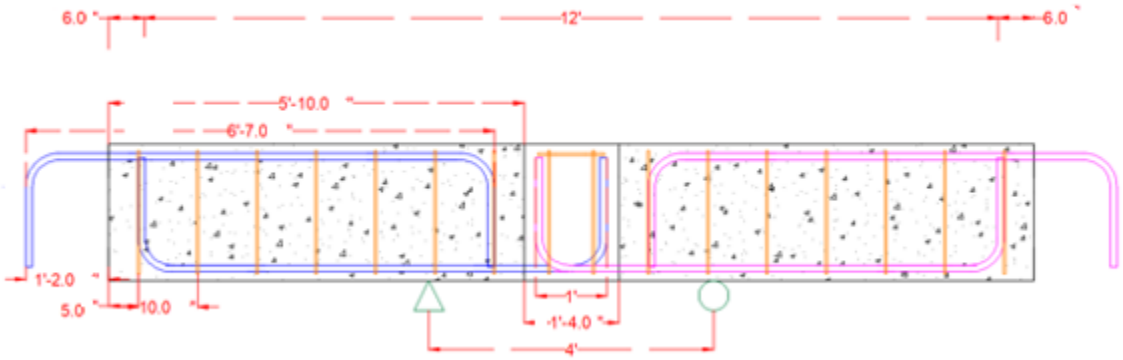

Figure 3-2 : Design for S4-#9-[S.Ends]

To construct the precast segments, the pieces were built on platforms constructed with six 2x4s cut to the width of the plywood and evenly spaced along the length.

Wood side forms were built to the height specified for the beam and a length greater than the specified length to allow for the formwork to be reused for different beam dimensions. The end caps had a removable piece such that the longitudinal hooks may be placed inside the beam.

The formwork was assembled by placing the end caps at the required length of the beam and screwing them into the platform. Then, the wood was lined with plastic for easier demolding and to potentially reuse the formwork when possible.

The hooks were placed into the beam, and the stirrups were moved approximately into place.

Figure 3-3 : Precast Construction

The hooks were then positioned such that the length of the hooks protruding from the precast segment had 2 in. of cover plus the splice length specified. Using tape, the hooks were fixed in place so they would remain vertical.

The stirrups were moved to the locations specified in the design and affixed to the reinforcing bars using ties. Then, two pieces of PVC pipe were placed in the beam as shown in Figure 3-3, to allow for the transport of the beams after the concrete has cured. The PVC allows for two pieces of reinforcing bars to be put through the beam that lifting straps could then be attached to.

Lastly, any gaps in the formwork are filled with caulk or spray-foam.

Then each set of formworks was cast with concrete and vibrated. 4”x8” and 6”x12” cylinders were cast using this concrete to test compressive strengths and tensile strength of the precast segments over various points in the construction and testing process.

See Figure 3-3 for an example of a precast concrete piece prior to the concrete pour.

3.4.2 CONSTRUCTION OF THE CLOSURE JOINT

After the precast pieces were allowed to cure to a minimum compressive strength of 4000 psi, they were demolded.

From there, if stirrups were required, they were placed under the hooks of one of the precast pieces. The crane is used to move the precast pieces together such that the splice length is within ¼ in. of the specified splice length, and the precast pieces were aligned. The stirrups were then moved to the locations specified in the closure and tied using a reinforcing bar gun.

Lastly, the formwork siding, as shown in Figure 3-4, was painted with form grease for easy removal and screwed into the building platforms. It was then reinforced with two clamps, and 2x4s connecting the two pieces of siding, and reinforcing the bottom of the form to prevent blowout during placement.

Figure 3-4: Closure Construction

For the beams that required steel fibers, the concrete was mixed with a dosage of 1% steel fibers by volume and then cast into the closure joint and vibrated. Separate 4”x8” and 6”x12” cylinders were cast using this concrete to test compressive strengths during construction and testing.

Concrete is cast into the closure and vibrated. 4”x8” and 6”x12” cylinders were cast to test compressive strengths and tensile strengths at various points in the construction and testing process.

The mixture properties for the cast in place concrete and the precast concrete were the same and are shown in Table 3-1.

Table 3-3: Concrete Mixture Properties

Material	**Weight (SSD) (lb/yd^3)**
Water	269
Type I Cement	445
Fly Ash	148
Coarse Aggregate #68	1,768
Natural Sand	638
Manmade Sand	679
Admixture	**Dosage (oz/cwt)**
Air-Entrainment	0.25
High Range Water Reducer	3.30

3.5 TESTING PROCEDURE

This section presents the testing setup and procedures during testing. Figure 3-6 demonstrates the test setup for a test specimen.

Figure 3-5: Test Setup

3.5.1 TESTING PREPERATION

Once the compressive strength of the closure joint reached approximately 3500 psi, the closure joints were demolded. Since the closure joints are cast with the hooks facing up and the beams are tested in negative bending, the beams needed to be flipped prior to testing. This is to ensure that the longitudinal steel would be in tension for the tests. The reason the beams are tested in negative bending, is so that the cracking around the reinforcement was visible at all points during testing.

To flip the beams, the crane and a forklift were used together, the beams were flipped so that the longitudinal steel was in tension for the tests. After this, the beams were painted to better see cracking, and the placement of the reinforcement was drawn onto the beam.

The beams were then loaded into the testing frame using the crane and placed such that the rams were 6 in. from the edge of the concrete on each side. Steel plates were stacked on either side of the beam such that the RAM's full extension would not be reached. A swivel head was placed on the steel plates to evenly distribute the load.

To capture cracking throughout the progression of the test, one camera was placed on each side of the closure joint. Another camera was placed above the closure joint.

To measure the deflections, string pots were attached at the mid-depth of the beam, 6 in. from the beam's edge at all four corners and at mid-depth of the beam in the closure joint. Load cells were

placed above each RAM to measure the load, and RTDAQ data acquisition tests were used for the duration of the tests.

3.5.2 TESTING

To begin each test, the rams are lowered to the point that they are touching the swivel head and a load of at least 400 lbs. is registered in the data acquisition system. The load is then zeroed through the data acquisition system.

The load is increased at intervals of 3 kips for No. 6 beams, 7 kips for No. 9 beams, and 10 kips for No. 11 beams. At each load increment, a loading placard is placed on each face of the closure in view of the camera, any visible cracks are traced with a sharpie and marked with the load, crack width is measured, and a picture is taken.

As peak load is approached -- indicated by the slope of the load deflection plot getting smaller – it is important to step away from the beam, as spalling and other failures could send concrete flying at individuals in the area. During this time stop marking cracks.

The load is increased until the load is at approximately half of the peak load. While still under this load, cracks are traced with a sharpie, and a final picture is taken. The load is then removed, the string pots, steel plates, and cameras are removed.

The beam is then removed from the test frame and sent to the back of the structures lab using the crane. Here, the closure joint is sawn out using a concrete saw and the two precast segments are brought back to the construction area where the second set of hooks are joined in a closure pour. After the flip side has been tested, the beam is disposed.

3.6 MATERIAL PROPERTIES

This section will detail how material properties were obtained.

To obtain the material properties of the transverse reinforcing steel and longitudinal steel, coupon tests were performed according to ASTM A370 and ASTM ASTM A615-16. The yield stress and the stress strain behavior of the reinforcing bars were determined using this standard.

To obtain the material properties of the concrete, splitting tensile and cylinder tests were performed in accordance with ASTM C469 The material properties obtained from these tests were the concrete compressive strength (f_{cm}) and the splitting tensile strength (f_{st}).

Additionally, the elastic modulus of concrete was found using ASTM C469/ C469M.

3.7 CALCULATIONS FOR BAR STRESS

3.7.1 BAR STRESS CALCULATION USING SECTIONAL ANALYSIS

The tensile strength of concrete was ignored in the analysis.

The stress-strain response of the steel reinforcement from coupon tests was used to calculate f_s, and the stress-strain response of concrete was modeled using the relationship produced by the Hognestad parabola.

To determine the steel stress of the longitudinal reinforcement using sectional analysis, the typical method to achieve this is as follows.

In a reinforced concrete section, the internal forces must balance the external loads. Thus, the total compressive force in the concrete must equal the tensile force in the steel. See figure 3-6 below, the compression in the concrete is labeled Cc and the tensile force of the steel is labeled T.

Next, the depth of the neutral axis, c, or the point where the concrete transitions from compression to zero stress. This value is iterated upon based on strain compatibility and equilibrium. Strain compatibility is determined by choosing a concrete strain value which is usually associated with concrete crushing, and using the strain profile of the steel to determine the steel strain with each iteration of c until equilibrium is reached. Then the steel stress is calculated from the value for the tension force that results in equilibrium using the equation $T = A_s * f_s$.

For the specimens in this test matrix, concrete strain is not a known value since the beams fail due to a bond failure. Since the peak moment at failure is known, this can be used to determine equilibrium for the point where the nominal moment capacity found using sectional analysis is equal to the experimental moment. Thus, the steel stress was found by iterating on the value of concrete strain and the neutral axis until the nominal moment capacity is equal to the experimental moment, and once equilibrium is achieved, the steel stress that caused failure is calculated from the value of T.

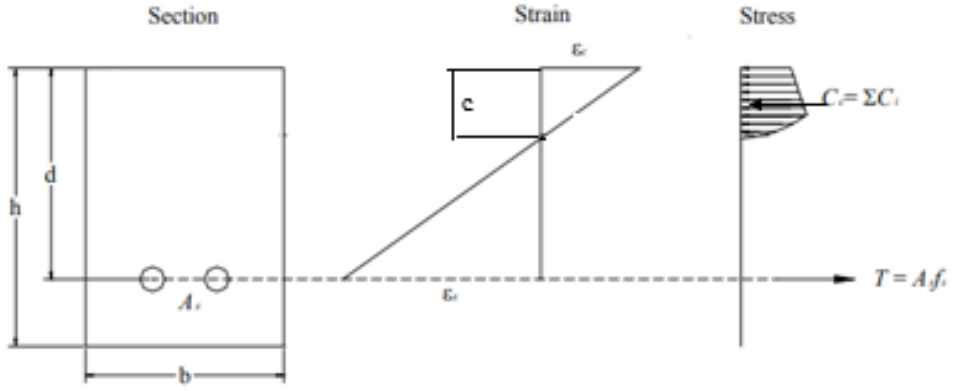

Figure 3-6: Sectional Analysis

Chapter 4 RESULTS AND DISCUSSION

4.1 INTRODUCTION

This chapter first details the overall cracking behavior for specimens whether they are confined or unconfined. From there, the results discussion is broken into sections by the parameter of interest. Each section discusses the moment deflection response and the normalized bar stress for beams from each series and the beams from Coleman (2024) which were compared to understand the influence of each parameter. Then each series was assessed for how well the descriptive equation predicted bar stress for that series. Since the descriptive equation underestimated bar stress by a substantial amount for all beams with the addition of 1% fiber volume fraction to the closure joint, a new term was developed for the equation to predict bar stress for a 1% fiber volume fraction of fibers to the closure joint.

As mentioned above, the bar stress developed was compared by normalizing the bar stress. The bar stress is normalized to be able to compare beams with similar conditions but without the influence of material properties or size parameters. The concrete strength (f_{cm}) and splice length (l_s) are typically normalized because of their contribution to bond strength. The equation used to normalize the bar stress was $f_s/(l_s^{0.67} f_{cm}^{0.33})$. This equation is frequently used in bond and anchorage studies and was developed based on empirical tests to normalize bar stress. The powers selected for this equation were verified by Coleman (2024).

Since Coleman (2024) did not verify that the normalized bar stress works when using steel fibers, Figure 4-1 and Figure 4-2 plot the splice length and the concrete compressive strength for beams with steel fibers to the test to predicted ratios using the descriptive equation from Coleman (2024). Since the lines for these values are horizontal, this equation treats the parameters of splice length and concrete compressive strength appropriately and the normalization can be used for beams with steel fibers.

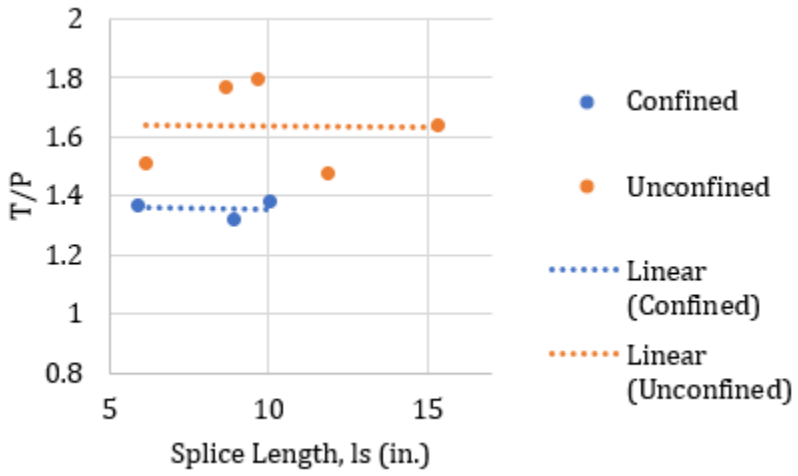

Figure 4-1: Splice length vs. test to predicted

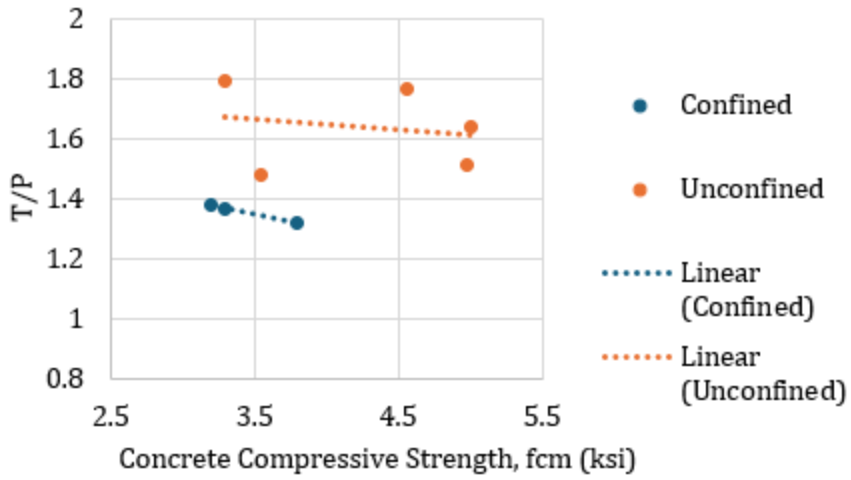

Figure 4-2: Concrete compressive strength vs. test to predicted

4.2 OVERALL BEHAVIOR

Figure 4-3 demonstrates the typical cracking behavior for an unconfined specimen in this test matrix. Not shown, at roughly 10% of the maximum loading cracks would begin to form along the interface and extend from the tension face to approximately 1/3 of the depth of the concrete and across the entire width. At approximately 50% of max loading, this depth of these cracks would increase to approximately ½ of the depth of the beam, and splitting cracks would begin to appear. For the example in Figure 4-3, splitting cracks occurred at 75% loading and are characterized by the cracks that run parallel to hooked bars over the bar. At 75% loading shown in Figure 4-3 (b) a flexural crack would appear splitting the beam down the middle. Then at failure for an unconfined specimen, cracks would spiderweb from the flexural crack in all directions, and diagonal cracks would propagate on the side of the closure from the radius of the edge hook to the tail end of the inner hook. All unconfined beams in this test matrix failed according to hook prying or hook side bulging consistent with the findings from Coleman (2024).

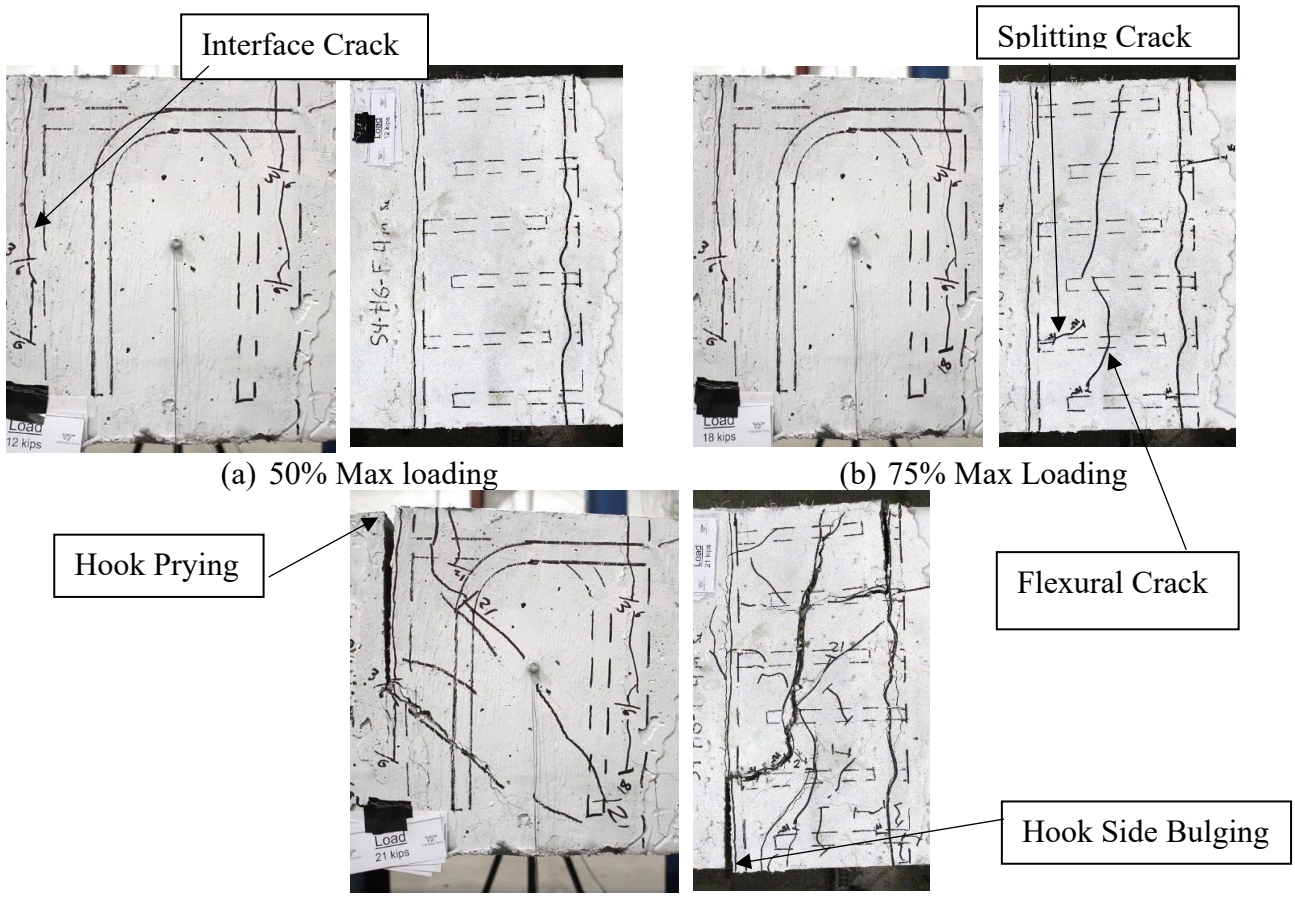

Figure 4-3: Crack Progression for an Unconfined Beam

Figure 4-4 demonstrates the typical cracking behavior for a confined specimen in this test matrix. At 10-20% of peak load, the interface crack would appear extending to approximately 1/3 or ½ of the overall depth. Then, at approximately 40% peak load splitting cracks would appear. At roughly 50% of peak load, as shown in Figure 4-4(a), a flexural crack down the middle of the top face of the closure pour would appear. At 75% of peak load, as shown in figure 4-4(b), diagonal cracks would appear on the top of the closure pour, and diagonal cracks would appear from the radius of the hooks propagating diagonally to the inside hook. At failure, the flexural crack would widen significantly, and the quantity of cracks would increase dramatically on the side faces of the concrete. Failures for confined specimens were driven by concrete crushing in the radius of the hooks or side face blow-out consistent with the findings of Coleman (2024). See Appendix A for the crack progression for all beams in this test matrix.

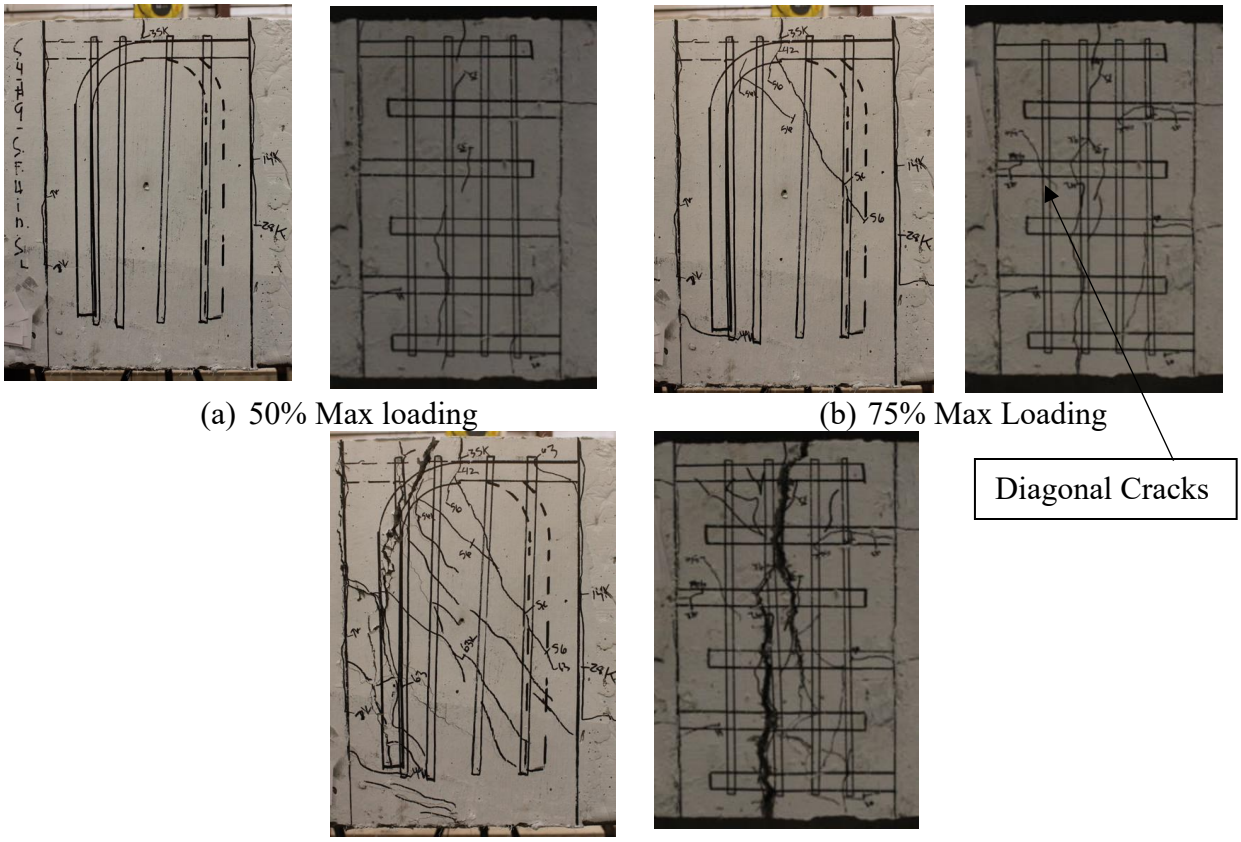

(a) 50% Max loading (b) 75% Max Loading

(c) At Failure

Figure 4-4: Crack Progression for a confined beam

The only beams which were outliers to this crack progression were those which had transverse reinforcement configurations [S.Ends]. For these beams, the crack progression and failure mode matched those for beams that were unconfined.

4.3 NUMBER OF SPLICES

4.3.1 QUALITATIVE DISCUSSION OF PARAMETER

Figures 4-5 and 4-6 provide a comparison of the moment-deflection behavior at the midspan of beams constructed with one more hooked bar lap splice pair for No. 6 and No. 11 reinforcing bars. These figures also compare this parameter with the addition of transverse reinforcing steel.

The overall flexural behavior can be characterized as follows: In the elastic range of the moment-deflection plots, the beams with one extra lap-splice demonstrate a greater stiffness than beams with fewer lap splices. This is because the amount of reinforcement increased, enhancing the overall stiffness of the material closure joint. Furthermore, the beams with more splices achieved a higher max moment than those without, and beams that had more transverse steel in combination with more longitudinal steel demonstrated a more ductile response.

In straight bar lap splices, the number of spliced bars does not have a substantial effect on bar stress and is therefore not factored into the development length equation. In figures 4-5 and 4-6 b, the bar stress developed independent of the number of splices. These findings corroborate with

the findings of the analytical study by Coleman (2024), which found that interior bars carry greater axial force than edge bars. For this reason, increasing interior bars increases splice strength, however this increase is relatively small and increasing the number of bars was found to improve the bar stress in the analytical study, thus since all experimental tests used a relatively small amount of splices the equation is expected to be conservative for this parameter in design.

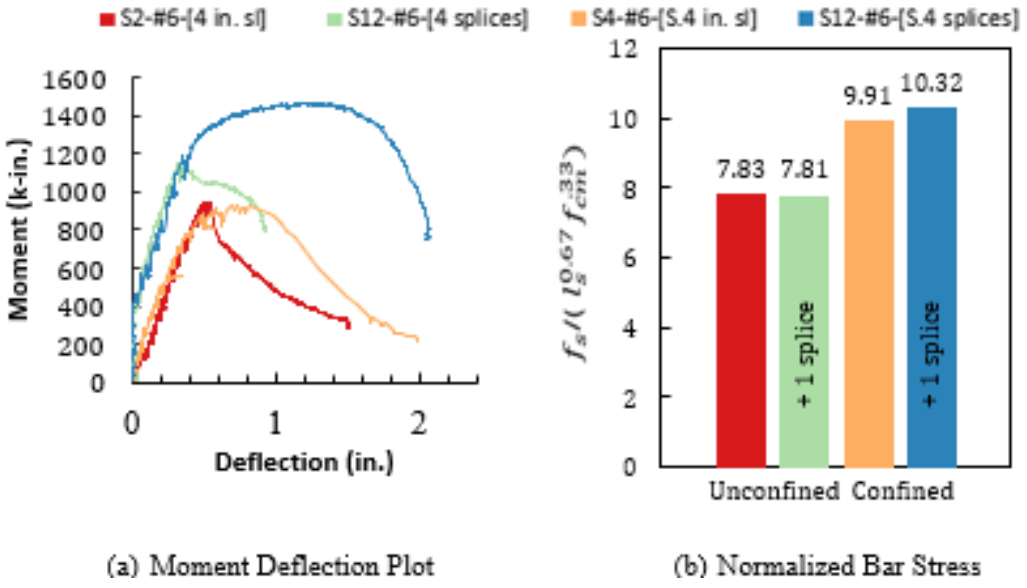

Figure 4-5: No. 6 Comparison Plots for Number of Splices Series

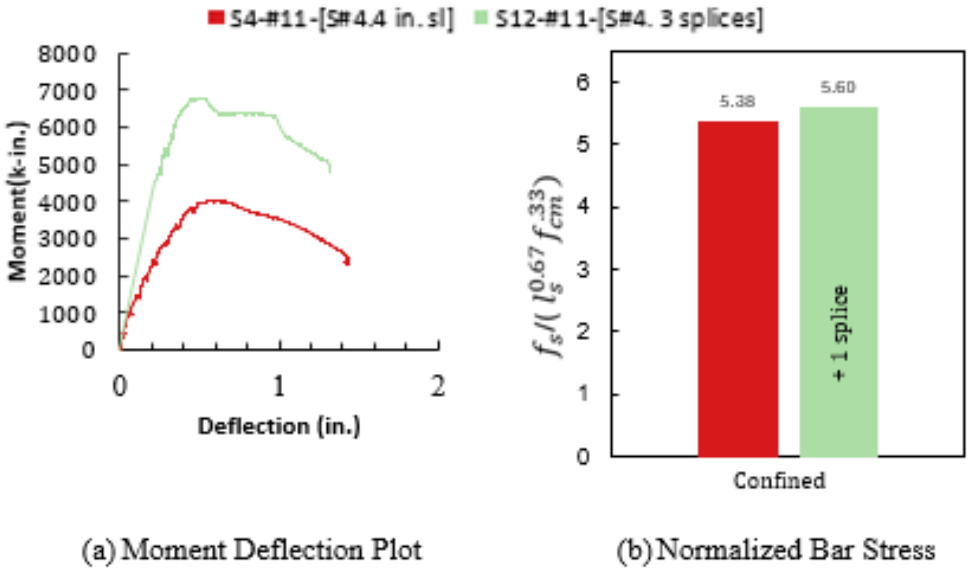

Figure 4-6: No. 11 Comparison Plots for Number of Splices Series

4.3.2 ASSESSMENT OF DESCRIPTIVE EQUATION

A comparison of predicted stresses to the experimental stresses is shown in Figure 4-7. The orange squares represent beams tested with the standard configuration of three splice pairs for No. 6 Beams or two splice pairs for No. 11 beams. The blue dots represent the beams with one

extra splice pair from the standard configuration (i.e. four splices for No. 6 beams or 3 splice pairs for No. 11 beams). The blue dashed line represents a slope of one which would mean that the equation exactly predicts bar stress. For these beams, it appears that the equation becomes a better prediction for bar stress when more splices are added. The point which has predicted bar stress of 88 and a experimental bar stress of 59, this beam was S4-#6-[S.4 in. s_l] and the discussion for why this is an outlier is included in the dissertation by Coleman (2024). For this series, the minimum test to predicted ratio was 0.93 where the maximum test to predicted ratio was 1.02. The average test to predicted ratio was 0.98 for this parameter, and the average coefficient of variation was 4.05%. Given these findings, it can be concluded that the descriptive equation can be used to reasonably predict bar stress regardless of the number of splices.

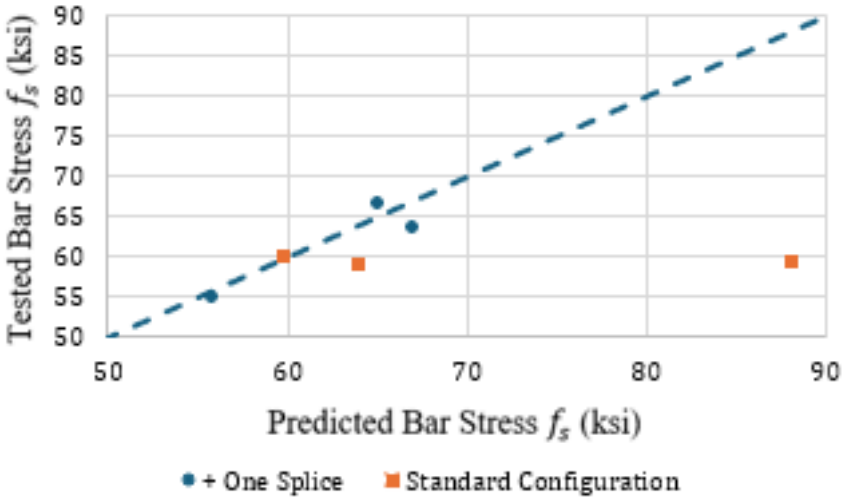

Figure 4-7: Test vs Predicted Plot for Bar Stress (Number of Splices)

4.4 TRANSVERSE REINFORCEMENT

4.4.1 QUALITATIVE DISCUSSION OF PARAMETER

Figures 4-8 through 4-9 provide a comparison of the moment-deflection behavior at the midspan of beams constructed with hooked bar lap splices and varying amounts and placement of transverse reinforcing steel for No. 6, No. 9, and No. 11 reinforcing bars.

The overall flexural behavior can be characterized as follows. In the elastic range of the moment-deflection plots, the beams had similar stiffness characteristics for the same bar size and did not vary with reinforcement.

One would assume that as the quantity of transverse reinforcement increases, the ductility of the beams would increase. In observing the moment deflection plots, this is not always the case. For all three bar sizes, the ductility is improved with the addition of confinement. As confinement is increased, there is less of a correlation between the amount of confinement and the ductility.

Furthermore, one would assume that as the transverse reinforcement increases, the bar stress developed would also increase. However, when comparing the normalized bar stress for each set of beams this is not always the case. In the beams with No. 6 hooks, the bar stress increases by

20% from the unconfined beam to the beam with confinement at only the ends of the lap splice. The beam with one additional piece of reinforcement in the middle experienced a decrease in the bar stress developed. One additional piece of reinforcement only had a 5% increase in bar stress from the beam with confinement at the ends. The decrease in bar stress for the beam with stirrups at the ends and middle of the closure joint can likely be explained by this beam being cracked along the interface prior to testing. These findings demonstrate that for No. 6 bars confinement is useful to substantially improve the bar stress developed, but that the most benefit in added confinement comes with adding confinement only at the ends of the splice.

For the beams with No. 9 hooks, there was a 30% increase in the bar stress developed from the unconfined specimen to the specimen with confinement only at the ends. The beam with stirrups spaced at $3d_b$ (four stirrups) experienced a 24% increase in the bar stressed developed. The beam with No. 4 stirrups spaced at $3d_b$ had a 7% increase in the bar stress developed from the beam with No. 3 stirrups at this spacing. For the beams in this series with No. 9 confining reinforcement, the hypothesis that as the amount of confinement increases the bar stress developed increased was true. However, consistent with the No. 6 beams, as confinement increased, the improvement from confinement at just the ends was not as high.

For the beams with No. 11 hooks, there were similar results to the beams with No. 6 hooks. From the unconfined beam to the beam with stirrups at the ends and middle of the lap splice, there was a 56% increase in the bar stress developed. The beam with stirrups spaced at $3d_b$(five stirrups) experienced a decrease in the stress developed in the steel. For this beam there is not an observation in testing which can explain this decrease in bar stress.

The findings in this study corroborate with the results of the analytical study by Coleman (2024), which found that when only adding two pieces of transverse reinforcement, these are most important to place at $2d_b$ from the edge of the hooks. This is likely because these hooks resist the failure mechanism of hook side bulging and hook prying. This study also suggests that it is most useful to put transverse reinforcement at the ends of the splice to improve the splice strength and that additional confinement may not be as necessary.

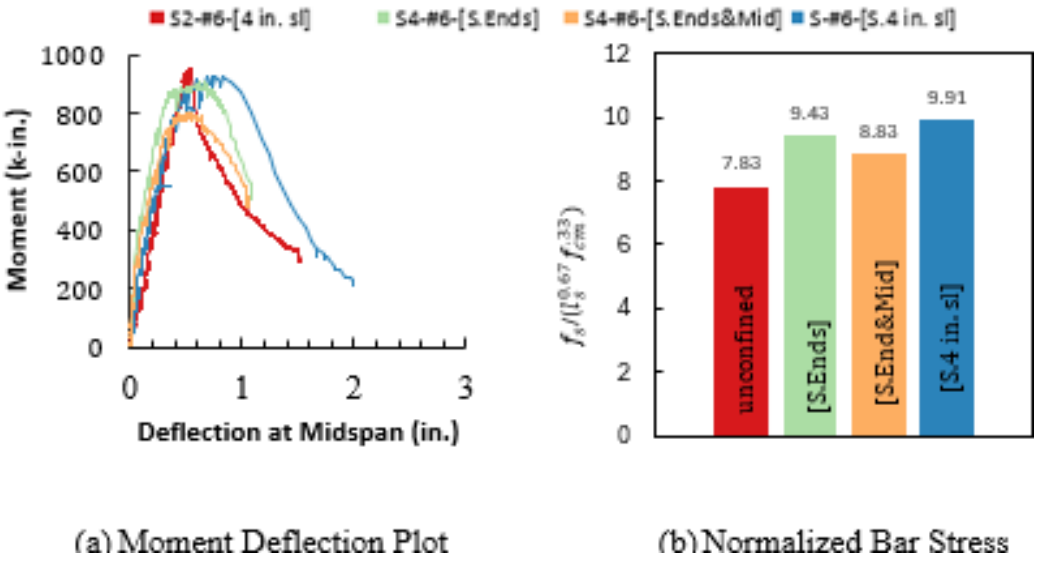

(a) Moment Deflection Plot (b) Normalized Bar Stress

Figure 4-8: No. 6 Comparison Plots for Transverse Reinforcement Series

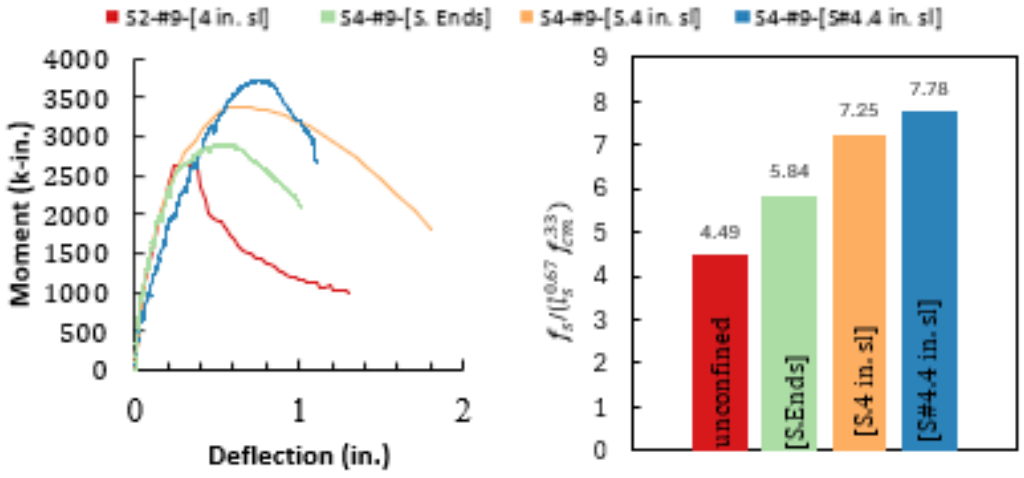

(a) Moment Deflection Plot (b) Normalized Bar Stress

Figure 4-9: No. 9 Comparison Plots for Transverse Reinforcement Series

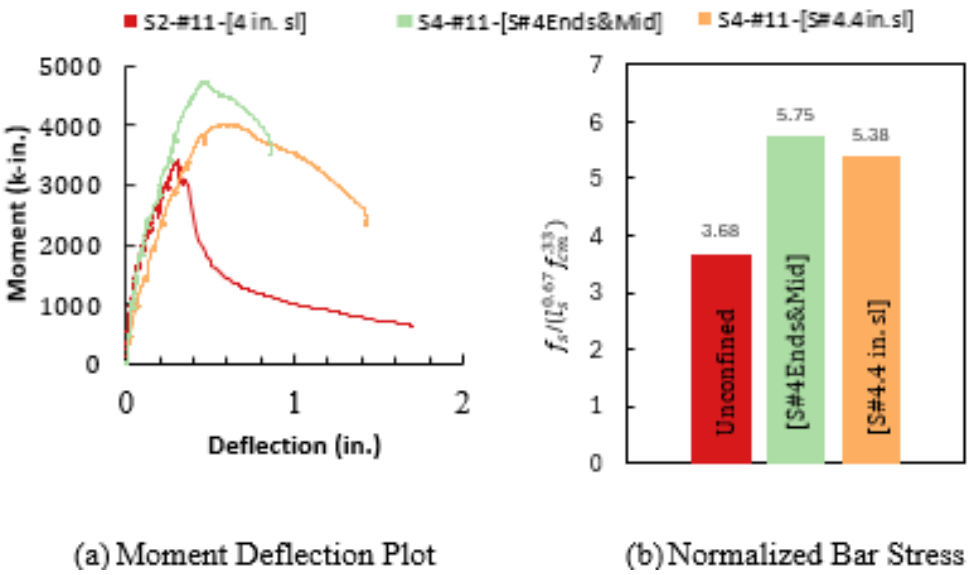

Figure 4-10: No. 11 Comparison Plots for Transverse Reinforcement Series

4.4.2 ASSESMENT OF DESCRIPTIVE EQUATION

For this series, to use the descriptive equation, it is important to understand how K_{tr} is used. The equation for this term is $K_{tr} = 6.5NA_{trl}$. In this series, the beams designated S.Ends have an N of 2 and the beams designated S.Ends&Mid have an N of 3. The beams with S.4 in. s_l have stirrups spaced at $3d_b$. These beams have a different number of stirrups depending on bar size. For No. 6 and No. 9 hooks, these beams had 4 stirrups i.e. N = 4, and for No. 11 hooks these beams had 5 stirrups i.e. N = 5.

A comparison of predicted stresses to the experimental stresses is shown in Figure 4-11. In this figure, the blue dots represent the beams tested in this thesis for this series. The dashed blue line represents a slope of one which indicates that the equation exactly predicts bar stress. For the beams that were unconfined, and the beams tested by compared from Coleman (2024), these beams were excluded from this figure as they were analyzed for their fit to the equation by Coleman. The dashed blue line represents a test to predicted ratio of one. For this series, the minimum test to predicted ratio was 0.89 and the maximum test to predicted ratio was 1.10. The average test to predicted ratio was 1.01 with an average coefficient of variation of 6.67%. Based on these findings, the descriptive equation is a good predictor of bar stress when the transverse reinforcement is varied.

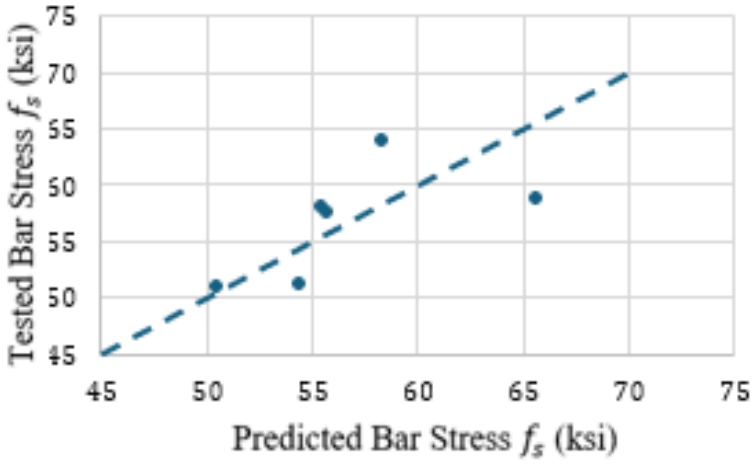

Figure 4-11: Test vs. Predicted Plot for Bar Stress (Transverse Reinforcement)

4.5 FIBERS

4.5.1 QUALITATIVE DISCUSSION OF PARAMETER

Figures 4-12 through 4-14 provide a comparison of the moment-deflection behavior at the midspan of beams constructed with hooked bar lap splices with and without the addition of steel fibers for No. 6, No. 9, and No. 11 reinforcing bars. Unconfined and confined beams are compared with and without fibers.

The overall flexural behavior can be characterized as follows. In the elastic range of the moment-deflection plots, the beams had similar stiffness characteristics for the same bar size and did not vary with the addition of steel fibers or confinement. Furthermore, beams with fibers achieved higher max moments than beams without fibers, except in the beam with stirrups for No. 9 beams for which the splice length was longer than the other beams being compared.

For beams with and without confinement, beams that had the addition of steel fibers in the closure joint saw an average of a 70% increase in the bar stress developed with the addition of fibers. Beams with confinement saw an average of a 26% increase in the bar stress developed with the addition of steel fibers. Furthermore, in all three bar sizes, beams with the addition of steel fibers had greater bar stress developed than those with confinement alone. The unconfined specimens with the addition of fibers developed nearly the same magnitude of bar stress as the beams with the addition of fibers and confinement.

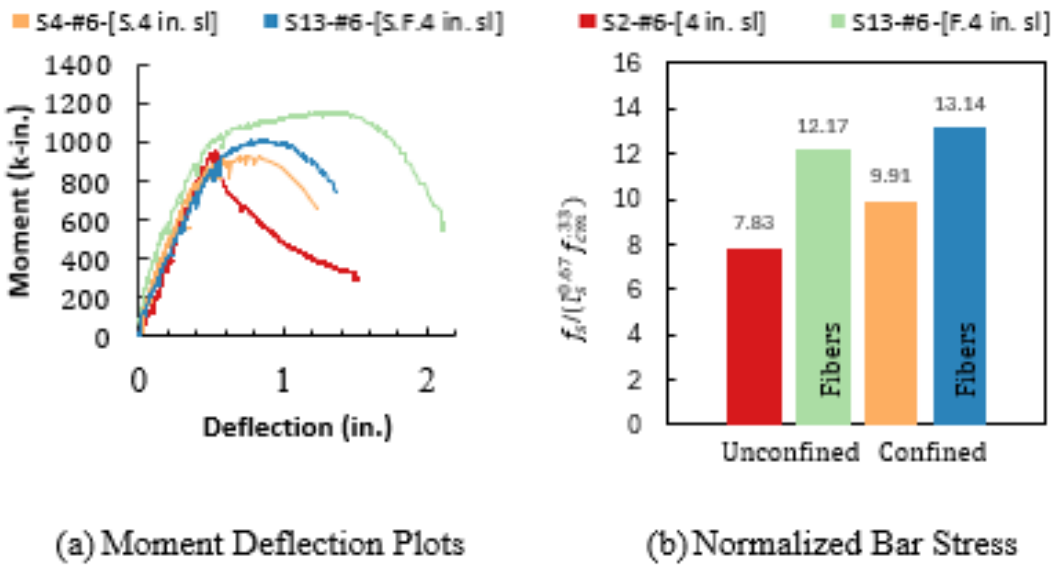

(a) Moment Deflection Plots (b) Normalized Bar Stress

Figure 4-12: No.6 Comparisons for Fibers Series

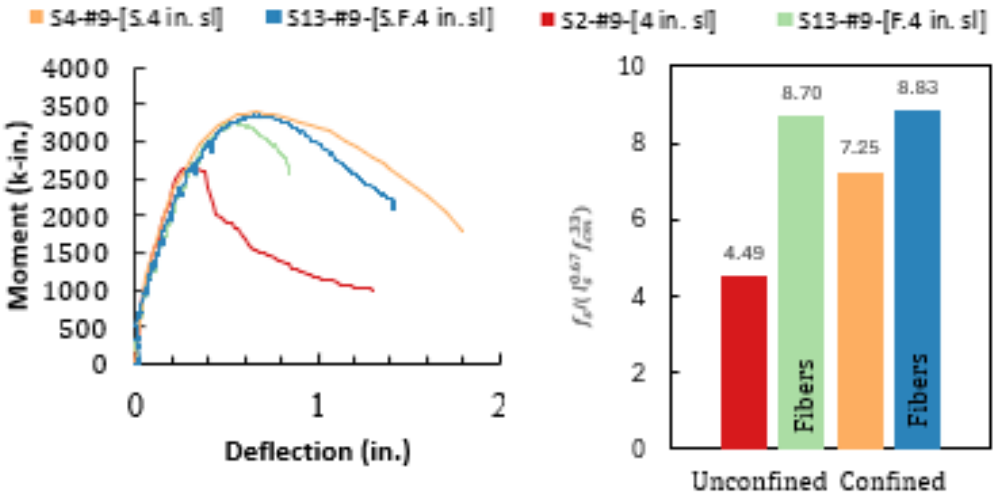

(a) Moment Deflection Plot (b) Normalized Bar Stress

Figure 4-13: No. 9 Comparisons for Fiber Series

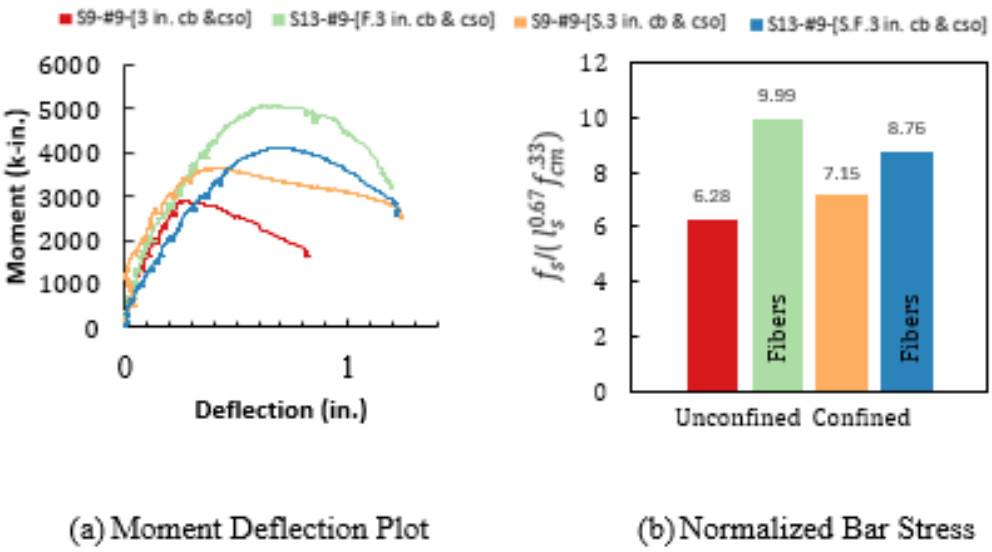

Figure 4-14: No. 9 and 3 in Cover Comparisons for Fiber Series

4.5.2 ASSESSMENT OF DESCRIPTIVE EQUATION

A comparison of predicted stresses to the experimental stresses is shown in Figure 4-15. In this figure, the purple squares represent beams with steel fibers in the closure joint without transverse reinforcement and the orange dots represent beams with steel fibers in the closure joint and transverse reinforcement. The dashed blue line represents a slope of one which indicates where the equation exactly predicts bar stress. For this series, the minimum test to predicted ratio was 1.32 and the maximum test to predicted ratio was 1.79. The average test to predicted ratio was 1.52 with a coefficient of variation of 12.51%.

For these tests, the equation underpredicted the bar stress by a large amount. For this reason, the design equation should be modified to reflect the contribution of steel fibers.

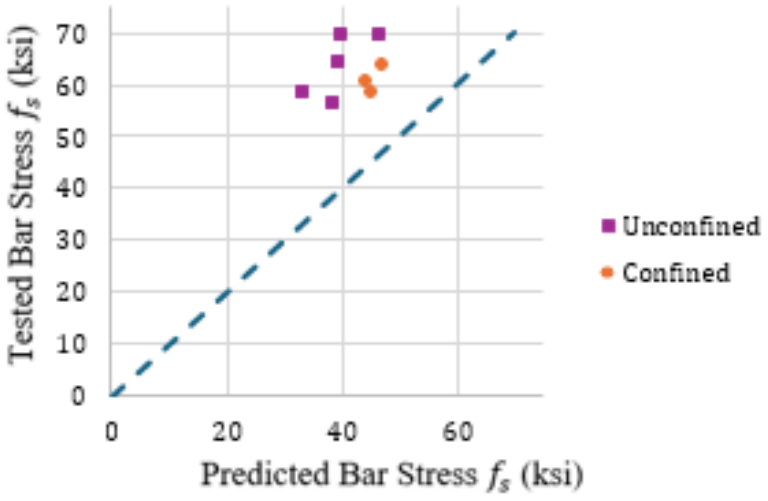

Figure 4-15: Test vs. Predicted Plot for Bar Stress (Steel Fibers)

From the qualitative discussion, and the test to predicted ratio, it appears that fibers have a greater effect when there is no confinement compared to when there is confinement. For this reason, two Ψ factors were developed for the unconfined and confined equations.

The factor for confined beams with a 1% fiber dosage Ψ_{fc} is 1.35, and the factor for unconfined beams with a 1% fiber dosage Ψ_{fu} is 1.63. The slope representing the equation with the factors applied are shown in Figure 4-14, where the dashed purple line represents a slope of 1.63 corresponding to the unconfined factor, and the dashed orange line represents a slope of 1.35 corresponding with the confined factor applied. When these factors are applied, the new minimum test to predicted ratio is 0.907, the maximum test to predicted ratio is 1.10. The average test to predicted ratio is 1.01 with a coefficient of variance of 6.31%.

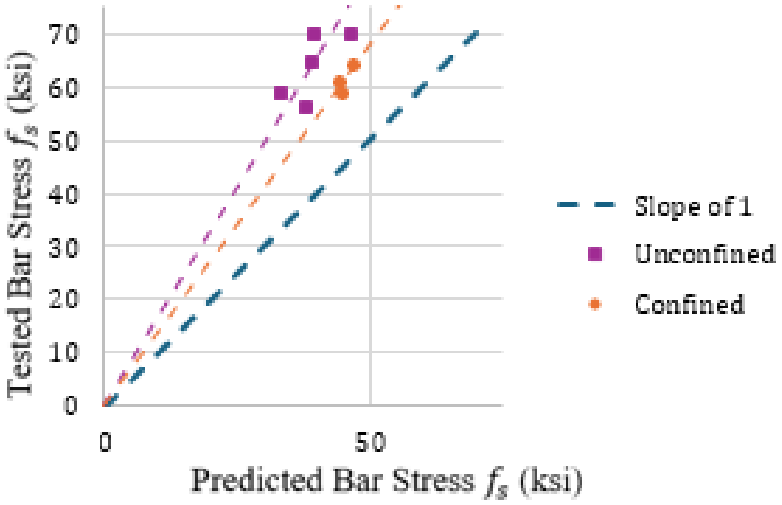

Figure 4-16: Test vs. Predicted Plot With Ψ Factors Applied

The descriptive equation with the proposed modification is as follows:

$$f_s^p = \frac{5.55 l_s^{0.67} f_{cm}^{0.33} \left(\frac{(0.1 c_{so} + 0.7 c_b)}{d_b} + K_{tr} \right)^{0.22} \Psi_f}{s_l^{0.033} d_b^{1.00}} \quad \text{Eq.2}$$

Where Ψ_f is the modification factor for a 1% fiber dosage by volume and is equal to:

Ψ_{fc} = 1.35 for specimens with transverse reinforcement in the form of stirrups perpendicular to the leads of the hooks.

Ψ_{fu} = 1.63 for specimens without transverse reinforcement

4.6 Design Equation for the Strength of Hooked Bar lap Splices

To develop a design equation from the descriptive equation, further simplification and a reduction factor are required. Using the simplification developed by Coleman (2024) and

applying the modification factors from this thesis, the simplification of the descriptive equation is shown in equation 3. The new COV for the simplified descriptive equation decreased from 6.31 to 6.26.

$$f_s^p = \frac{5.41 l_s^{0.67} f_{cm}^{0.33} \left(\frac{c_{min}}{d_b} + K_{tr}\right)^{0.22} \Psi_f}{s_l^{0.033} d_b^{1.00}} \quad \text{Eq.3}$$

c_{min} = The minimum cover of the bottom and side cover ($c_{min} = \min\{c_b, c_{so}\}$

To determine the minimum required splice length, Equation 3 was multiplied by a strength reduction factor of (0.75) and the splice strength f_s was replaced with yield strength f_y, which gives equation 4 (Coleman, 2024).

$$f_y = \frac{(0.75)5.41 l_s^{0.67} f_{cm}^{0.33} \left(\frac{c_{min}}{d_b} + K_{tr}\right)^{0.22} \Psi_f}{s_l^{0.033} d_b^{1.00}} \quad \text{Eq.4}$$

Rearranging this equation to solve for the minimum splice length gives Equation 5.

$$l_s = \left(\frac{f_y^{1.5} s_l^{0.05}}{8\sqrt{f_{cm}} + \left(\frac{c_{min}}{d_b} + K_{tr}\right)^{0.33} \Psi_f^{1.5}} \right) d_b^{1.5} \quad \text{Eq.5}$$

When solving for splice strength as a function of splice length using Equation 5, results in an average splice strength to test ratio of 1.31 and a COV of 6.23% based on the 17 beams in this test matrix. Which is comparable to the average splice strength test ratio of 1.33 and COV of 6% for the 58 beams from Coleman (2024). Figure 4-15 demonstrates that the steel strengths calculated using the design equation in Equation 5 are conservative. The slope of 0.76 represented by the inverse of the 1.31 splice strength to test ratio is shown by the dashed orange line in Figure 4-17. The blue line in Figure 4-17 represents a slope of one, where anything above this line would indicate that the equation over predicts the steel stress and the beam would fail. This indicates that design strengths are consistently about 76% of test values. This shows that the design equation provides a safe and conservative estimate for the minimum required splice length for hooked bar lap splices.

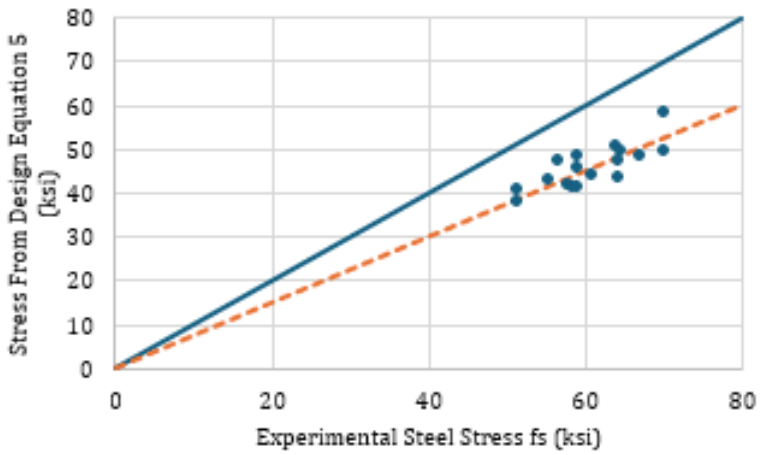

Figure 4-17: Calculated Splice Strengths using Design Equation Eq. 5 for Hooked Bar Lap Splices compared against Corresponding Experimental Strengths.

Since the Ψ factors were based on a limited number of tests, a simplification of the design equation was made to make the equation more conservative. This simplification is to remove the Ψ factor for the unconfined beams and use the conservative estimate that the $\Psi_f^{1.5}$ term is equal to 1.5. This simplification gives equation 6

$$l_s = \left(\frac{f_y^{1.5} s_l^{0.05}}{8\sqrt{f_{cm}} + \left(\frac{c_{min}}{d_b} + K_{tr}\right)^{0.33} \Psi_F} \right) d_b^{1.5} \qquad \text{Eq. 6}$$

Where Ψ_F = 1.5 for both confined and unconfined beams.

Solving splice strength as a function of splice length using equation 6, results in an average splice strength to test ratio of 1.40 based on the 17 beams in this test matrix. This indicates that design strengths are consistently about 71% of test values. With the simplification of the equation, the coefficient of variance increases to 10.3% which makes sense since the new equation is very conservative for beams that are unconfined with fiber reinforcement. See figure 4-18 for the stress from the design equation compared to the experimental stress. In this figure, the blue line represents a slope of 1, where values above this line indicate the equation would overpredict bar stress and the beam would fail, and the yellow dashed line represents a slope of .714 representing the average design equation stress over the experimental stress.

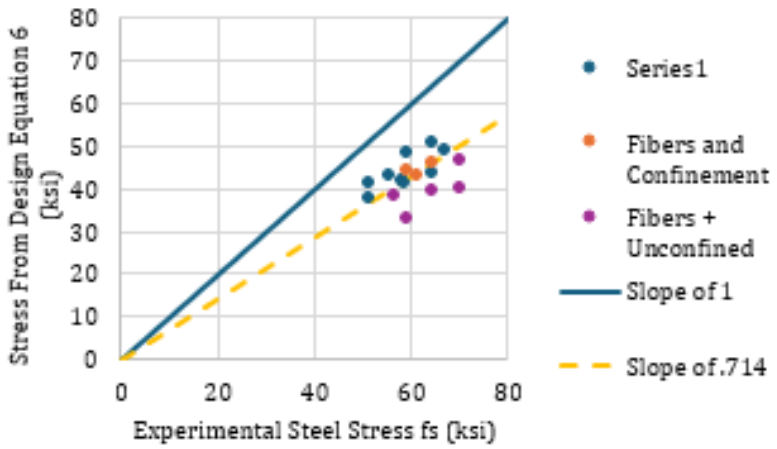

Figure 4-18: Calculated Splice Strengths using Design Equation Eq. 6 for Hooked Bar Lap Splices compared against Corresponding Experimental Strengths

4.6.1 USE AND RESTRICTIONS OF THE DESIGN EQUATION FOR HOOKED BAR LAP SPLICES WITH A 1% DOSAGE OF FIBERS BY VOLUME

This design equation is expected to yield safe design guidance when applied within the range of construction parameters used in this study and the study by Coleman (2024).

For this study, a 1% dosage of fibers by volume was used for all beams containing fibers in this test matrix. Therefore, the design equation is only expected to yield safe results when a 1% dosage of fibers by volume is used in the closure joint.

Though simplification was made due to limited test data, more tests should be done which vary the confinement, since the improvement from fibers was higher for unconfined beams. Furthermore, the findings from this series on fibers paired with the findings that transverse reinforcement is most beneficial at the ends of the splice, it may be most beneficial to design beams with transverse reinforcement at the ends of the splice and use steel fibers for the most benefit in reducing splice lengths. Tests should be done which vary the transverse reinforcement as a term could be proposed which scales with the amount of reinforcement similar to the way the K_{tr} term scales.

The confinement term was based on beams with No. 3 stirrups spaced at 3 d_b in the closure joint; however, since the improvement from fibers is greater for beams that are unconfined, this should be a conservative estimate when using less transverse reinforcement.

Since the Ψ factors proposed in this study were developed based on a limited number of tests, more beams should be tested that are unconfined and confined varying other bond parameters to confirm that the equation can be used over the entire set of bond parameters studied by Coleman (2024).

See Table 4-1 for a complete table for the results of each of the beams in this test matrix, and the beams that are compared from Coleman (2024).

Table 4-1: Results

Series	Beam ID	f_{cm} (ksi)	f_y (ksi)	f_{yt} (ksi)	l_s (in.)	b (in.)	h (in.)	c_{so} (in.)	c_b (in.)	s_l (in.)	n	N	A_{trl} (in^2)	f_s (ksi)	l_{eq} (in.)
4	S4-#6-[S.Ends]	3.58	66.1	72.9	7.96	24.19	15.84	1.62	1.64	4.32	3	2	0.11	57.7	13.66
	S4-#6-[S.Ends&Mid.]	3.11	66.1	72.9	7.88	24.25	15.81	1.51	1.45	4.67	3	3	0.11	51.2	14.12
	S4-#9-[S.Ends]	4.53	61.6	72.9	12.13	24.13	23.25	1.62	1.45	4.06	3	2	0.11	51.1	24.52
	S4-#9-[S#4.4 in. s_l]	3.58	61.6	60.6	12.38	24.28	23.25	1.85	1.64	3.96	3	4	0.20	63.9	20.44
	S4-#11-[S#4.4 in. s_l]	3.51	66.4	60.6	17.06	16.69	27.94	1.67	1.74	4.18	2	5	0.20	59.0	27.57
	S4-#11-[S#4.Ends&Mid.]	4.37	66.4	60.6	17.25	16.69	28.06	1.55	1.71	4.45	2	3	0.20	58.2	28.61
12	S12-#6-[4 splices]	3.11	66.1	-	10.59	32.00	15.75	1.57	1.56	4.44	4	-	-	55.2	17.62
	S12-#6-[S.4 splices]	4.37	66.1	72.9	7.84	31.88	15.75	1.84	1.96	3.82	4	4	0.11	66.7	10.79
	S12-#6-[S#4.3 splices]	5.04	66.4	60.6	17.04	24.25	28.25	1.51	2.00	4.01	3	5	0.20	63.8	23.07
13	S13-#6-[F.4 in s_l]	4.98	66.1	-	6.15	24.13	15.88	1.77	1.68	3.93	3	-	-	69.8	N/A
	S13-#6-[S.F.4 in s_l]	3.29	66.1	72.9	5.92	24.06	16.06	1.63	1.83	4.38	3	3	0.11	64.0	N/A
	S13-#9-[F.4 in s_l]	3.29	61.6	-	9.67	24.25	23.25	1.89	1.56	3.93	3	-	-	59.0	N/A
	S13-#9-[S.F.4 in s_l]	3.20	61.6	72.9	10.04	24.13	23.25	1.50	1.71	4.29	3	4	0.11	60.8	N/A
	S13-#9-[F.3 in c_b&c_{so}]	4.56	61.6	-	8.63	27.13	26.25	3.18	3.24	4.19	3	-	-	69.8	N/A
	S13-#9-[S.F.3 in c_b&c_{so}]	3.80	61.6	72.9	8.92	27.13	27.00	3.51	3.57	3.72	3	4	0.11	59.0	N/A
Beams from Coleman (2024)															
2	S2-#6-[4 in. s_l]*	3.50	66.1	-	11.29	24.00	15.67	1.74	1.42	4.00	3	-	-	60.1	17.04
	S2-#9-[4 in. s_l]*	4.01	70.0	-	16.92	24.06	23.29	1.59	1.46	4.08	3	-	-	47.3	33.42
	S2-#11-[4 in. s_l]*	3.65	66.8	-	21.44	16.63	27.69	1.55	1.43	4.11	2	-	-	44.0	53.12
4	S4-#6-[S.4 in. s_l]*	3.50	66.1	69.5	7.83	24.00	15.70	1.64	1.61	4.04	3	4	0.11	59.5	12.34
	S4-#9-[S.4 in. s_l]*	4.01	70.0	69.5	11.92	24.00	23.23	1.45	1.44	4.05	3	4	0.11	60.3	22.66
9	S9-#9-[3 in c_b&c_{so}]*	3.65	66.3	-	13.00	27.13	26.07	3.03	3.32	4.14	3	-	-	49.2	27.45
	S9-#9-[S.3 in c_b&c_{so}]*	3.67	66.3	69.5	13.583	27.125	26.25	2.98	3.069	4.248	5	3	0.11	60.5	20.72
13	S13-#9-[F.6 in. s_l]*	3.55	66.3	-	11.88	34.25	23.40	1.46	1.62	6.17	3	-	-	56.3	N/A
	S13-#11-[F.8 in. s_l]*	5.01	66.8	-	15.30	28.63	27.75	1.52	1.60	8.30	2	-	-	64.3	N/A

[a]Definitions: f_{cm} = concrete compressive strength; f_y = yield strength of hooked bars; f_{yt} = yield strength of secondary reinforcement; l_s = lap length; b = beam width; h = beam height; c_{so} = side cover; c_b = vertical cover; s_l = spacing of lapped bars; n = number of lapped bars; N = number of legs of secondary reinforcement within one outer hook diameter from splices; A_{trl} = area of one leg of secondary reinforcement; f_s = peak stress developed in bars at the critical section based on moment-curvature analysis; l_{eq} = required lap length per Eq. (2) to develop yield strength of Grade 60 bars

[b]Bracketed Terms: [S.Ends] = one piece of transverse reinforcement was placed at $2d_b$ from either splice end; [S.Ends&Mid.] = one piece of transverse reinforcement was placed at $2d_b$ from either splice end and at the middle of the splice; [180° Hook] = specimen contained 180° hooks in place of 90° hooks; [U-Bar] = specimen contained U-Bars in place of 90° hooks. Beams with an (*) are from Coleman (2024).

Chapter 5 CONCLUSIONS

5.1 SUMMARY OF WORK

Engineers are using non-contact hooked bar lap splices to connect pre-cast elements without proper design guidance. The goal of this work was to broaden the understanding of non-contact hooked bar lap splices and provide design recommendations for the minimum required lap length of hooked bars. The following tasks were accomplished in this thesis:

1.) A literature review on the parameters of focus in this study, which were the number of splices, transverse reinforcement, and steel fiber usage.
2.) To evaluate the influence of the parameters on bond and anchorage, fifteen beam-splice specimens containing No. 6, No. 9, or No. 11 hooked bars were tested.
3.) Test results from the fifteen beam-splice specimens were compared against calculated strengths using the descriptive equation proposed by Coleman (2024).
4.) Design recommendations regarding the use of steel fibers in closure joints for non-contact hooked bar lap splices was proposed.

5.2 CONCLUSIONS

Based on the work in this thesis, the following conclusions have been developed.

1.) Increasing the number of spliced bars from three pairs to four for beams with No. 6 bars and increasing the number of spliced bars from two to three pairs has a negligible effect on the splice strength. For this reason, the number of spliced bars does not need to be factored into the descriptive equation.
2.) The existence of confinement at a minimum of 1 transverse tie spaced at $2d_b$ from the splice ends provides a substantial increase in splice strength.
3.) A 1% dosage of steel fibers by volume significantly increases the splice strength.
4.) The use of a 1% dosage of steel fibers by volume is more influential on improving splice strength than the use of transverse reinforcement alone. However, the use of steel fibers in a 1% dosage by volume is beneficial for improving splice strength in both unconfined and confined beams.
5.) The improvement of a 1% dosage of steel fibers by volume was distinctly higher for beams that were unconfined when compared to beams that were confined.
6.) A factor has been proposed based on fibers to apply to the descriptive and design equations. Since this factor was proposed based on a limited number of tests, future work should be done to validate these factors.

5.3 FUTURE WORK

From the findings of this research, and the limitations of the scope of this research, the following opportunities for future work are provided.

1.) Additional tests should be conducted examining increasing the number of splices varying bar size, to confirm the findings of this study.
2.) Additional tests should be conducted examining the placement of transverse reinforcement for transverse reinforcement to confirm the findings of this study.
3.) Steel fibers were found to be very effective at improving the splice strength. However, since the improvement in splice strength was different for splices with confinement and without confinement, further tests should be conducted to verify the Ψ factors developed in this study. Specifically, more tests should be done varying the amount of confinement. Since this term was based on the maximum amount of confinement and the improvement for confined beams is less than that for unconfined beams, it is expected that this term should be conservative. Furthermore, more tests should be done varying the size of the hooks.
4.) Since this study only tested beams with a fiber volume fraction of 1%, future work should be done which changes the fiber volume fraction.
5.) Full – scale beams should be tested to verify the findings in this study.

Bibliography

318-19 Building Code Requirements for Structural Concrete and Commentary. (2019). American Concrete Institute. https://doi.org/10.14359/51716937

Altera, A., Bayraktar, O., Bodur, B., & Kaplan, G. (2021). Investigation of the Usage Areas of Different Fiber Reinforced Concrete. *Journal of Engineering and Sciences*.

Bekaert. (2018, October 22). *Steel Fiber Concrete Reinforcement - How Does it Work* [Video recording].

Canbay Erdem, & Frosch Robert. (2006). Design of Lap-Spliced Bars: Is Simplification Possible? *ACI Structural Journal*, *103-S47*.

Coleman, Z. W. (2024). *Hooked Bar Anchorages and their Use in Noncontact Lap Splices*.

Hamad Bilal, Abou Haidar Elias, & Harajili Mohamad. (2011). *43 ACI Structural Journal*.

Hamad Bilal, Harajli Mohamad, & Jumaa Ghaida. (2001). Effect of Fiber Reinforcement on Bond Strength of Tension Lap Splices in High- Strength Concrete. *ACI Structural Journal*, *98-S61*.

Harajli, M. H., & Salloukh, K. A. (1997). Effect of Fibers on Development/Splice Strength of Reinforcing Bars in Tension. In *ACI Materials Journal* (Vol. 94, Issue 4).

Marques, J. L. G., & Jirsa, J. 0. (1975). *TITLE NO. 72-18 A Study of Hooked Bar Anchorages in Beam-Column Joints*.

McLean David, & Smith Carol. (1997). *NONCONTACT LAP SPLICES IN BRIDGE COLUMN-SHAFT CONNECTIONS*.

Metelli, G., Marchina, E., & Plizzari, G. A. (2017). Experimental study on staggered lapped bars in fiber reinforced concrete beams. *Composite Structures*, *179*, 655–664. https://doi.org/10.1016/j.compstruct.2017.07.069

Specification for Deformed and Plain Carbon-Steel Bars for Concrete Reinforcement. (2016). ASTM International. https://doi.org/10.1520/A0615_A0615M-16

Test Method for Splitting Tensile Strength of Cylindrical Concrete Specimens. (1996). ASTM International. https://doi.org/10.1520/C0496-96

Test Methods and Definitions for Mechanical Testing of Steel Products. (2015). ASTM International. https://doi.org/10.1520/A0370-15

Appendix A

Test Data from Beam-Splice Specimens

Table A-1: Initial Test Matrix of Large-Scale Beam-Splice Specimens

Specimen Description [Identifier]	Cross-Sectional Dimensions (b x h in.) for each Bar Size		
	No. 6	**No. 9**	**No. 11**
Series 4 — Series to Investigate the Influence of transverse reinforcement			
No. 3 transverse reinforcement at ends of lap splice	24.0 x 15.5	24.0 x 23.0	
No. 3 transverse reinforcement at ends and middle of lap splice	24.0 x 15.5		16.5 x 27.5
No. 4 transverse reinforcement at 4 in. offset		24.0 x 23.0	16.5 x 27.5
Series 12 — Series to Investigate the Influence of Multiple Splices			
Use of 4 lap splices	32.0 x 15.5		
Use of 4 lap splices and No. 3 transverse reinforcement at $3d_b$	32.0 x 15.5		
Use of 3 lap splices and No. 4 transverse reinforcement at $3d_b$			24.41 x 27.5
Series 13 — Series to Investigate the Influence of Steel Fibers			
1% steel-fiber dosage [F.4 in. s_l]	24.0 x 15.5	24.0 x 23.0	
1% steel-fiber dosage w/ No. 3 transverse reinforcement at $3d_b$ [F.4 in. s_l]	24.0 x 15.5	24.0 x 23.0	
1% steel fiber dosage with 3 in. cover		26.0 x 27.0	
1% steel fiber dosage with 3 in. cover and No. 3 transverse reinforcement at $3d_b$		26.0 x 27.0	

Table A-2: Lettering Designation in Names of Beam-Splice Specimens

Specimen Identifier	Unique Feature
F.	1% dosage of steel fibers
S.	Transverse ties or stirrups at $3d_b$ enclosing spliced hooks

Table A-3: First and Second Beam Tested with Each Pair of Precast Segments

First Beam Tested	Second Beam Tested
S4-#6-[S. Ends]	S4-#6-[S. Ends&Mid]
S4-#9-[S.#4.4in. s_l]	S4-#9-[S.Ends]
S4-#11-[S#4 Ends&Mid]	S4-#11-[S#4.4 in. s_l]
S12-#6-[4 splices]	S12-#6-[S.4 splices]
S12-#11-[S#4.3 splices]	None

S13-#6-[F.4 in. s_l]	S13-#6-[S.F.in. s_l]
S13-#9-[F.4 in. s_l]	S13-#9-[S.F.4 in. s_l]
S13-#9-[F.3 in. c_b & c_{so}]	S13-#9-[S.F.3 in. c_b & c_{so}]

Table A-4: Constitutive Properties and Deformations of Longitudinal Steel

Imperial Bar Size	f_y **(psi)**	ε_y **(με)**	ε_{sh} **(με)**	E_h **(ksi)**	h_r **(in.)**	w_r **(in.)**	s_r **(in.)**
6	66,100	2,279	6,500	1,377	0.062	0.113	0.430
9	61,600	2,124	19,200	539	0.055	0.179	0.700
11	66,790	2,303	11,770	1,039	0.088	0.184	0.891

Concrete for all specimens used air-entrained concrete with a specified compressive strength of 4,000 psi and an air content of 5-8%. Specimens with steel fibers used a Fiber Volume Fraction of 1% in the closure joint. BEKAERT 3D 80/30BGP steel fibers (length of 1.18 in. and diameter of 15 mil.) were used.

Table A-5: Concrete Mixture Proportions for Beam-Splice Specimens

Material	**Weight (SSD) (lb/yd^3)**
Water	269
Type I Cement	445
Fly Ash	148
Coarse Aggregate #68	1,768
Natural Sand	638
Manmade Sand	679
Admixture	**Dosage (oz/cwt)**
Air-Entrainment	0.25
High Range Water Reducer	3.30

Hardened concrete properties including the compressive strength, static modulus of elasticity, and splitting tensile strength were determined on the day of beam testing in accordance with ASTM C39 (2020), C469 (2014), and C496 (2017) specifications, respectively

S4-#6-[S.Ends]

Summary:

Specimen S4-#6-[S.Ends] was designed to determine if the placement of the stirrups affects bond strength. For this Beam, No. 3 stirrups are placed at $2d_b$ from either spliced End.

Testing Notes:

None

Table B-1: S4-#6-[S.Ends] Specimen Properties

Configuration of Closure Joint

c_b (in.)	c_{so} (in.)	c_{si} (in.)	c_{th} (in.)	s_l (in.)	l_s (in.)	b (in.)	h (in.)	Secondary Reinforcement
1.64	1.62	1.43	2.198	4.32	7.96	24.19	15.84	No. 3 stirrups at $2d_b$ from either spliced end

Properties of Constitutive Materials

Precast Concrete			Cast-in-Place Concrete			Steel Reinforcing Bars		
f_{cm} (psi)	f_{stm} (psi)	E_{cm} (ksi)	f_{cm} (psi)	f_{stm} (psi)	E_{cm} (ksi)	d_b (in.)	f_y (psi)	R_r
5730	400	3900	3,580	330	3350	0.75	66,100	.130

Table B-7: S4-#6-[S.Ends] Fresh Concrete Properties

Precast Concrete			Cast-in-Place Concrete		
Air Content (%)	Unit Weight (pcf)	Slump (in.)	Air Content (%)	Unit Weight (pcf)	Slump (in.)
6	143.1	6	8	138	7.5

Table B-8: S4-#6-[S.Ends] Loading Configuration and Test Results

A (in.)	B (in.)	C (in.)	δ_u (in.)	P_u (lb)	M_u (kip-in.)	$f_{s,mc}$ (ksi)
48	48	6	1.095	18,872	968.5844	57.683

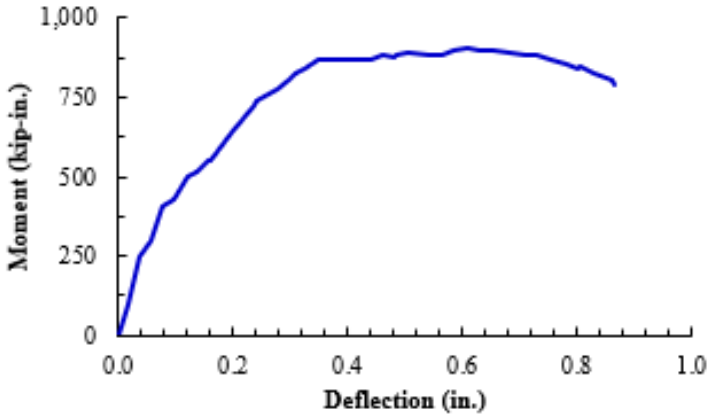

Figure B-1: S4-#6-[S.Ends] Applied Moment Against Midspan Deflection

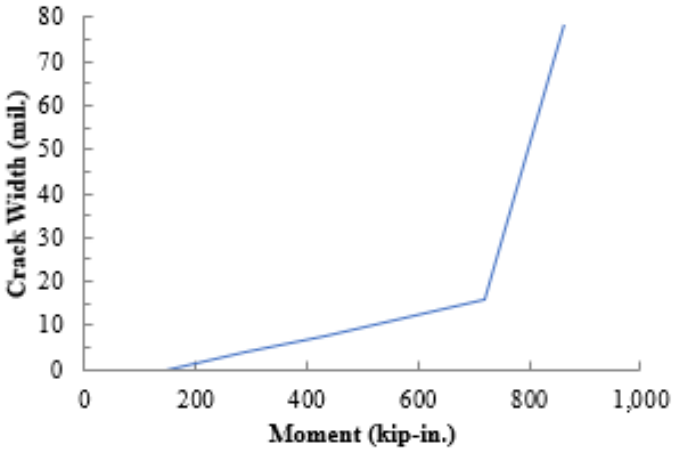

Figure B-2: S4-#6-[S.Ends] Interface Crack Growth Under Loading

	Side View of Splice Region	Top View of Splice Region
50% Maximum Loading	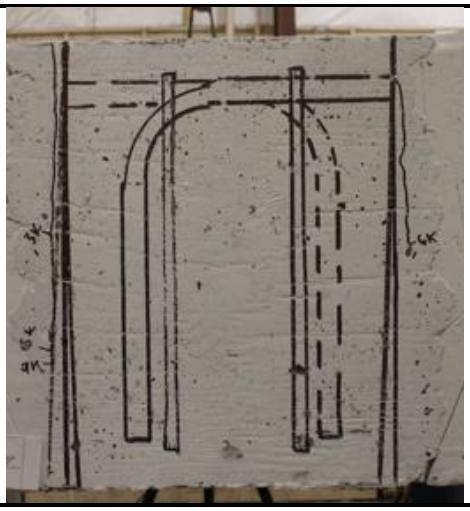	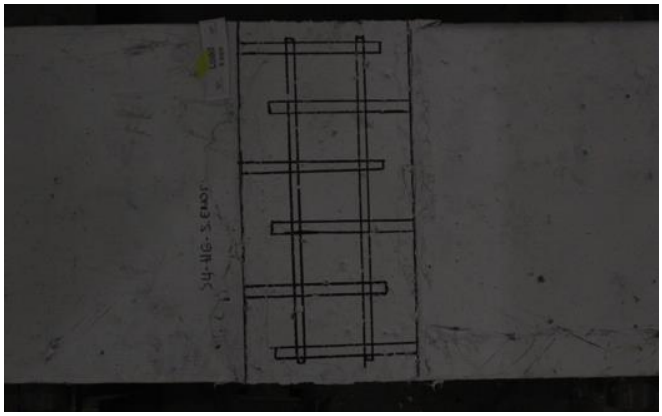
75% Maximum Loading	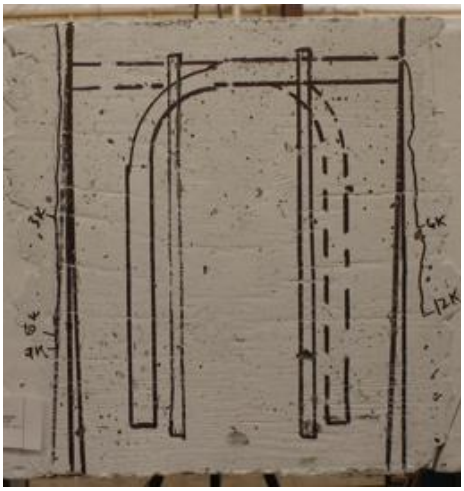	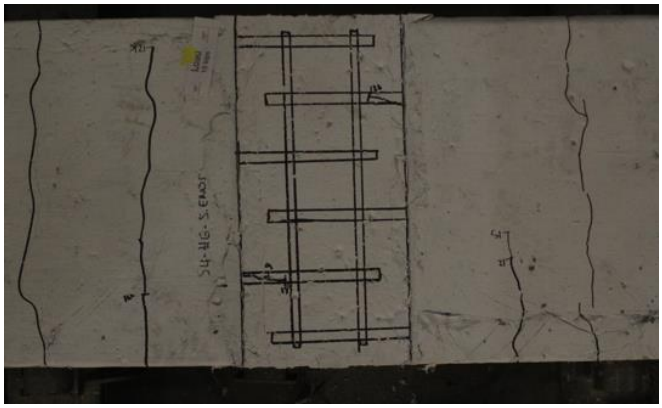
At Failure	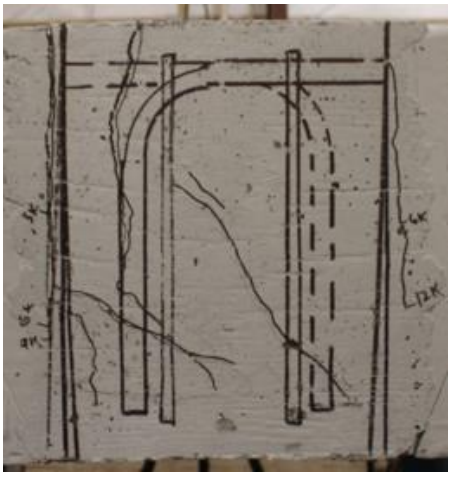	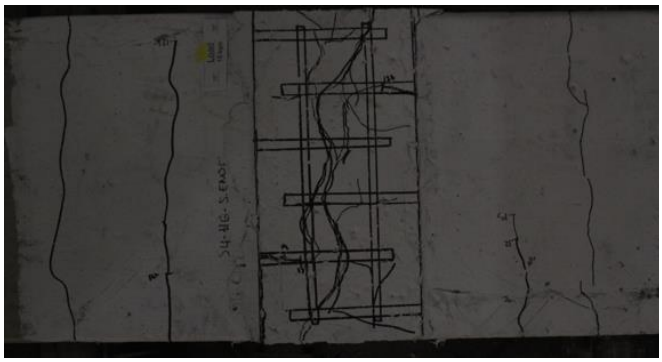

Figure B-7: Progression of Damage in Closure Joint of S4-#6-[S. Ends]

S4-#6-[S.Ends&Mid]

Summary:

Specimen S4-#6-[S.Ends&Mid] was designed to determine if the placement of the stirrups affects bond strength. For this Beam, No. 3 stirrups are placed at $2d_b$ from either spliced end with one No.3 stirrup placed midway through the closure.

Testing Notes:

Interface between closure joint and precast piece cracked prior to testing

Table B-36: S4-#6-[S.Ends&Mid] Specimen Properties

Configuration of Closure Joint

c_b (in.)	c_{so} (in.)	c_{si} (in.)	c_{th} (in.)	s_l (in.)	l_s (in.)	b (in.)	h (in.)	Secondary Reinforcement
1.447	1.506	1.247	2.208	4.667	7.875	24.25	15.813	No. 3 stirrups at $2d_b$ from either spliced end and one No. 3 stirrup at the middle of the splice length

Properties of Constitutive Materials

Precast Concrete			Cast-in-Place Concrete			Steel Reinforcing Bars		
f_{cm} (psi)	f_{stm} (psi)	E_{cm} (ksi)	f_{cm} (psi)	f_{stm} (psi)	E_{cm} (ksi)	d_b (in.)	f_y (psi)	R_r
5740	410	3950	3110	280	3130	0.75	66,100	0.130

Table B-37: S4-#6-[S.Ends&Mid] Fresh Concrete Properties

Precast Concrete			Cast-in-Place Concrete		
Air Content (%)	Unit Weight (pcf)	Slump (in.)	Air Content (%)	Unit Weight (pcf)	Slump (in.)
6	143.1	6	8	-	8

Table B-38: S4-#6-[S.Ends&Mid] Loading Configuration and Test Results

A (in.)	B (in.)	C (in.)	δ_u (in.)	P_u (lb)	M_u (kip-in.)	$f_{s,mc}$ (ksi)
48	48	6.00	1.061	16,732	866.84	51.2

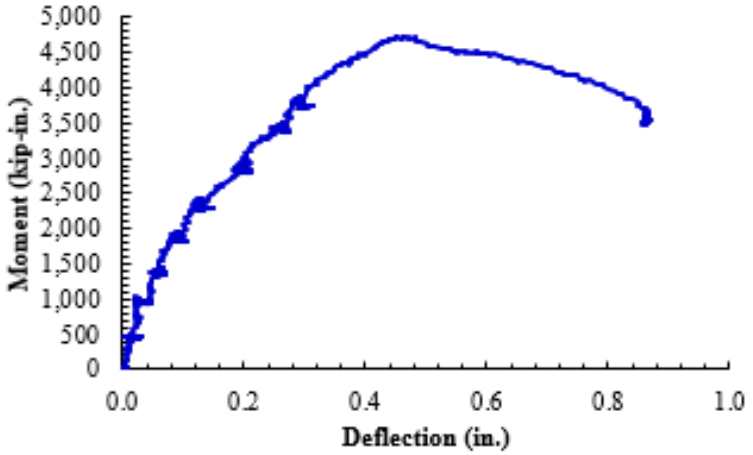

Figure B-42: S4-#6-[S.Ends&Mid] Applied Moment Against Midspan Deflection

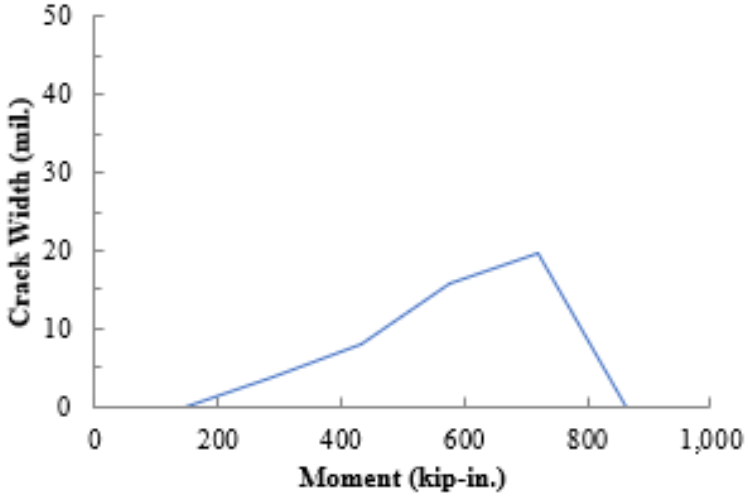

Figure B-43: S4-#6-[S.Ends&Mid] Interface Crack Growth Under Loading

	Side View of Splice Region	Top View of Splice Region
50% Maximum Loading	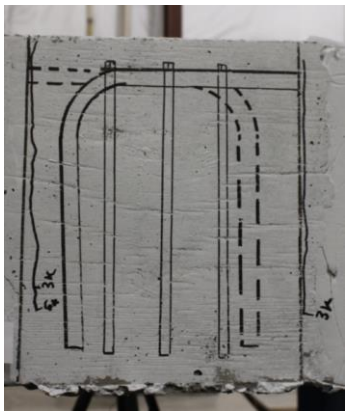	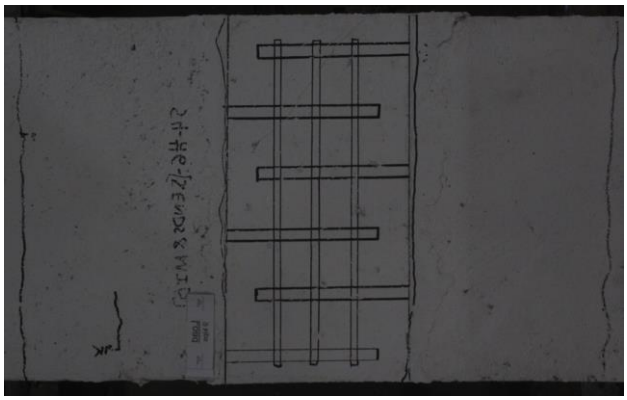
75% Maximum Loading	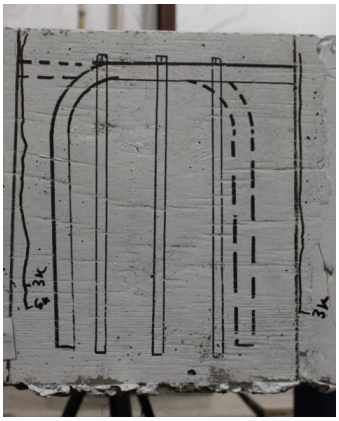	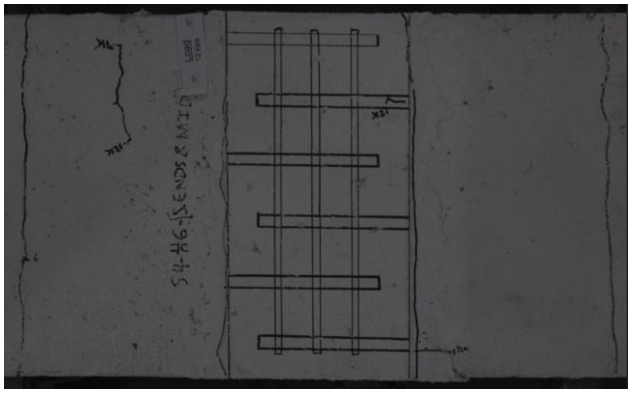
At Failure	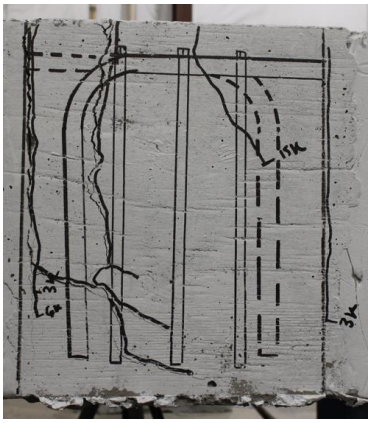	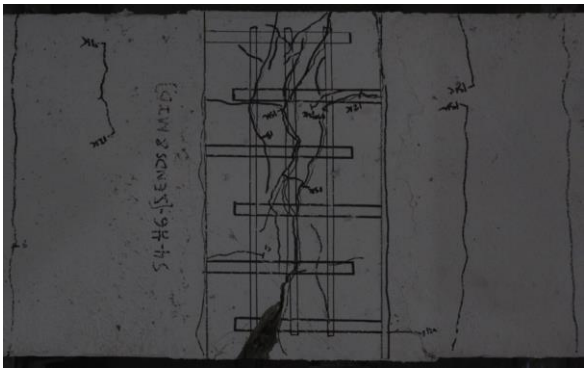

Figure B-44: Progression of Damage in Closure Joint of S4-#6-[F.4 in. s_l]

S4-#9-[S#4.4in. s_l]

Summary:

Specimen S4-#9-[S#4.4in. s_l] was designed to determine if the bar size of the stirrups affects bond strength. For this Beam, No. 4 stirrups are placed at $3d_b$ over the splice length.

Testing Notes:

None.

Table B-36: S4-#9-[S#4.4 in. s_l] Specimen Properties

Configuration of Closure Joint

c_b (in.)	c_{so} (in.)	c_{si} (in.)	c_{th} (in.)	s_l (in.)	l_s (in.)	b (in.)	h (in.)	Secondary Reinforcement
1.639	1.847	1.332	1.563	3.958	12.375	24.25	23.25	No. 4 stirrups placed at $3d_b$

Properties of Constitutive Materials

Precast Concrete			Cast-in-Place Concrete			Steel Reinforcing Bars		
f_{cm} (psi)	f_{stm} (psi)	E_{cm} (ksi)	f_{cm} (psi)	f_{stm} (psi)	E_{cm} (ksi)	d_b (in.)	f_y (psi)	R_r
3,650	350	3,400	4,980	690	3,600	1.128		0.07

Table B-37: S4-#9-[S#4.4 in. s_l] Fresh Concrete Properties

Precast Concrete			Cast-in-Place Concrete		
Air Content (%)	Unit Weight (pcf)	Slump (in.)	Air Content (%)	Unit Weight (pcf)	Slump (in.)
7.8	138.1	8	8	140	7.5

Table B-38: S4-#9-[S#4.4 in. s_l] Loading Configuration and Test Results

A (in.)	B (in.)	C (in.)	δ_u (in.)	P_u (lb)	M_u (kip-in.)	$f_{s,mc}$ (ksi)
48	48	6.00	1.115	77,596	3808.62	63.941

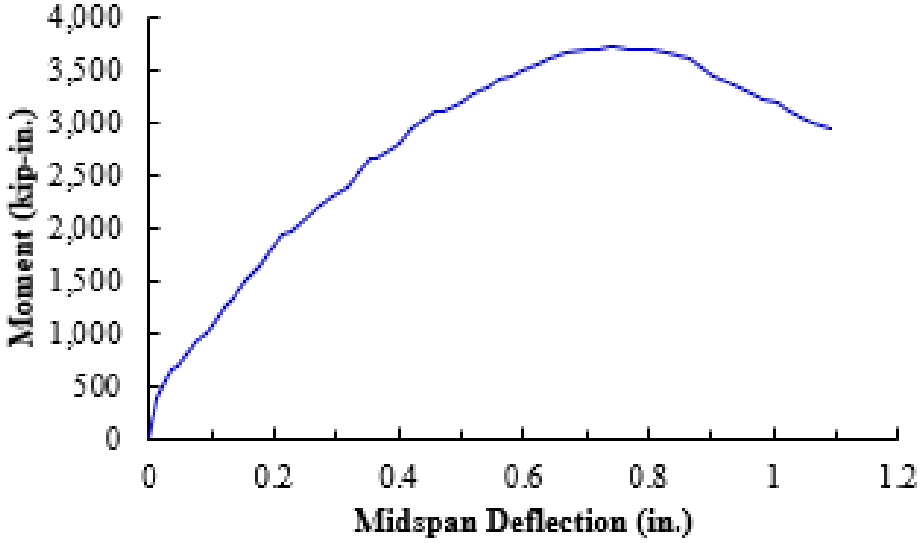

Figure B-42: S4-#9-[S#4.4 in. s_1] Applied Moment Against Midspan Deflection

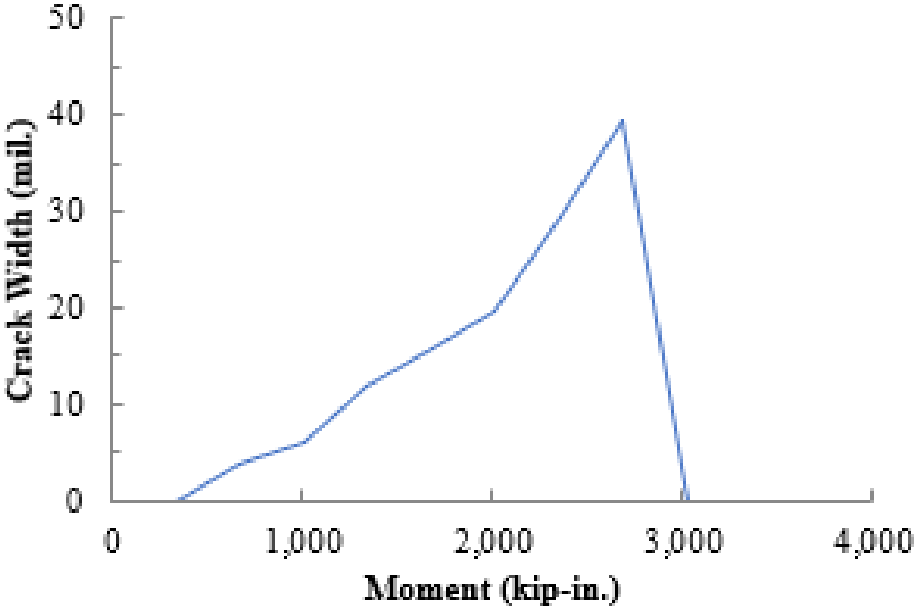

Figure B-43: S4-#9-[S#4.4 in. s_1] Interface Crack Growth Under Loading

	Side View of Splice Region	Top View of Splice Region
50% Maximum Loading	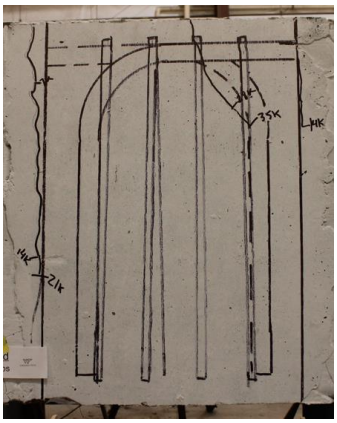	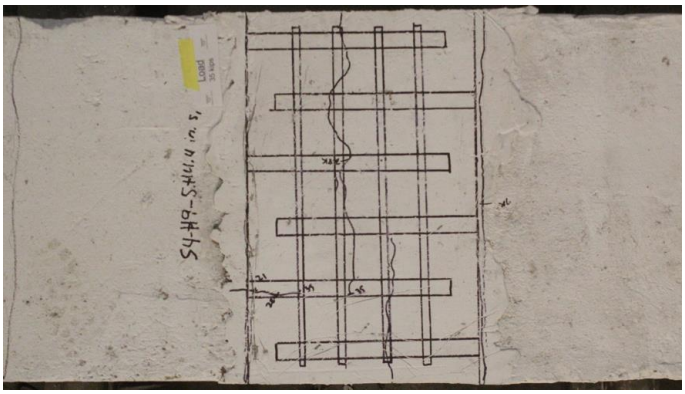
75% Maximum Loading	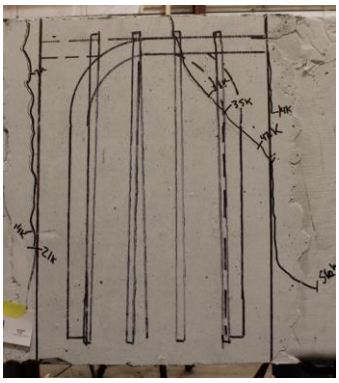	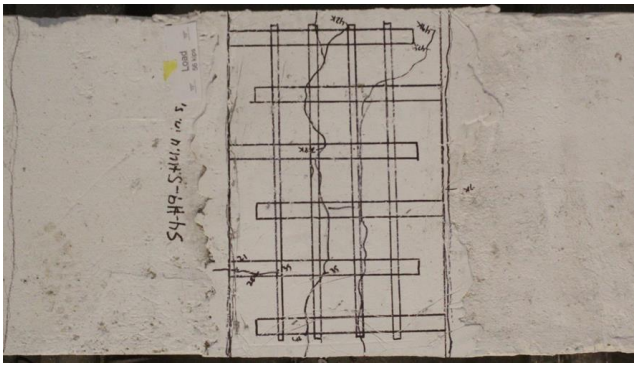
At Failure	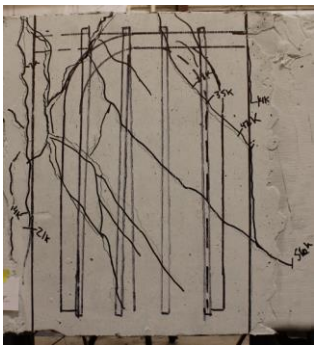	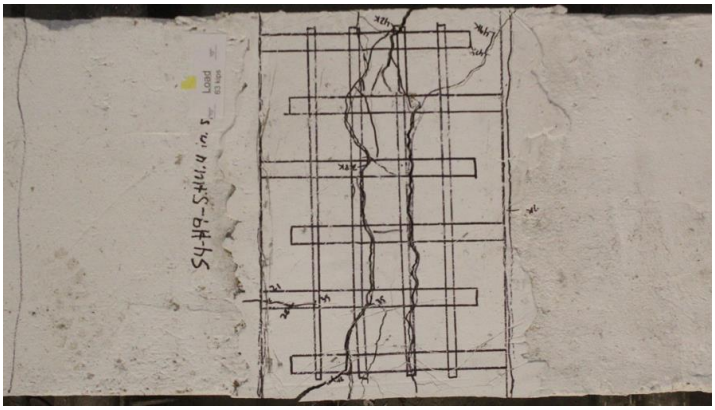

Figure B-44: Progression of Damage in Closure Joint of S4-#9-[S#4.4 in. s_l]

S4-#9-[S.Ends]

Summary:

Specimen S4-#9-[S.Ends] was designed to determine if the placement of the stirrups affects bond strength. For this Beam, No. 3 stirrups are placed at $2d_b$ from either spliced End.

Testing Notes:

Deflections on west end may be too high due to roller moving.

Table B-36: S4-#9-[S.Ends] Specimen Properties

Configuration of Closure Joint

c_b (in.)	c_{so} (in.)	c_{si} (in.)	c_{th} (in.)	s_l (in.)	l_s (in.)	b (in.)	h (in.)	Secondary Reinforcement
1.454	1.62	1.333	2.064	4.057	12.125	24.125	23.25	No. 3 stirrups at $2d_b$ from either spliced end

Properties of Constitutive Materials

Precast Concrete			Cast-in-Place Concrete			Steel Reinforcing Bars		
f_{cm} (psi)	f_{stm} (psi)	E_{cm} (ksi)	f_{cm} (psi)	f_{stm} (psi)	E_{cm} (ksi)	d_b (in.)	f_y (psi)	R_r
3650	350	3400	4530	435	4750	1.128	61600	.07

Table B-37: S4-#9-[S.Ends] Fresh Concrete Properties

Precast Concrete			Cast-in-Place Concrete		
Air Content (%)	Unit Weight (pcf)	Slump (in.)	Air Content (%)	Unit Weight (pcf)	Slump (in.)
7.8	138.1	8	6	143.1	6

Table B-38: S4-#9-[S.Ends] Loading Configuration and Test Results

A (in.)	B (in.)	C (in.)	δ_u (in.)	P_u (lb)	M_u (kip-in.)	$f_{s,mc}$ (ksi)
48	48	6	1.014	60,197	2973.07	51.139

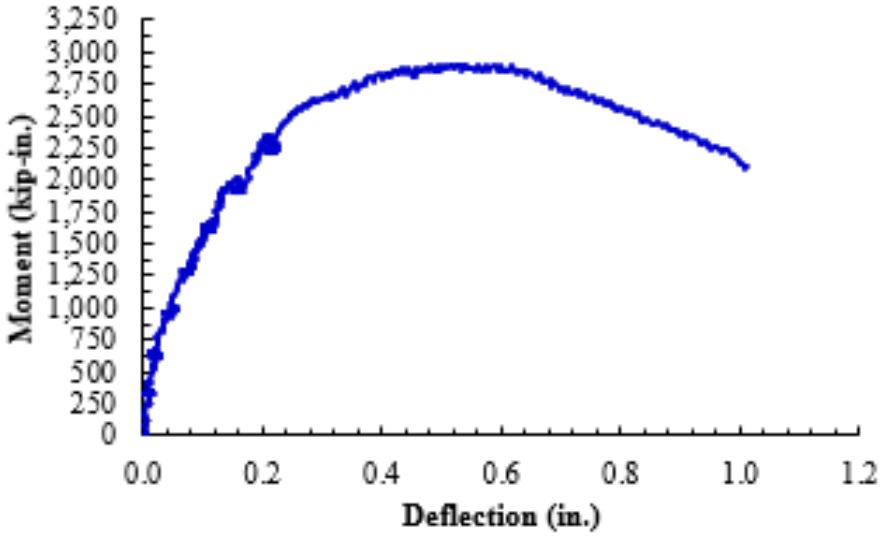

Figure B-42: S4-#9-[S.Ends] Applied Moment Against Midspan Deflection

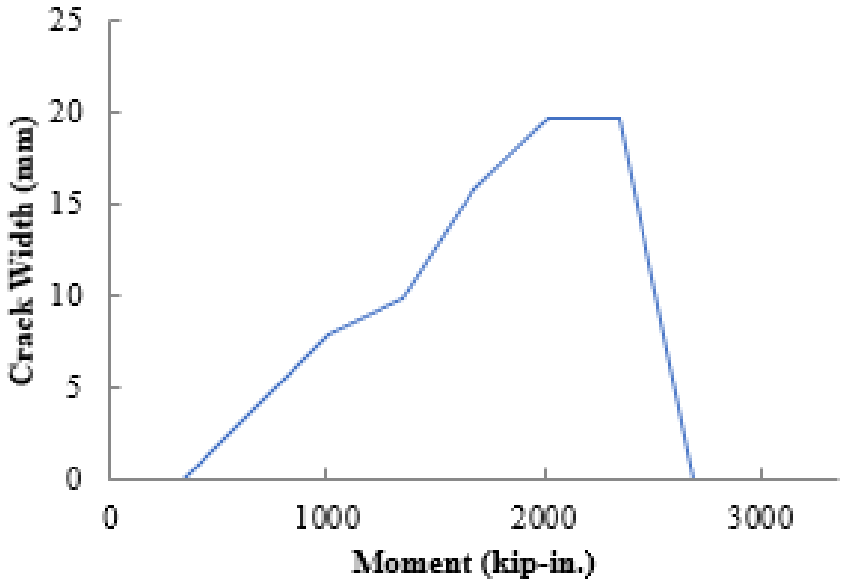

Figure B-43: S4-#9-[S.Ends] Interface Crack Growth Under Loading

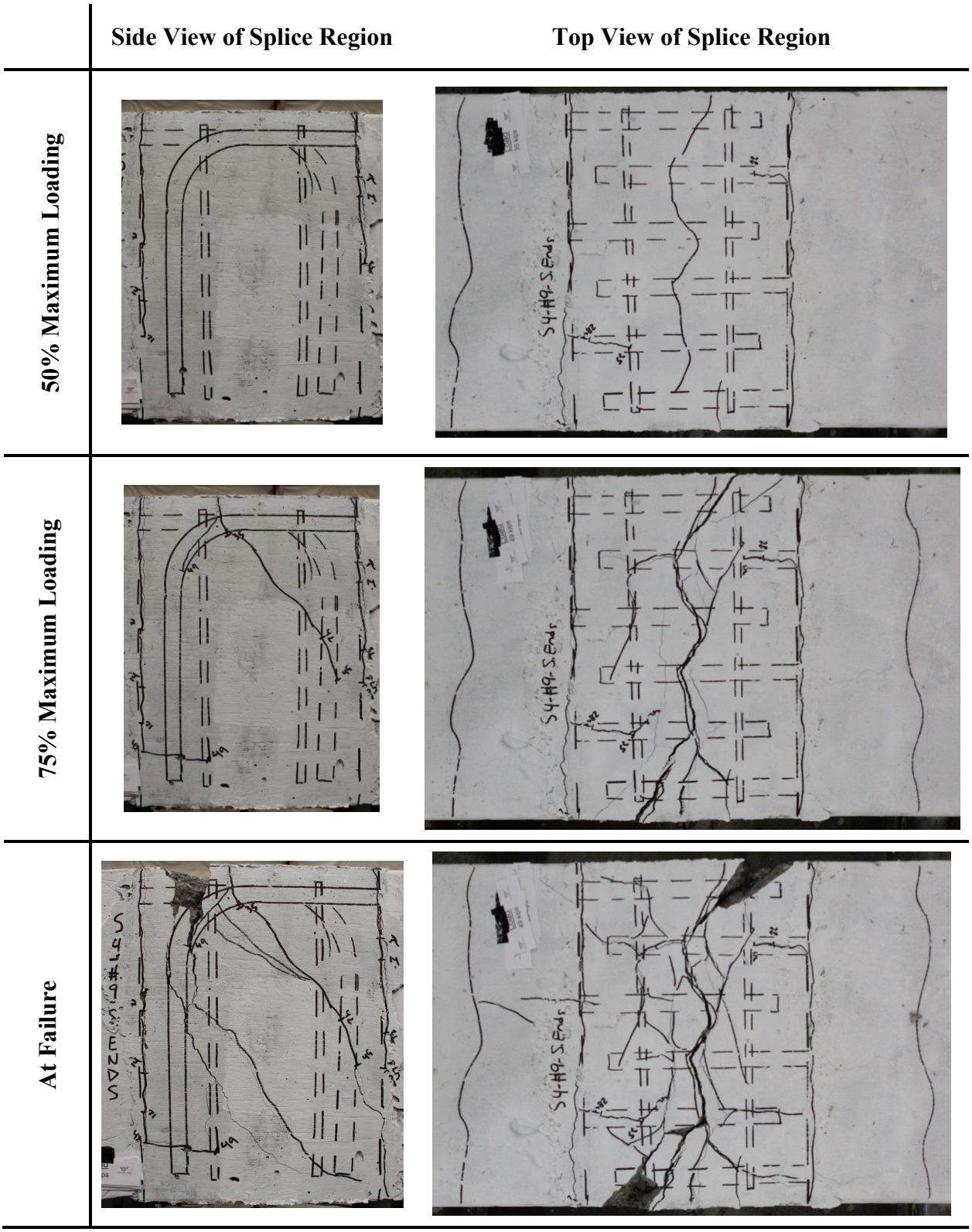

Figure B-44: Progression of Damage in Closure Joint of S4-#9-[S.Ends]

S4-#11-[S#4 Ends & Mid]

Summary:

Specimen S4-#11-[S.#4Ends&Mid] was designed to determine if the placement of the stirrups affects bond strength. For this Beam, No. 4 stirrups are placed at $2d_b$ from either spliced end with one No.3 stirrup placed midway through the closure.

Testing Notes:

Real support span was 5 ft. for this test.

Table B-36: S4-#11-[S.Ends&Mid] Specimen Properties

Configuration of Closure Joint

c_b (in.)	c_{so} (in.)	c_{si} (in.)	c_{th} (in.)	s_l (in.)	l_s (in.)	b (in.)	h (in.)	Secondary Reinforcement
1.71	1.551	0.936	1.621	4.448	17.250	16.688	28.063	No. 4 stirrups at $2d_b$ from either spliced end and one No. 4 stirrup at the middle of the splice length

Properties of Constitutive Materials

Precast Concrete			Cast-in-Place Concrete			Steel Reinforcing Bars		
f_{cm} (psi)	f_{stm} (psi)	E_{cm} (ksi)	f_{cm} (psi)	f_{stm} (psi)	E_{cm} (ksi)	d_b (in.)	f_y (psi)	R_r
3360	325	3250	4370	410	3400	1.41	66400	.0859

Table B-37: S4-#11-[S.Ends&Mid] Fresh Concrete Properties

Precast Concrete			Cast-in-Place Concrete		
Air Content (%)	Unit Weight (pcf)	Slump (in.)	Air Content (%)	Unit Weight (pcf)	Slump (in.)
8	135.4	8	5.2	147.7	4.5

Table B-38: S4-#11-[S.Ends&Mid] Loading Configuration and Test Results

A (in.)	B (in.)	C (in.)	δ_u (in.)	P_u (lb)	M_u (kip-in.)	$f_{s,mc}$ (ksi)
42	60	6	0.881	98,603	4194.3	58.168

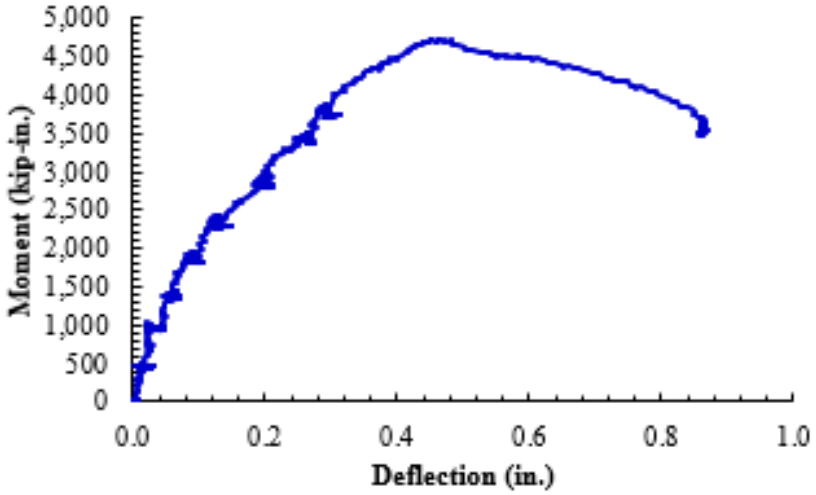

Figure B-42: S4-#11-[S.Ends&Mid] Applied Moment Against Midspan Deflection

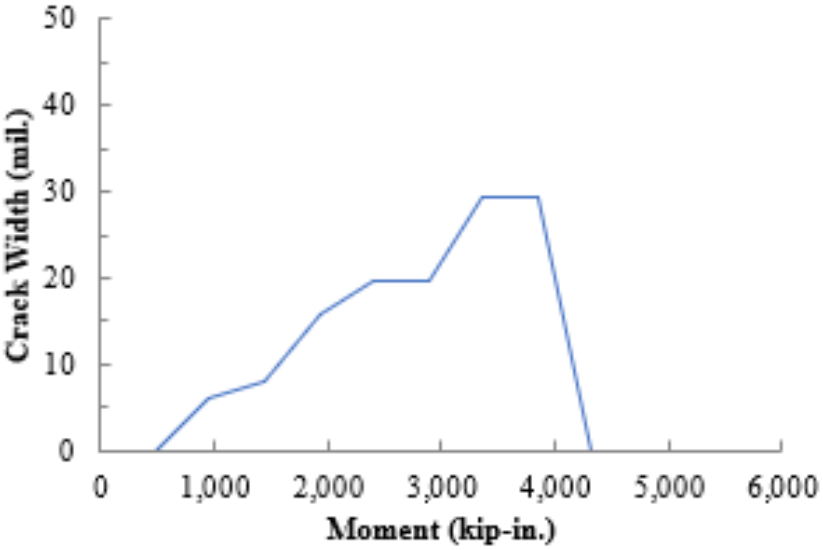

Figure B-43: S4-#11-[S.Ends&Mid] Interface Crack Growth Under Loading

	Side View of Splice Region	Top View of Splice Region
50% Maximum Loading	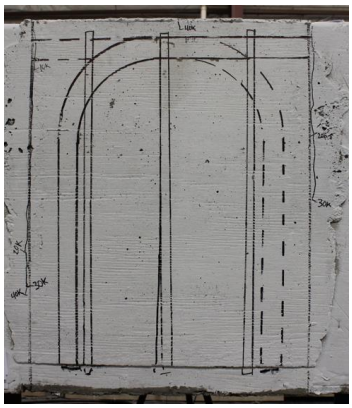	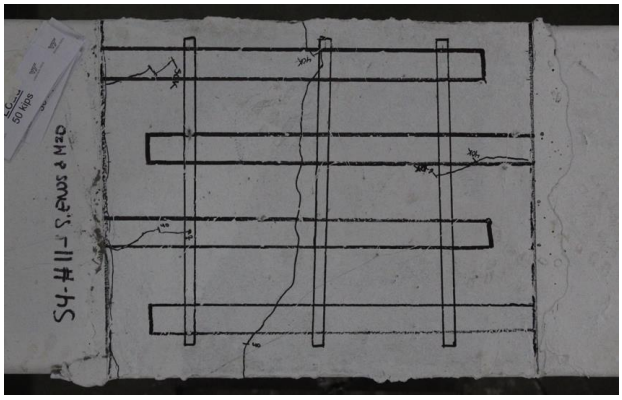
75% Maximum Loading	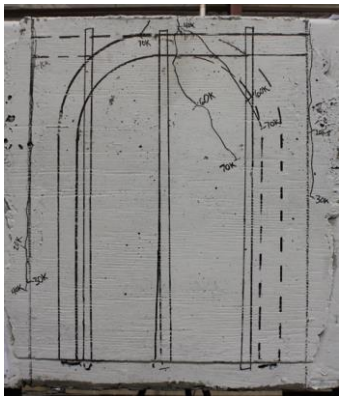	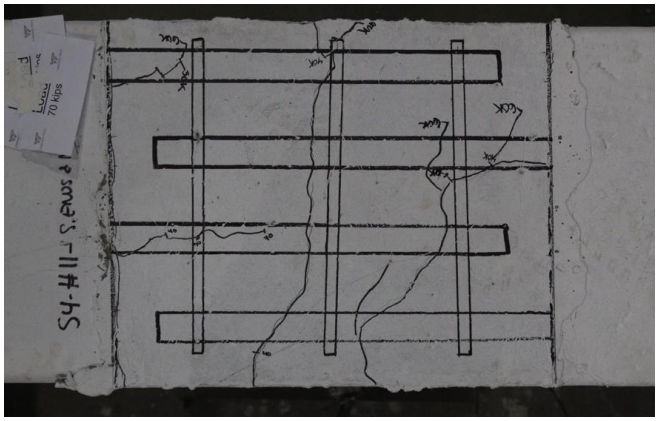
At Failure	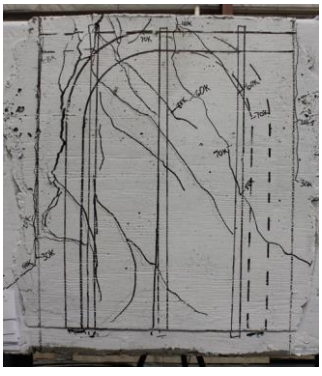	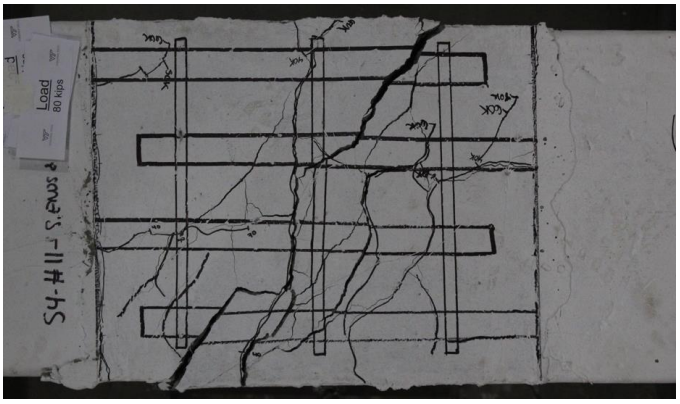

Figure B-44: Progression of Damage in Closure Joint of S4-#11-[S.Ends&Mid]

S4-#11-[S#4.4in. s_l]

Summary:

Specimen S4-#11-[S#4.4in. s_l] was designed to determine if the bar size of the stirrups affects bond strength. For this Beam, No. 4 stirrups are placed at $3d_b$ over the splice length.

Testing Notes:

None.

Table B-36: S4-#11-[S#4.4 in. s_l] Specimen Properties

Configuration of Closure Joint

c_b (in.)	c_{so} (in.)	c_{si} (in.)	c_{th} (in.)	s_l (in.)	l_s (in.)	b (in.)	h (in.)	Secondary Reinforcement
1.737	1.668	1.09	1.549	4.177	17.063	16.688	27.938	No. 4 stirrups placed at $3d_b$

Properties of Constitutive Materials

Precast Concrete			Cast-in-Place Concrete			Steel Reinforcing Bars		
f_{cm} (psi)	f_{stm} (psi)	E_{cm} (ksi)	f_{cm} (psi)	f_{stm} (psi)	E_{cm} (ksi)	d_b (in.)	f_y (psi)	R_r
3490	345	3350	3510	315	3200	1.41	66400	.07

Table B-37: S4-#11-[S#4.4 in. s_l] Fresh Concrete Properties

Precast Concrete			Cast-in-Place Concrete		
Air Content (%)	Unit Weight (pcf)	Slump (in.)	Air Content (%)	Unit Weight (pcf)	Slump (in.)
8	135.4	8	5.3	146.5	7

Table B-38: S4-#11-[S#4.4 in. s_l] Loading Configuration and Test Results

A (in.)	B (in.)	C (in.)	δ_u (in.)	P_u (lb)	M_u (kip-in.)	$f_{s,mc}$ (ksi)
48	48	6	1.444	83,720	4092.7	58.966

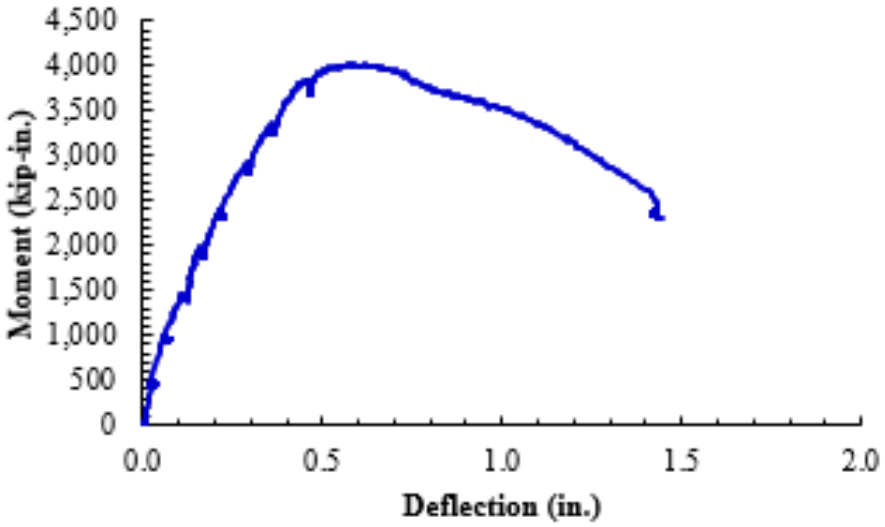

Figure B-42: S4-#11-[S#4.4 in. s_l] Applied Moment Against Midspan Deflection

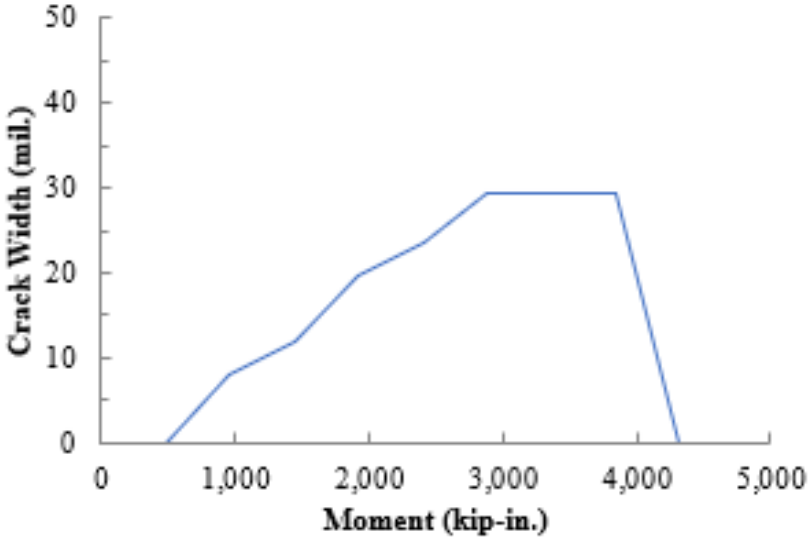

Figure B-43: S4-#11-[S#4.4 in. s_l] Interface Crack Growth Under Loading

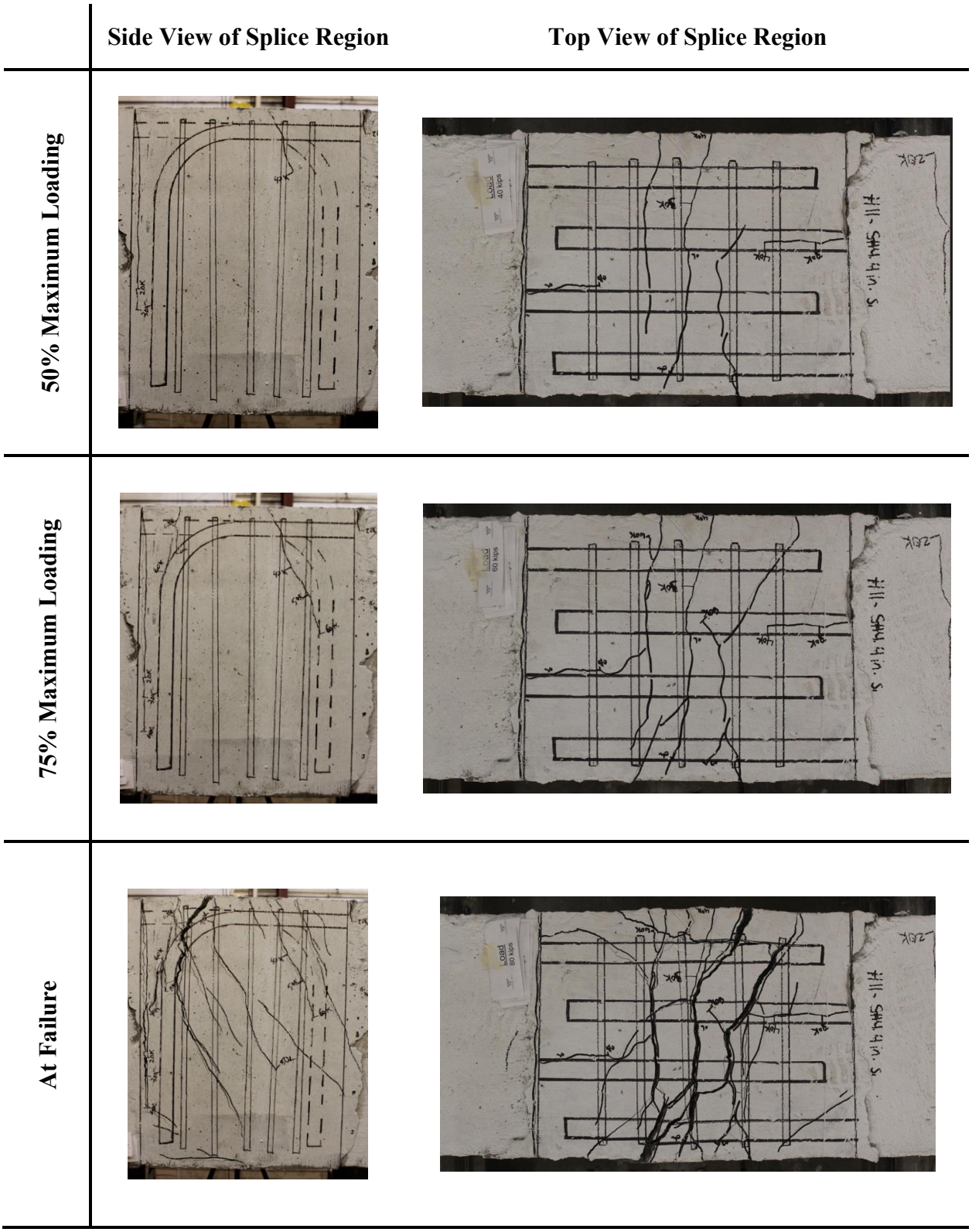

Figure B-44: Progression of Damage in Closure Joint of S4-#11-[S#4.4 in. s_l]

S12-#6-[4 splices]

Summary:

Specimen S12-#6-[4 splices] was designed to determine if the number of splices affects splice strength.

Testing Notes:

Real resistance might be slightly higher. Held load during last map cracking then it fell.

Table B-36: S12-#6-[4 splices] Specimen Properties

Configuration of Closure Joint								
c_b (in.)	c_{so} (in.)	c_{si} (in.)	c_{th} (in.)	s_l (in.)	l_s (in.)	b (in.)	h (in.)	Secondary Reinforcement
1.56	1.57	-	2.469	4.438	10.594	32	15.75	none

Properties of Constitutive Materials								
Precast Concrete			**Cast-in-Place Concrete**			**Steel Reinforcing Bars**		
f_{cm} (psi)	f_{stm} (psi)	E_{cm} (ksi)	f_{cm} (psi)	f_{stm} (psi)	E_{cm} (ksi)	d_b (in.)	f_y (psi)	R_r
3670	330	3400	3110	280	3130	.75	66100	.1304

Table B-37: S12-#6-[4 splices] Fresh Concrete Properties

Precast Concrete			Cast-in-Place Concrete		
Air Content (%)	Unit Weight (pcf)	Slump (in.)	Air Content (%)	Unit Weight (pcf)	Slump (in.)
8	138	3	8	-	8

Table B-38: S12-#6-[4 splices] Loading Configuration and Test Results

A (in.)	B (in.)	C (in.)	δ_u (in.)	P_u (lb)	M_u (kip-in.)	$f_{s,mc}$ (ksi)
48	48	6	0.931	24,062	1228.4	55.188

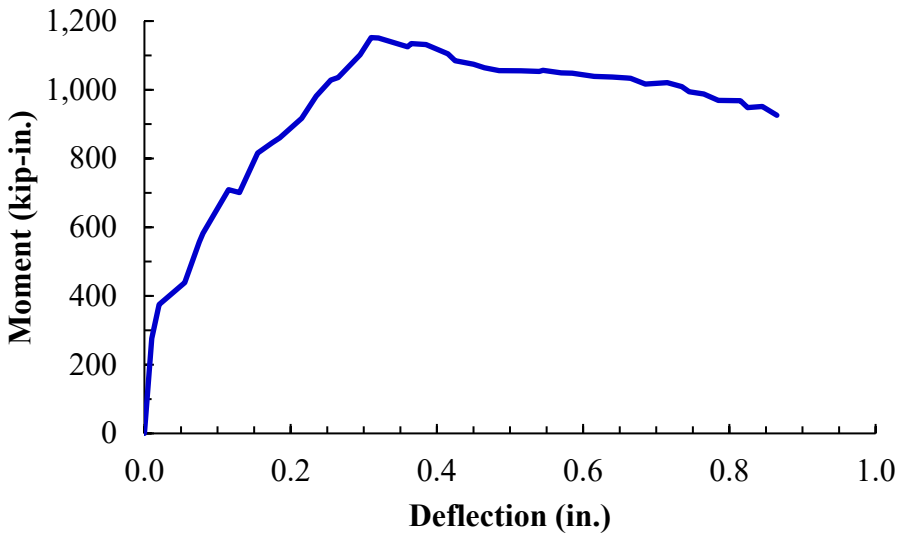

Figure B-42: S12-#6-[4 splices] Applied Moment Against Midspan Deflection

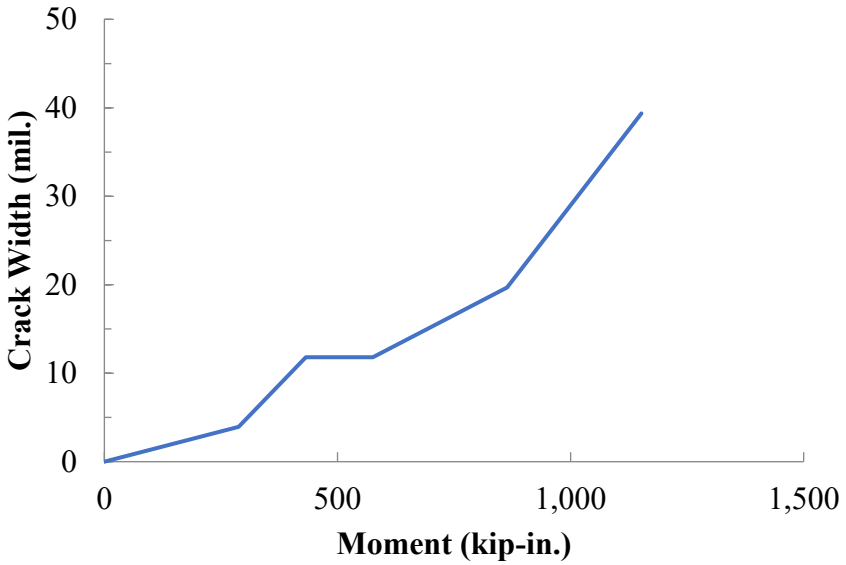

Figure B-43: S12-#6-[4 splices] Interface Crack Growth Under Loading

	Side View of Splice Region	Top View of Splice Region
50% Maximum Loading	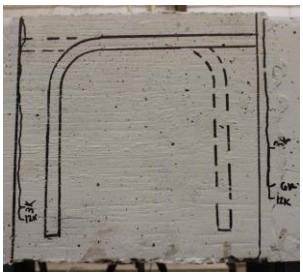	
75% Maximum Loading	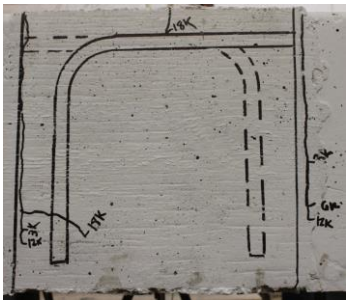	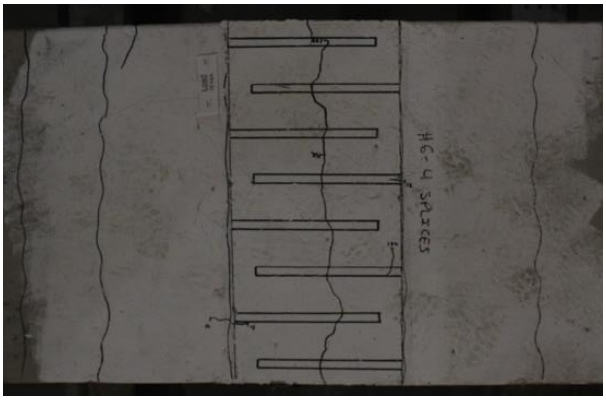
At Failure	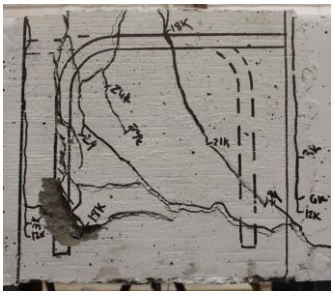	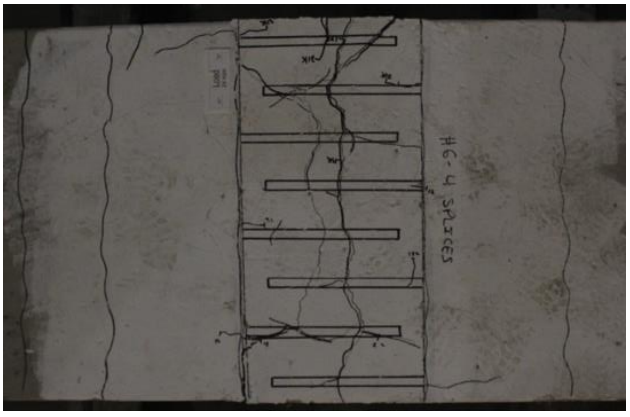

Figure B-44: Progression of Damage in Closure Joint of S12-#6-[4 splices]

S12-#6-[S.4 splices]

Summary:

Specimen S12-#6-[S.4 splices] was designed to determine if the number of splices affects splice strength. This specimen also has confinement in the form of No. 3 stirrups placed at $3d_b$ along the closure joint.

Testing Notes:

None.

Table B-36: S12-#6-[S.4 Splices] Specimen Properties

Configuration of Closure Joint

c_b (in.)	c_{so} (in.)	c_{si} (in.)	c_{th} (in.)	s_l (in.)	l_s (in.)	b (in.)	h (in.)	Secondary Reinforcement
1.958	1.844	-	1.811	3.820	7.844	31.875	16.125	No. 3 stirrups placed at $3d_b$

Properties of Constitutive Materials

Precast Concrete			Cast-in-Place Concrete			Steel Reinforcing Bars		
f_{cm} (psi)	f_{stm} (psi)	E_{cm} (ksi)	f_{cm} (psi)	f_{stm} (psi)	E_{cm} (ksi)	d_b (in.)	f_y (psi)	R_r
3790	390	3500	4370	410	3400	.75	66100	.1304

Table B-37: S12-#6-[S.4 Splices] Fresh Concrete Properties

Precast Concrete			Cast-in-Place Concrete		
Air Content (%)	Unit Weight (pcf)	Slump (in.)	Air Content (%)	Unit Weight (pcf)	Slump (in.)
8	138	3	5.2	147.7	4.5

Table B-38: S12-#6-[S.4 Splices] Loading Configuration and Test Results

A (in.)	B (in.)	C (in.)	δ_u (in.)	P_u (lb)	M_u (kip-in.)	$f_{s,mc}$ (ksi)
48	48	4.25	2.076	30,646	1541.1	66.686

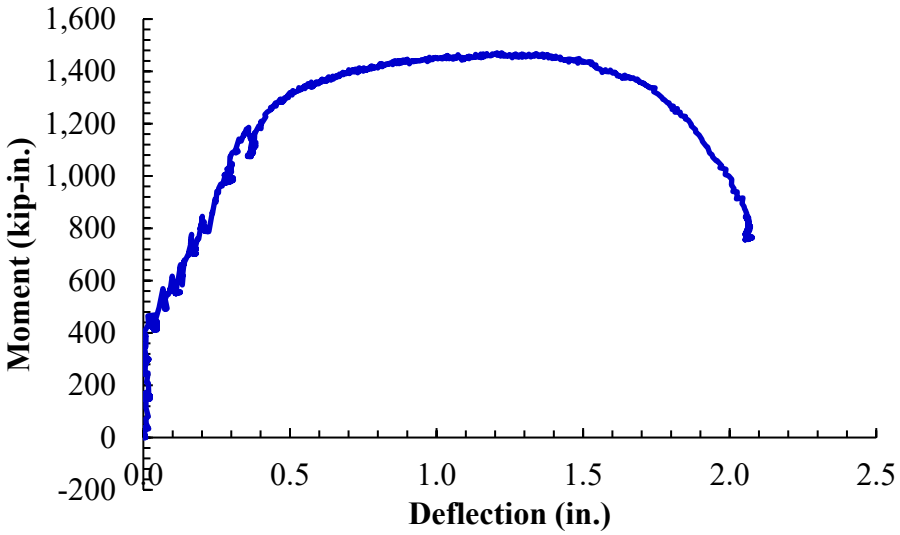

Figure B-42: S12-#6-[S.4 Splices] Applied Moment Against Midspan Deflection

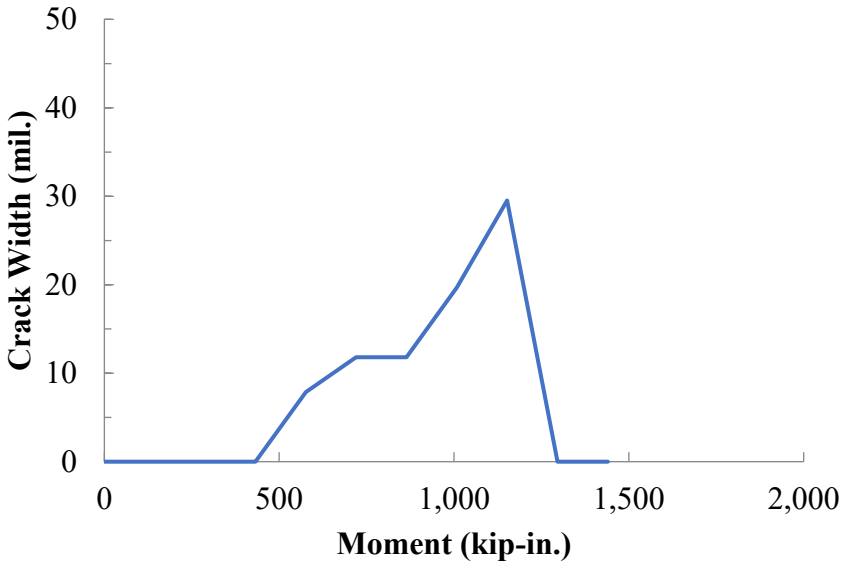

Figure B-43: S12-#6-[S.4 Splices] Interface Crack Growth Under Loading

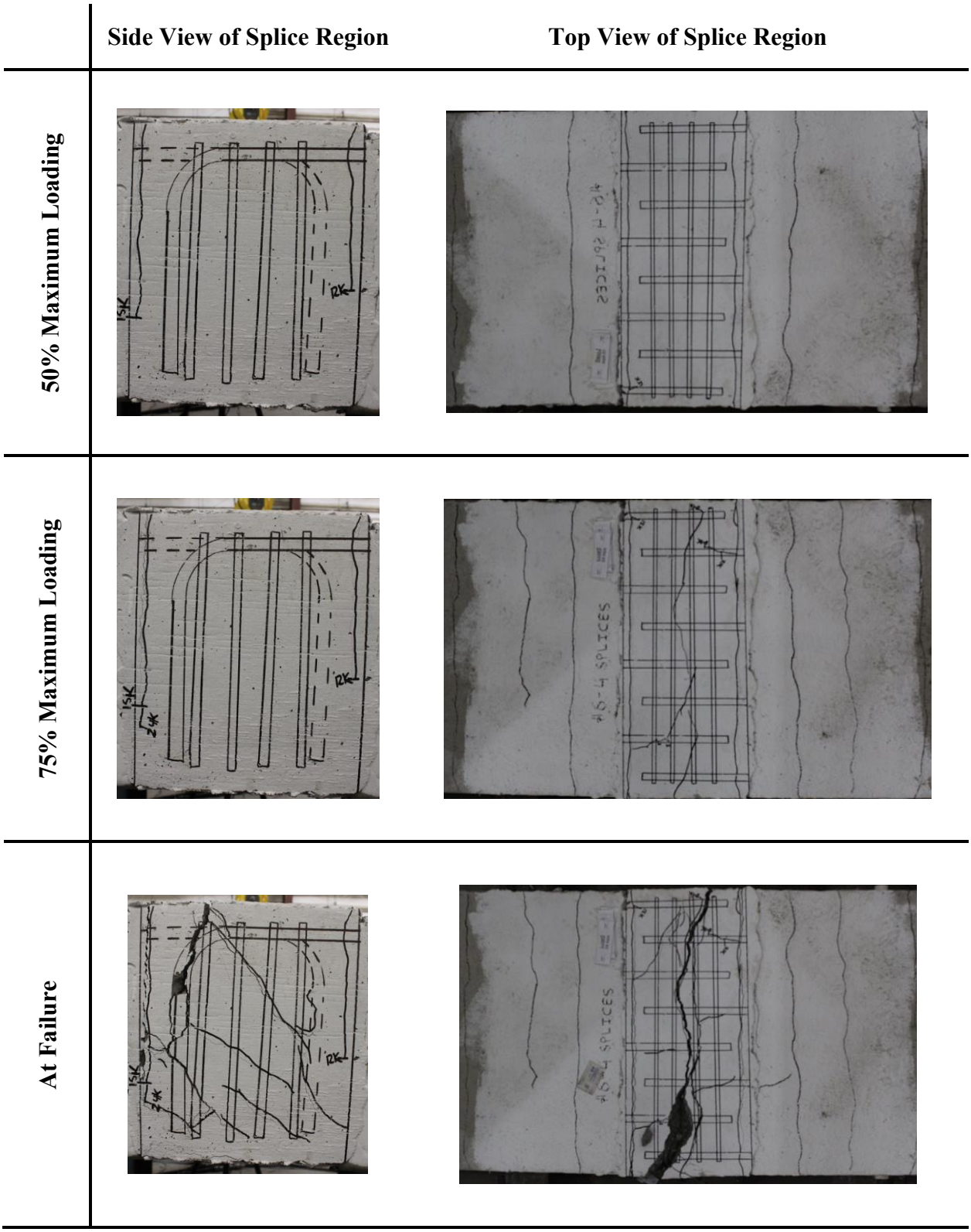

Figure B-44: Progression of Damage in Closure Joint of S12-#6-[S.4 Splices]

S12-#11-[S#4.3 splices]

Summary:

Specimen S12-#11-[S#4. 3 splices] was designed to determine if the number of splices affects splice strength. This specimen also has confinement in the form of No. 4 stirrups placed at $3d_b$ along the closure joint.

Testing Notes:

None.

Table B-36: S12-#11-[S#4.3 splices] Specimen Properties

Configuration of Closure Joint

c_b (in.)	c_{so} (in.)	c_{si} (in.)	c_{th} (in.)	s_l (in.)	l_s (in.)	b (in.)	h (in.)	Secondary Reinforcement
1.998	1.51	1.246	1.73	4.006	17.042	24.25	25.25	No. 4 stirrups placed at $3d_b$

Properties of Constitutive Materials

Precast Concrete			Cast-in-Place Concrete			Steel Reinforcing Bars		
f_{cm} (psi)	f_{stm} (psi)	E_{cm} (ksi)	f_{cm} (psi)	f_{stm} (psi)	E_{cm} (ksi)	d_b (in.)	f_y (psi)	R_r
5700	385	3750	6040	455	3650	1.41	66400	.0859

Table B-37: S12-#11-[S#4.3 splices] Fresh Concrete Properties

Precast Concrete			Cast-in-Place Concrete		
Air Content (%)	Unit Weight (pcf)	Slump (in.)	Air Content (%)	Unit Weight (pcf)	Slump (in.)
5.2	147	4.5	6	148.3	5

Table B-38: S12-#11-[S#4.3 splices] Loading Configuration and Test Results

A (in.)	B (in.)	C (in.)	δ_u (in.)	P_u (lb)	M_u (kip-in.)	$f_{s,mc}$ (ksi)
48	48	4	1.341	141,519	6888	63.86

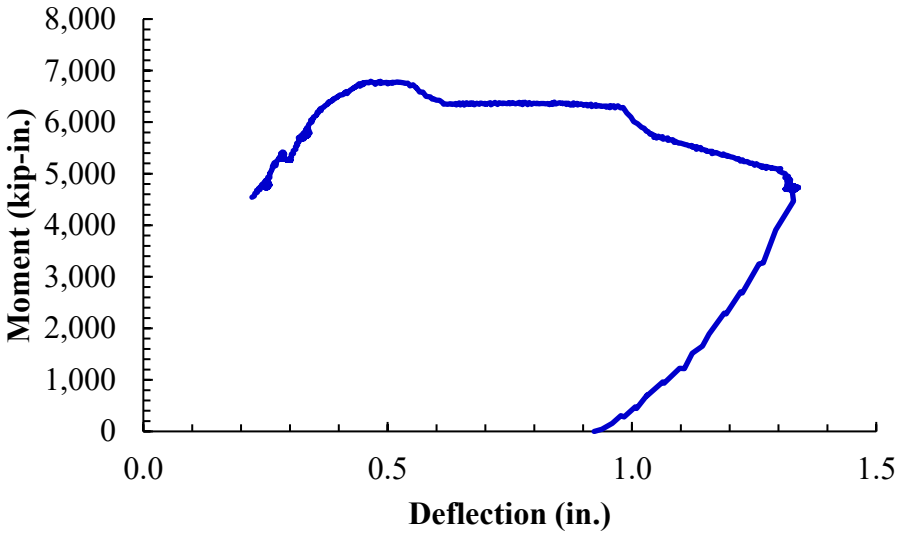

Figure B-42: S12-#11-[S#4.3 splices] Applied Moment Against Midspan Deflection

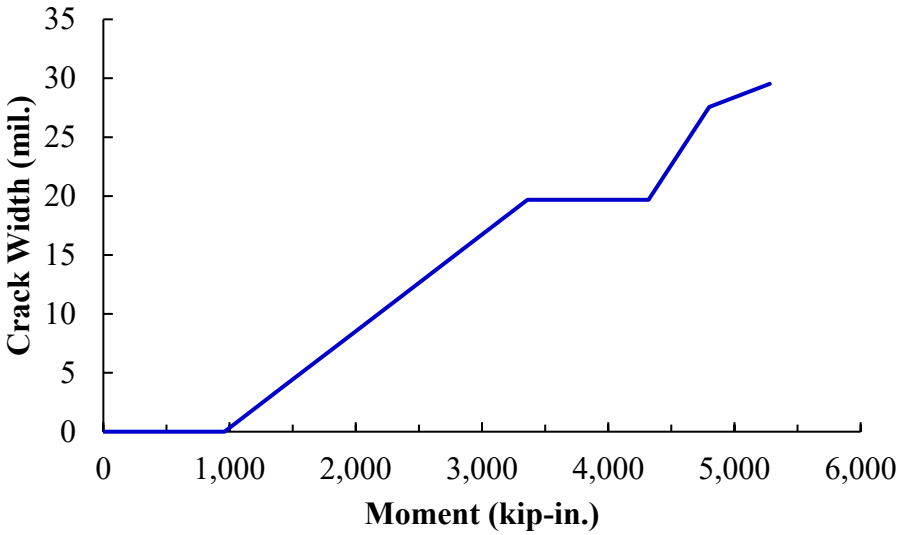

Figure B-43: S12-#11-[S#4.3 splices] Interface Crack Growth Under Loading

	Side View of Splice Region	Top View of Splice Region
50% Maximum Loading	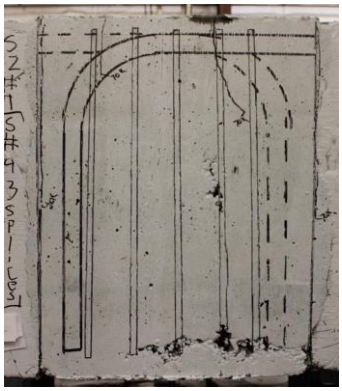	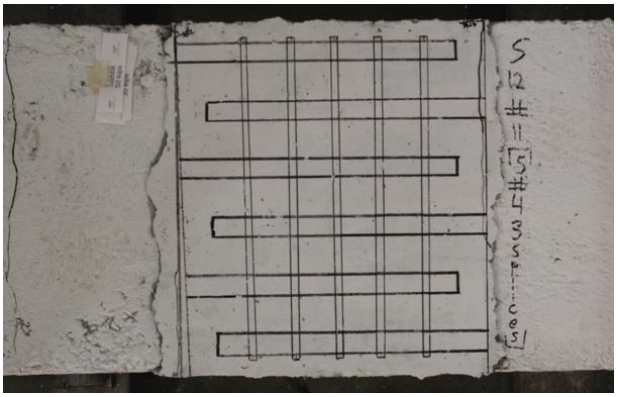
75% Maximum Loading	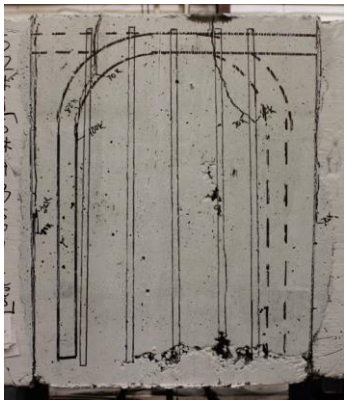	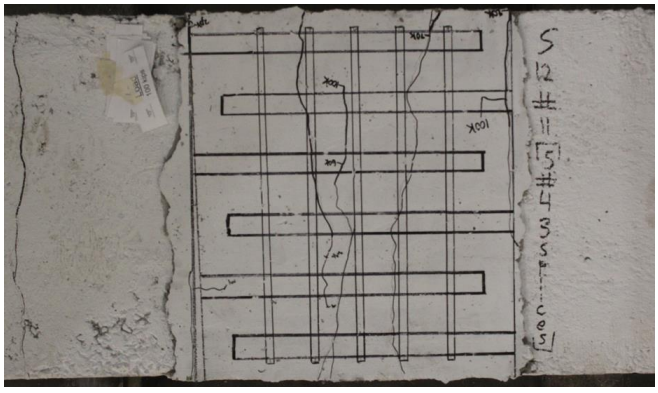
At Failure	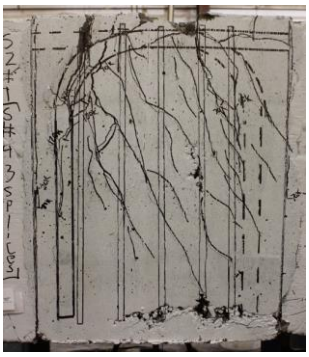	

Figure B-44: Progression of Damage in Closure Joint of S12-#11-[S#4.3 splices]

S13-#6-[F.4 in. s_l]

Summary:

Specimen S13-#6-[F.4 in. s_l] was designed to investigate the influence of a 1% steel fiber dosage on the performance of noncontact hooked bar lap splices. The specimen failed due to hook side bulging after yielding of the hooked bars. Face-splitting cracks were present.

Testing Notes:

None.

Table B-36: S13-#6-[F.4 in. s_l] Specimen Properties

Configuration of Closure Joint

c_b (in.)	c_{so} (in.)	c_{si} (in.)	c_{th} (in.)	s_l (in.)	l_s (in.)	b (in.)	h (in.)	Secondary Reinforcement
1.679	1.774	1.633	1.406	3.932	6.146	24.125	15.875	none

Properties of Constitutive Materials

Precast Concrete			Cast-in-Place Concrete			Steel Reinforcing Bars		
f_{cm} (psi)	f_{stm} (psi)	E_{cm} (ksi)	f_{cm} (psi)	f_{stm} (psi)	E_{cm} (ksi)	d_b (in.)	f_y (psi)	R_r
3,650	350	3,400	4,980	690	3,600	0.75	66,100	0.130

Table B-37: S4-#6-[F.4 in. s_l] Fresh Concrete Properties

Precast Concrete			Cast-in-Place Concrete		
Air Content (%)	Unit Weight (pcf)	Slump (in.)	Air Content (%)	Unit Weight (pcf)	Slump (in.)
7.8	138.0	8.0	6.0	145.8	2.0

Table B-38: S4-#6-[F.4 in. s_l] Loading Configuration and Test Results

A (in.)	B (in.)	C (in.)	δ_u (in.)	P_u (lb)	M_u (kip-in.)	$f_{s,mc}$ (ksi)
48	48	6.00	1.39	24,129	1,220	69.824

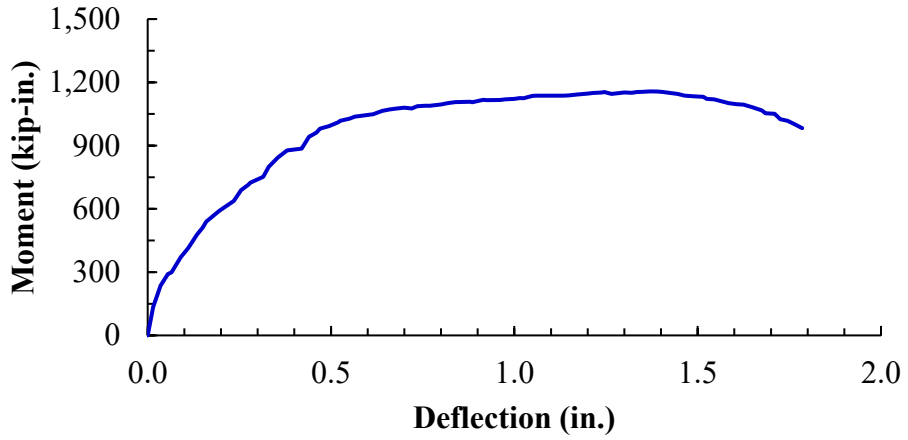

Figure B-42: S4-#6-[F.4 in. s_1] Applied Moment Against Midspan Deflection

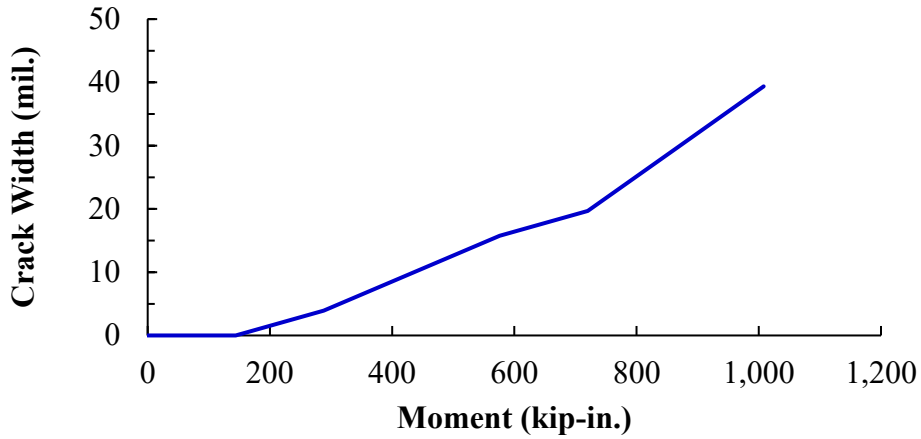

Figure B-43: S4-#6-[F.4 in. s_1] Interface Crack Growth Under Loading

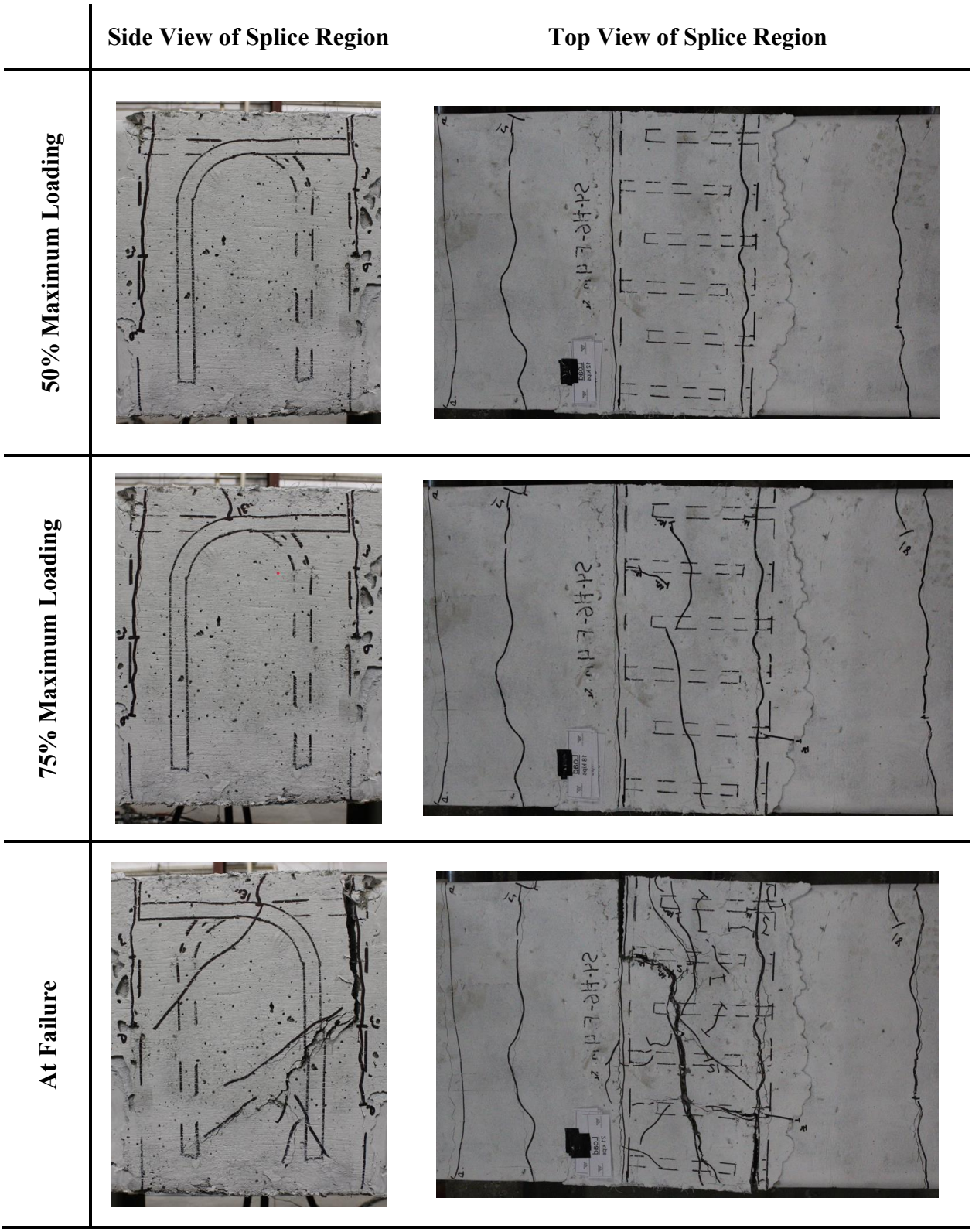

Figure B-44: Progression of Damage in Closure Joint of S4-#6-[F.4 in. s_l]

S13-#6-[S.F.4in. s_l]

Summary:

Specimen S13-#6-[S.F.4 in. s_l] was designed to investigate the influence of a 1% steel fiber dosage on the performance of noncontact hooked bar lap splices. This beam investigates fiber dosage with the addition of confinement in the form of No. 3 stirrups placed at $3d_b$.

Testing Notes:

Steel Fibers not mixed perfectly.

Table B-36: S13-#6-[S.F.4 in. s_l] Specimen Properties

Configuration of Closure Joint

c_b (in.)	c_{so} (in.)	c_{si} (in.)	c_{th} (in.)	s_l (in.)	l_s (in.)	b (in.)	h (in.)	Secondary Reinforcement
1.71	1.495	1.219	1.813	4.292	10.042	24.125	23.25	No. 3 stirrups placed at $3d_b$

Properties of Constitutive Materials

Precast Concrete			Cast-in-Place Concrete			Steel Reinforcing Bars		
f_{cm} (psi)	f_{stm} (psi)	E_{cm} (ksi)	f_{cm} (psi)	f_{stm} (psi)	E_{cm} (ksi)	d_b (in.)	f_y (psi)	R_r
5740	410	3950	3200	460	3300	.75	66100	.1304

Table B-37: S13-#6-[S.F.4 in. s_l] Fresh Concrete Properties

Precast Concrete			Cast-in-Place Concrete		
Air Content (%)	Unit Weight (pcf)	Slump (in.)	Air Content (%)	Unit Weight (pcf)	Slump (in.)
6	143.1	6	8	-	3

Table B-38: S13-#6-[S.F.4 in. s_l] Loading Configuration and Test Results

A (in.)	B (in.)	C (in.)	δ_u (in.)	P_u (lb)	M_u (kip-in.)	$f_{s,mc}$ (ksi)
48	48	6	1.368	69800	3435.62	60.784

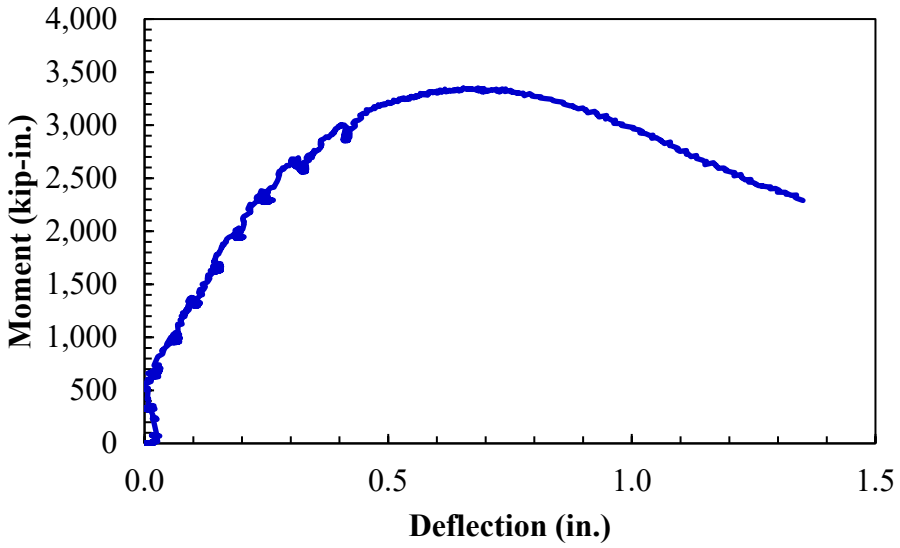

Figure B-42: S13-#6-[S.F.4 in. s_l] Applied Moment Against Midspan Deflection

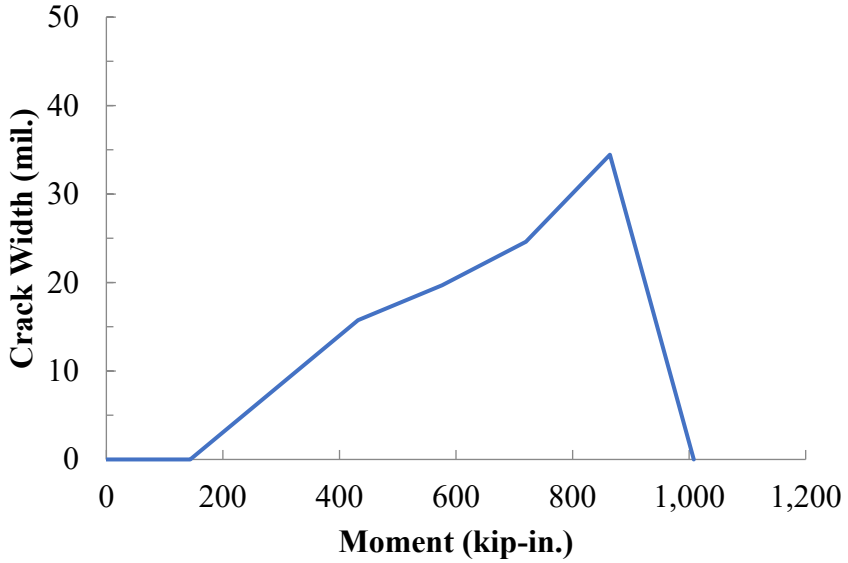

Figure B-43: S13-#6-[S.F.4 in. s_l] Interface Crack Growth Under Loading

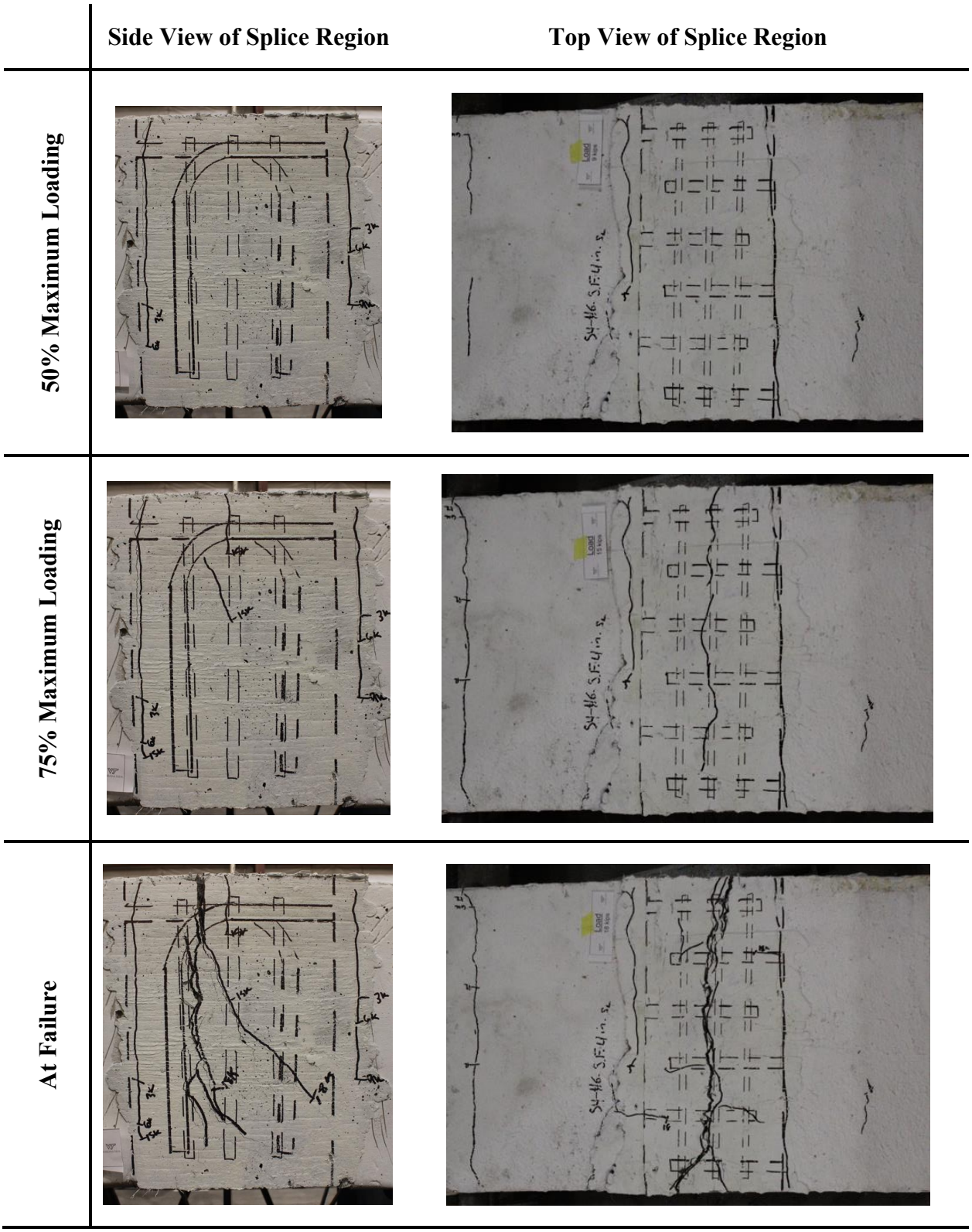

Figure B-44: Progression of Damage in Closure Joint of S13-#6-[S.F.4 in. s_l]

S13-#9-[F.4 in. s_l]

Summary:

Specimen S13-#9-[F.4 in. s_l] was designed to investigate the influence of a 1% steel fiber dosage on the performance of noncontact hooked bar lap splices.

Testing Notes:

East deflection is higher because the roller is there, which suggests the higher deflection is due to the roller.

Table B-36: S13-#9-[F.4 in. s_l] Specimen Properties

Configuration of Closure Joint								
c_b (in.)	c_{so} (in.)	c_{si} (in.)	c_{th} (in.)	s_l (in.)	l_s (in.)	b (in.)	h (in.)	Secondary Reinforcement
1.563	1.891	1.325	2.094	3.928	9.667	24.25	23.25	none

Properties of Constitutive Materials								
Precast Concrete			Cast-in-Place Concrete			Steel Reinforcing Bars		
f_{cm} (psi)	f_{stm} (psi)	E_{cm} (ksi)	f_{cm} (psi)	f_{stm} (psi)	E_{cm} (ksi)	d_b (in.)	f_y (psi)	R_r
5730	400	3900	3290	465	3100	1.128	61600	.07

Table B-37: S13-#9-[F.4 in. s_l] Fresh Concrete Properties

Precast Concrete			Cast-in-Place Concrete		
Air Content (%)	Unit Weight (pcf)	Slump (in.)	Air Content (%)	Unit Weight (pcf)	Slump (in.)
6	143.1	6	8	141.5	3

Table B-38: S13-#9-[F.4 in. s_l] Loading Configuration and Test Results

A (in.)	B (in.)	C (in.)	δ_u (in.)	P_u (lb)	M_u (kip-in.)	$f_{s,mc}$ (ksi)
48	48	6.5	0.853	68,210	3360.91	58.958

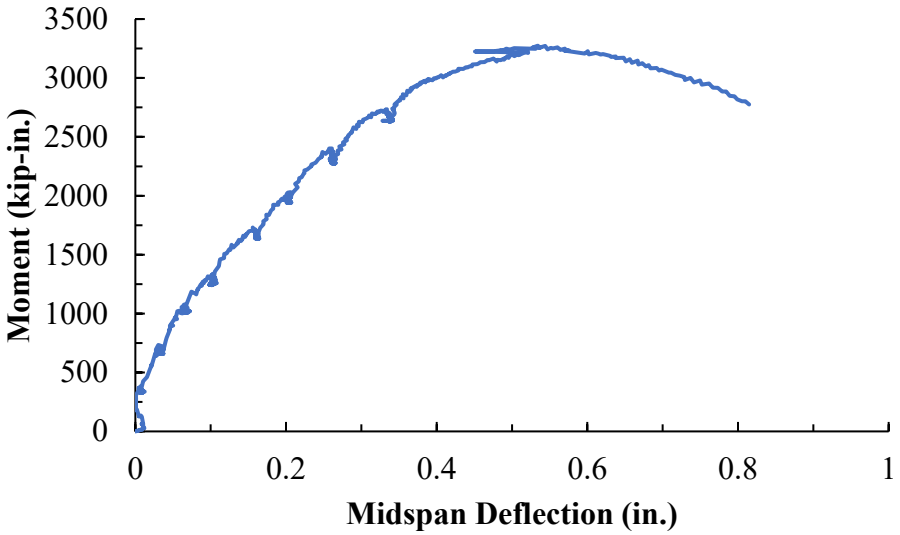

Figure B-42: S13-#9-[F.4 in. s_l] Applied Moment Against Midspan Deflection

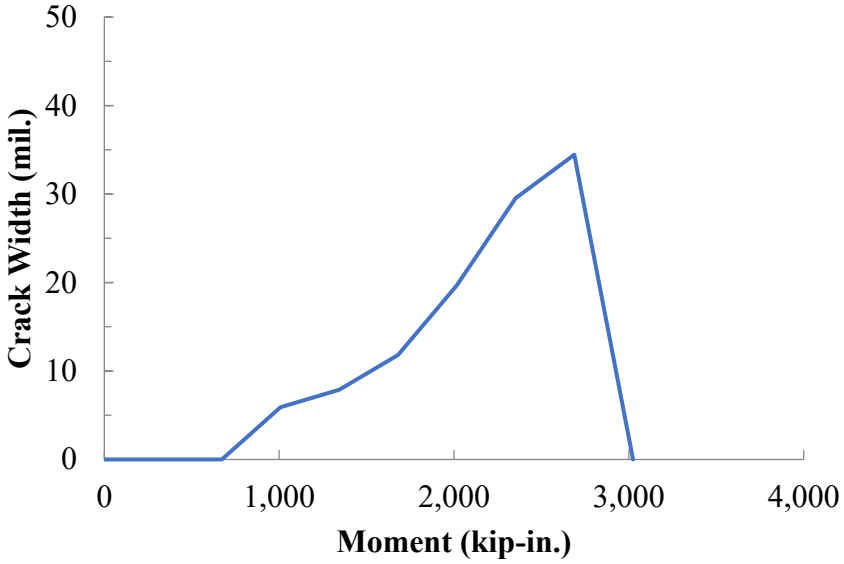

Figure B-43: S13-#9-[F.4 in. s_l] Interface Crack Growth Under Loading

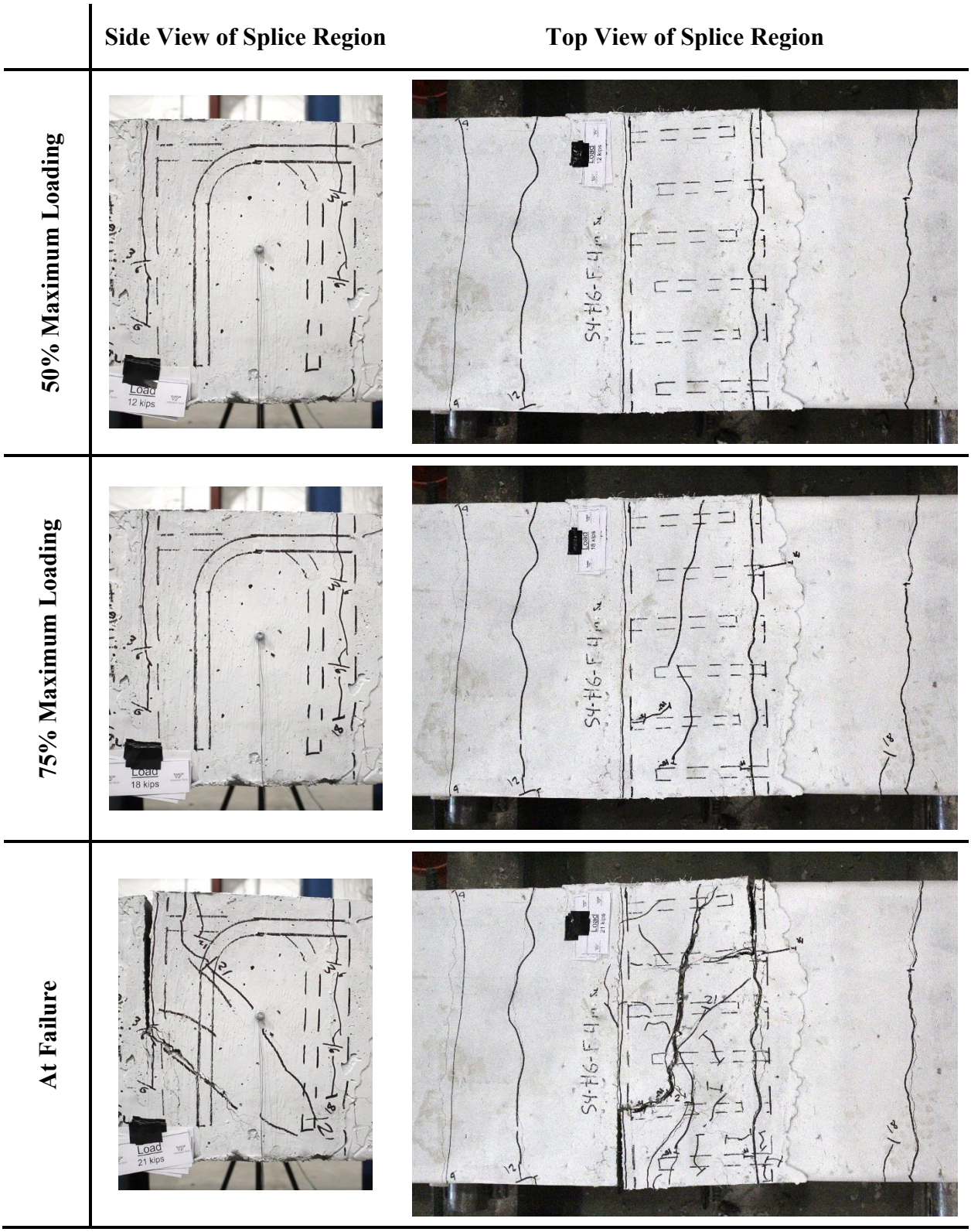

Figure B-44: Progression of Damage in Closure Joint of S13-#9-[F.4 in. s_l]

S13-#9-[S.F.4 in. s_l]

Summary:

Specimen S13-#9-[S.F.4 in. s_l] was designed to investigate the influence of a 1% steel fiber dosage on the performance of noncontact hooked bar lap splices. This beam investigates fiber dosage with the addition of confinement in the form of No. 3 stirrups placed at $3d_b$.

Testing Notes:

None.

Table B-36: S13-#9-[S.F.4 in. s_l] Specimen Properties

Configuration of Closure Joint								
c_b (in.)	c_{so} (in.)	c_{si} (in.)	c_{th} (in.)	s_l (in.)	l_s (in.)	b (in.)	h (in.)	**Secondary Reinforcement**
1.71	1.495	1.1.219	1.813	4.292	10.042	24.125	23.25	No. 3 stirrups placed at $3d_b$

Properties of Constitutive Materials								
Precast Concrete			**Cast-in-Place Concrete**			**Steel Reinforcing Bars**		
f_{cm} (psi)	f_{stm} (psi)	E_{cm} (ksi)	f_{cm} (psi)	f_{stm} (psi)	E_{cm} (ksi)	d_b (in.)	f_y (psi)	R_r
5740	410	3950	3200	460	3300	1.128	61600	.07

Table B-37: S13-#9-[S.F.4 in. s_l] Fresh Concrete Properties

Precast Concrete			**Cast-in-Place Concrete**		
Air Content (%)	**Unit Weight (pcf)**	**Slump (in.)**	**Air Content (%)**	**Unit Weight (pcf)**	**Slump (in.)**
6	143.1	6	8	-	3

Table B-38: S13-#9-[S.F.4 in. s_l] Loading Configuration and Test Results

A (in.)	B (in.)	C (in.)	δ_u (in.)	P_u (lb)	M_u (kip-in.)	$f_{s,mc}$ (ksi)
48	48	6	1.483	69.799	3435.62	60.784

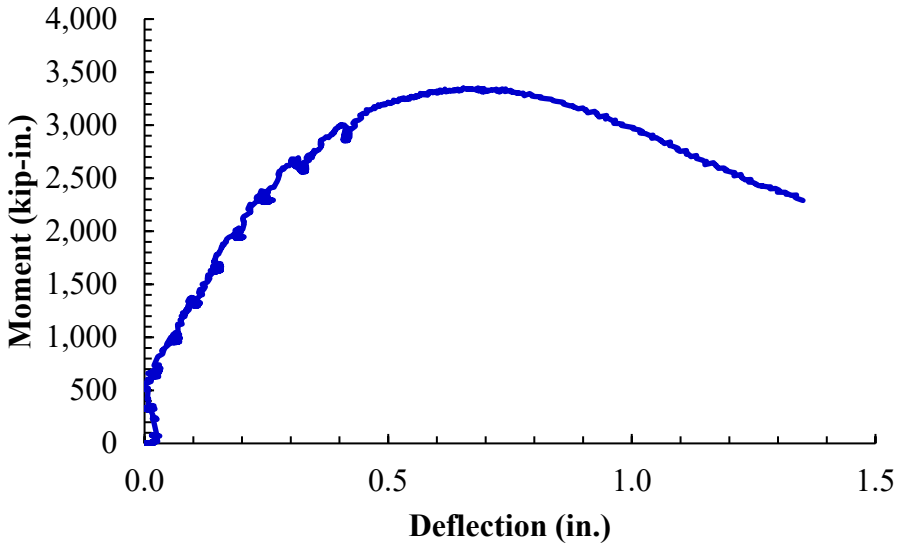

Figure B-42: S4-#6-[F.4 in. s_l] Applied Moment Against Midspan Deflection

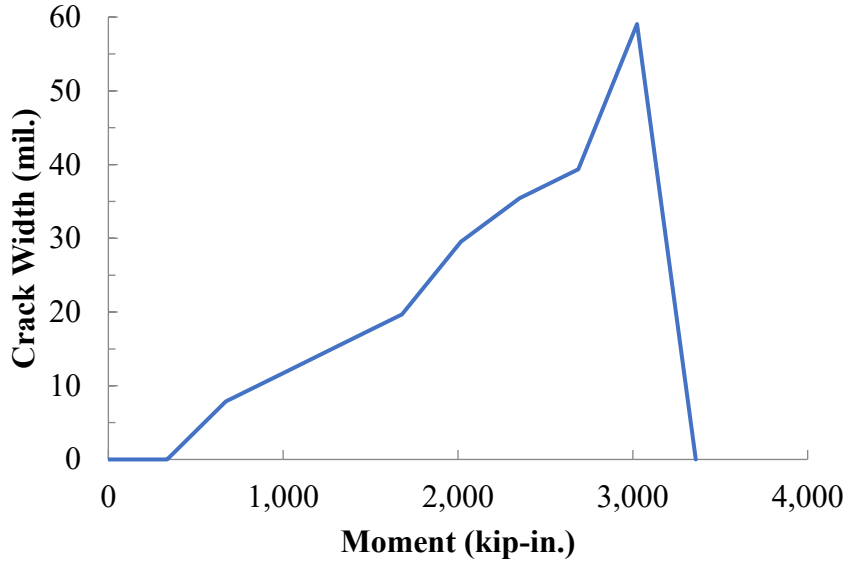

Figure B-43: S4-#6-[F.4 in. s_l] Interface Crack Growth Under Loading

	Side View of Splice Region	Top View of Splice Region
50% Maximum Loading	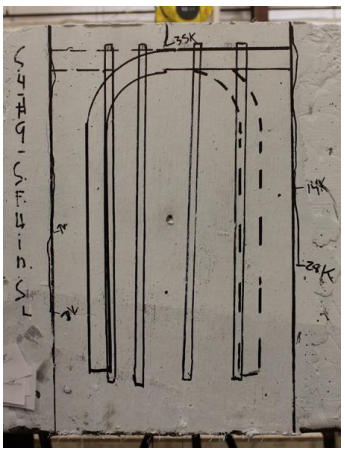	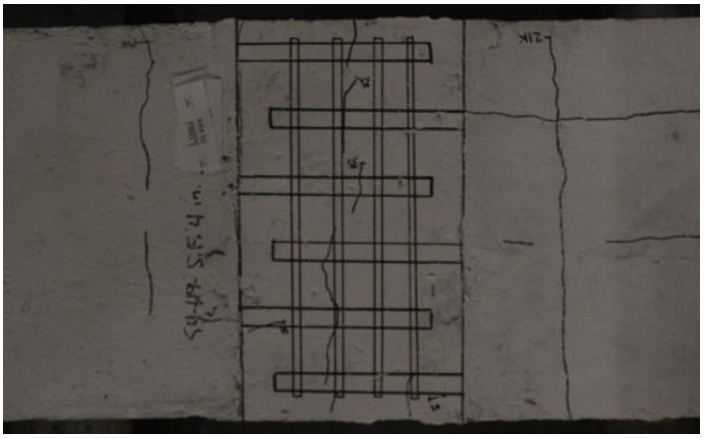
75% Maximum Loading	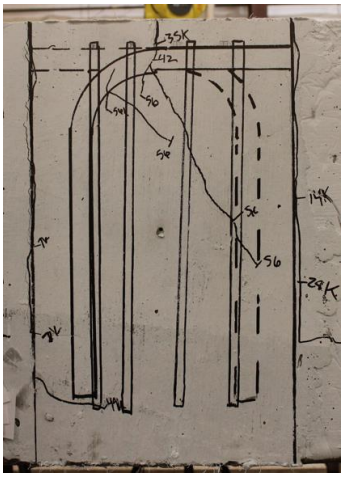	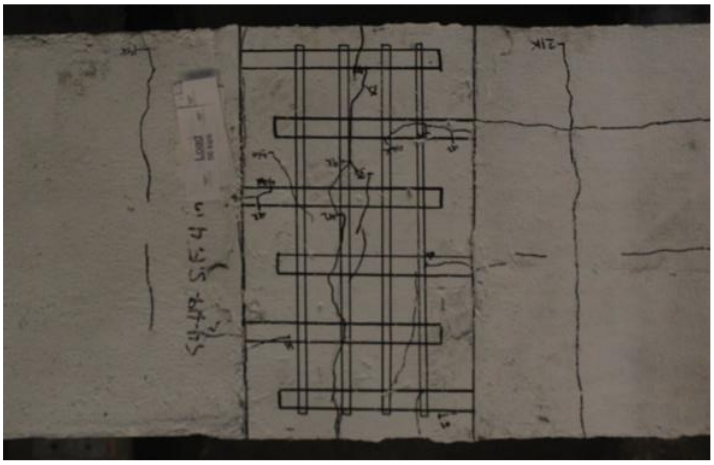
At Failure	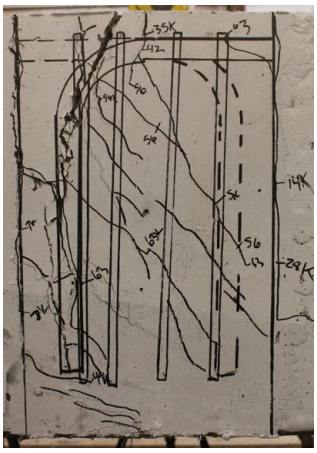	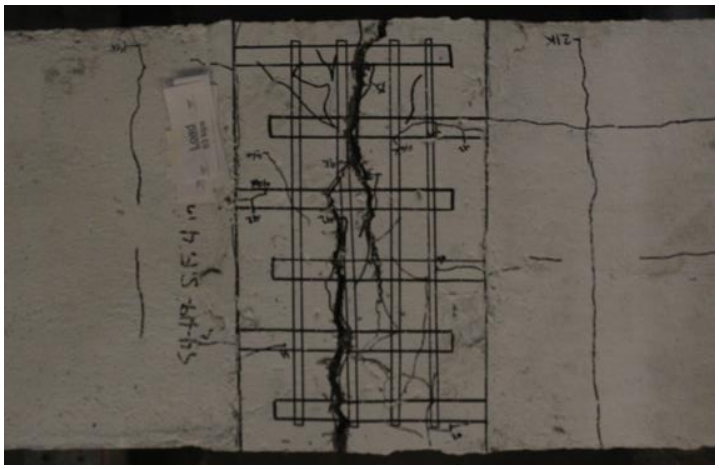

Figure B-44: Progression of Damage in Closure Joint of S13-#9-[S.F.4 in. s_l]

S13-#9-[F.3in. c_b&c_{so}]

Summary:

Specimen S13-#6-[S.F.4 in. s_l] was designed to investigate the influence of a 1% steel fiber dosage on the performance of noncontact hooked bar lap splices. This beam investigates fiber dosage with the addition of confinement in the form of 3 in. of bottom and side cover.

Testing Notes:

Real support span was 5 ft. for this test.

Table B-36: S13-#9-[F.3 in. c_b &c_{so}] Specimen Properties

Configuration of Closure Joint								
c_b (in.)	c_{so} (in.)	c_{si} (in.)	c_{th} (in.)	s_l (in.)	l_s (in.)	b (in.)	h (in.)	Secondary Reinforcement
3.24	3.175	1.203	2.135	4.193	8.625	27.125	26.25	3 in. concrete cover

Properties of Constitutive Materials								
Precast Concrete			**Cast-in-Place Concrete**			**Steel Reinforcing Bars**		
f_{cm} (psi)	f_{stm} (psi)	E_{cm} (ksi)	f_{cm} (psi)	f_{stm} (psi)	E_{cm} (ksi)	d_b (in.)	f_y (psi)	R_r
3360	325	3250	4560	640	3550	1.128	61600	.07

Table B-37: S13-#9-[F.3 in. c_b &c_{so}] Fresh Concrete Properties

Precast Concrete			Cast-in-Place Concrete		
Air Content (%)	Unit Weight (pcf)	Slump (in.)	Air Content (%)	Unit Weight (pcf)	Slump (in.)
8	135.4	8	5.2	151.9	1

Table B-38: S13-#9-[F.3 in. c_b &c_{so}] Loading Configuration and Test Results

A (in.)	B (in.)	C (in.)	δ_u (in.)	P_u (lb)	M_u (kip-in.)	$f_{s,mc}$ (ksi)
42	60	6	1.229	105,825	4510.79	69.829

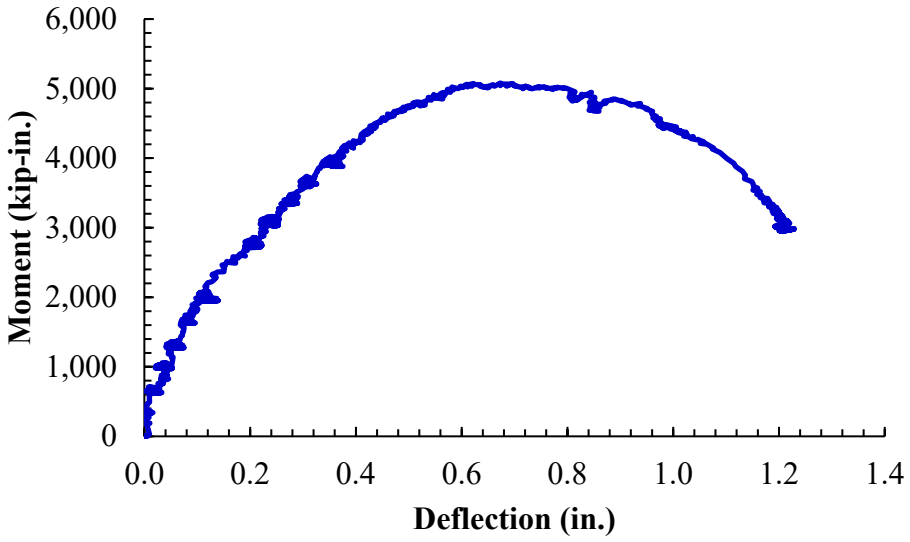

Figure B-42: S13-#9-[F.3 in. c_b &c_{so}] Applied Moment Against Midspan Deflection

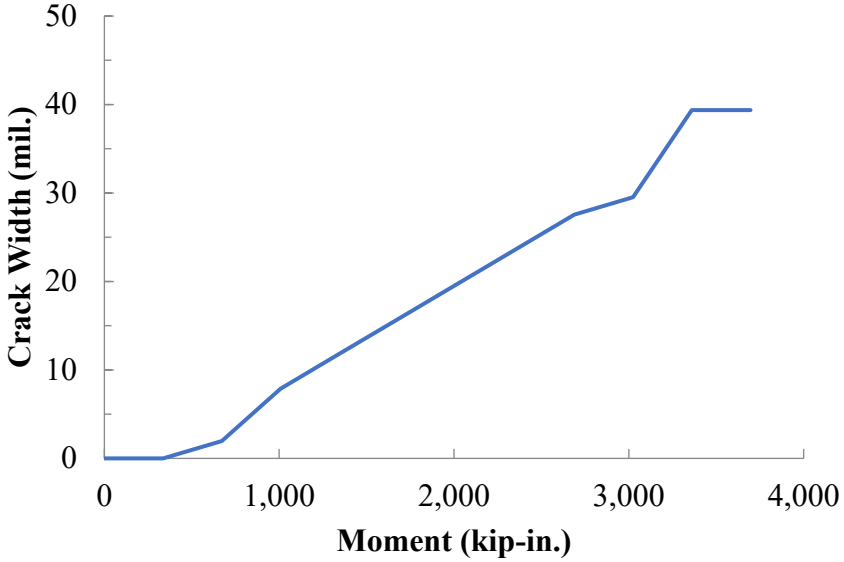

Figure B-43: S13-#9-[F.3 in. c_b &c_{so}] Interface Crack Growth Under Loading

*Photos not available for this beam due to camera malfunction during tests.

S13-#9-[S.F.3in. c_b&c_{so}]

Summary:

Specimen S13-#6-[S.F.4 in. s_l] was designed to investigate the influence of a 1% steel fiber dosage on the performance of noncontact hooked bar lap splices. This beam investigates fiber dosage with the addition of confinement in the form of 3 in. of bottom and side cover and No. 3 stirrups placed at $3d_b$.

Testing Notes:

None.

Table B-36: S13-#9-[S.F.3 in. c_b &c_{so}] Specimen Properties

Configuration of Closure Joint								
c_b (in.)	c_{so} (in.)	c_{si} (in.)	c_{th} (in.)	s_l (in.)	l_s (in.)	b (in.)	h (in.)	**Secondary Reinforcement**
3.567	3.51	1.392	2.149	3.719	8.917	27.125	27	No. 3 stirrups placed at $3d_b$ and 3 in. concrete cover

Properties of Constitutive Materials								
Precast Concrete			**Cast-in-Place Concrete**			**Steel Reinforcing Bars**		
f_{cm} (psi)	f_{stm} (psi)	E_{cm} (ksi)	f_{cm} (psi)	f_{stm} (psi)	E_{cm} (ksi)	d_b (in.)	f_y (psi)	R_r
3490	345	3350	3800	585	3600	1.128	61600	.07

Table B-37: S13-#9-[S.F.3 in. c_b &c_{so}] Fresh Concrete Properties

Precast Concrete			**Cast-in-Place Concrete**		
Air Content (%)	**Unit Weight (pcf)**	**Slump (in.)**	**Air Content (%)**	**Unit Weight (pcf)**	**Slump (in.)**
8	135.4	8	5.3	150.9	3

Table B-38: S13-#9-[S.F.3 in. c_b &c_{so}] Loading Configuration and Test Results

A (in.)	B (in.)	C (in.)	δ_u (in.)	P_u (lb)	M_u (kip-in.)	$f_{s,mc}$ (ksi)
48	48	6	1.263	85,692	3694.14	58.966

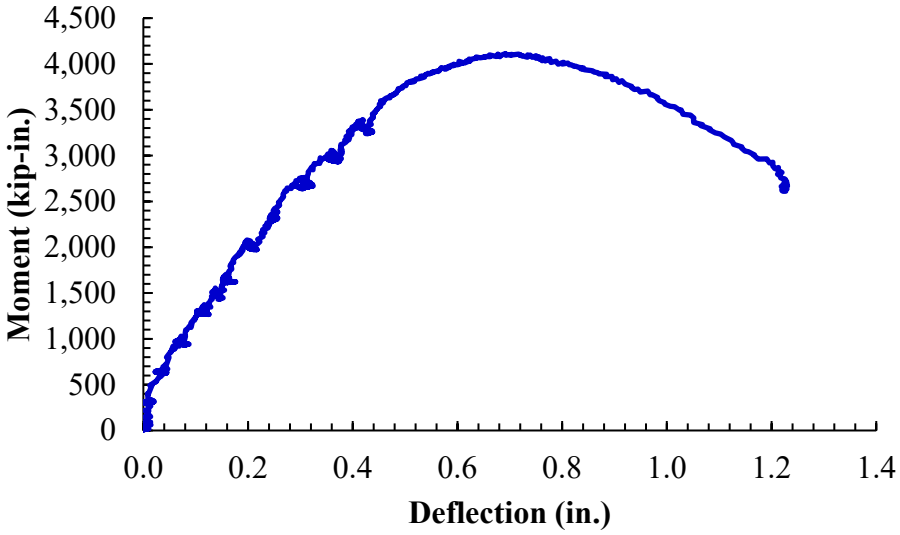

Figure B-42: S13-#9-[S.F.3 in. c_b &c_{so}] Applied Moment Against Midspan Deflection

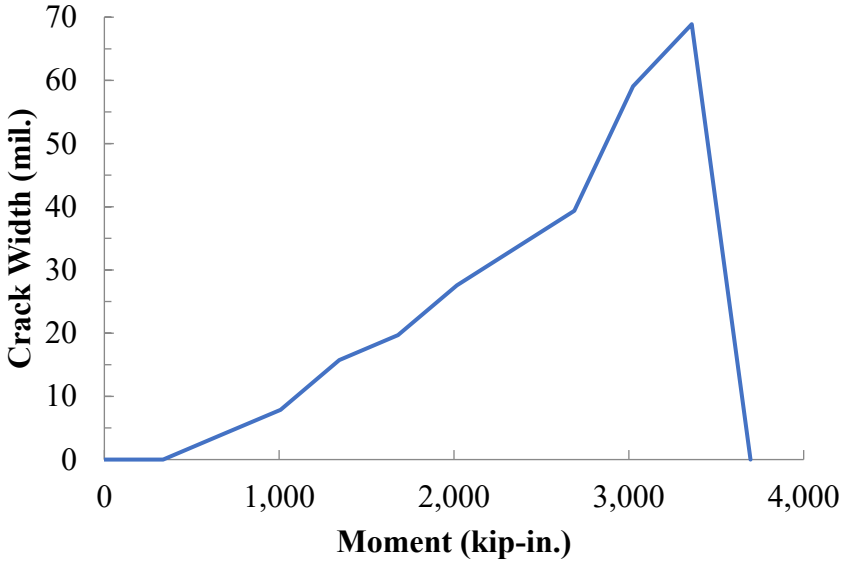

Figure B-43: S13-#9-[S.F.3 in. c_b &c_{so}] Interface Crack Growth Under Loading

	Side View of Splice Region	Top View of Splice Region
50% Maximum Loading	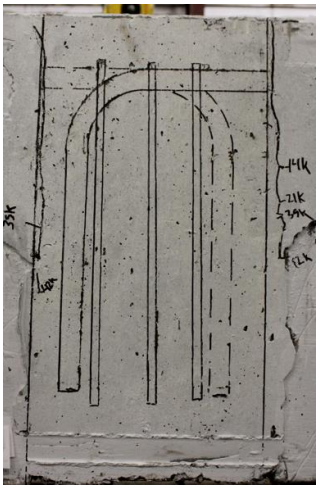	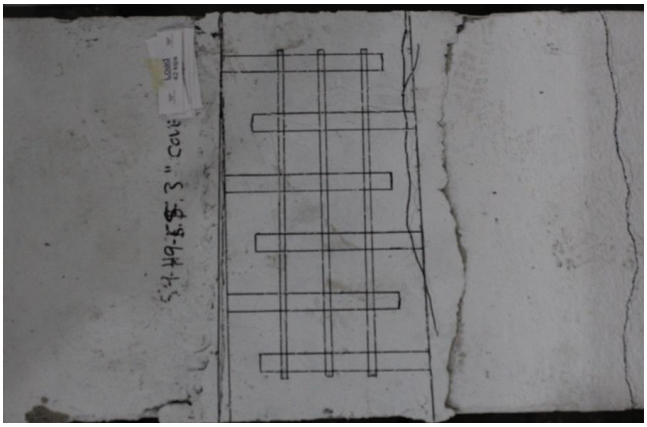
75% Maximum Loading	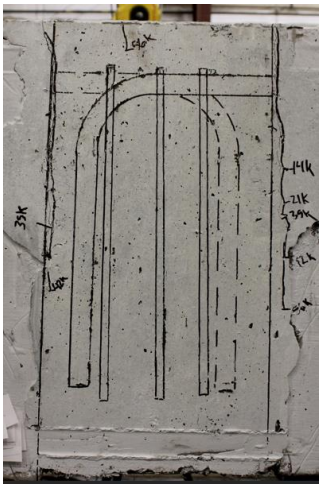	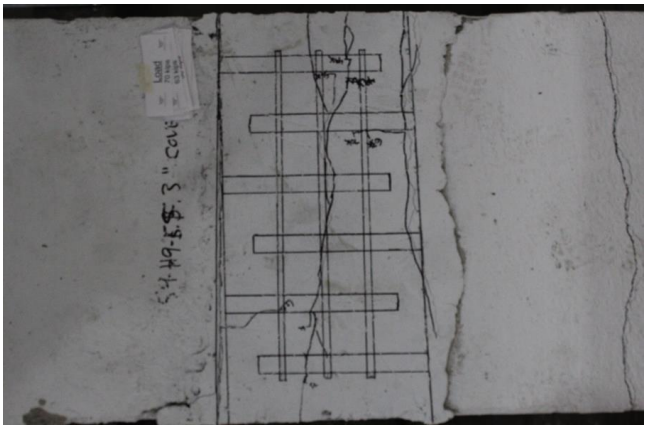
At Failure	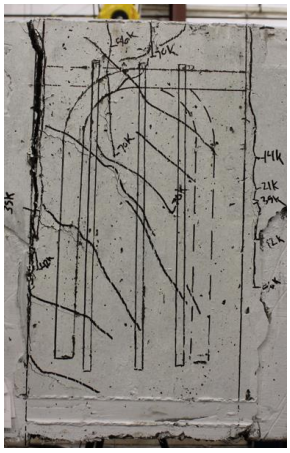	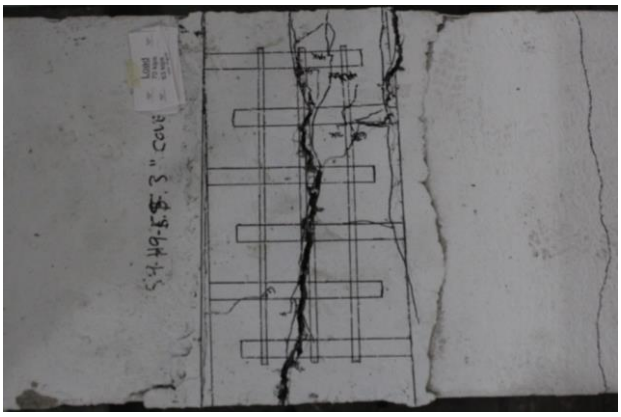

Figure B-44: Progression of Damage in Closure Joint of S13-#9-[S.F.3 in. c_b &c_{so}]

APPENDIX A NOTATION LIST

A Center-to-center distance between an applied point load and nearest support

AUC_F Energy required to fracture notched three-point bending specimens

b Measured beam width at the closure-joint region

B Center-to-center distance between supports in the midspan region

c_b The vertical clear cover to the spliced bar

c_{si} One-half of the clear distance between bars of adjacent lap splices, measured at the middle of the splices

c_{so} Cover measured from edge of bar to closest beam edge, measured at the middle of the splice

c_{th} Tail cover measured from the outer point of tangency of a hooked bar to the precast concrete

C Distance between end of beam and nearest point load

d_b Nominal bar diameter of lapped reinforcement

E_{cm} Static modulus of elasticity of concrete measured per ASTM C469

E_h Modulus of strain hardening of steel reinforcement

f_c' Specified concrete compressive strength

f_{cm} Uniaxial concrete compressive strength measured per ASTM C39

$f_{s,mc}$ Peak stress of the lapped bars determined using moment-curvature analysis

f_{stm} Concrete splitting tensile strength measured per ASTM C496

f_y Measured yield strength of reinforcement

h Measured beam height at the closure-joint region

h_r Height of bar ribs

l_s Length of lap splice of hooked bars measured between the outside ends of hooks bars at their points of tangency

M_u Moment at the splice ends due to combined effects of applied loads, beam self-weight, and weight of testing equipment

P_u One-half of total applied point loads not including self-weight of beam or weight of testing equipment

R_r Relative rib area, defined as the ratio of bar bearing area to shearing area

s_l Center-to-center spacing of paired bars in a lap splice

s_r Center-to-center spacing of bar ribs

w_r Width of bar ribs

δ_u Midspan deflection at peak applied load

ε_{sh} Strain at the onset of hardening

ε_y Yield strain